AtkinsRéalis

Upper Liard Flood Mapping Study – Modelling Report

Yukon Government

March 16, 2026

705450-0000-4HER-0003_00

UPPER LIARD FLOOD MAPPING STUDY – MODELLING REPORT

Signature Page

Prepared by:

Felix Nguyen, Ph.D.
Specialist – Hydrology/hydraulics

AtkinsRéalis – Engineering Services Canada

William Xing, MSc.
Professional – Surveyor

AtkinsRéalis – Engineering Services Canada

Francis Lepage, MSc., P.Eng.
Lead – Hydraulics, Hydrology & Climate Impacts
Engineers Yukon License N. 3998

AtkinsRéalis – Engineering Services Canada

Verified by:

March 16, 2026

Ahmed Bouayad, P.Eng.
Senior Technical Review
OIQ license: 102656

AtkinsRéalis – Engineering Services Canada

Approved by:

Francis Lepage, MSc., P.Eng.
Project Manager
Engineers Yukon License N. 3998

AtkinsRéalis – Engineering Services Canada

Notice

This document and its contents have been prepared and are intended solely as information for Yukon Government and use in relation to Report

AtkinsRéalis Canada Inc. assumes no responsibility to any other party in respect of or arising out of or in connection with this document and/or its contents.

Document history

Document title: **Upper Liard Flood Mapping Study**

Document reference: Revision	Purpose description	Originated	Reviewed	Date
705450-0000-4HER-0003 – PA	Preliminary version based on commented preliminary modelling input memo	FN, WX, FL	AB	November 10th, 2025
705450-0000-4HER-0003 – 00	Final	FN, FL	AB	March 16th 2026

Contents

Tables

Figures

1. Introduction

1.1 Background

Upper Liard is a Liard First Nation, Kaska Dena community (Government of Yukon, 2025). The community has a population of approximately 130 and is located on the Liard River (Nêt'ił Tué') at the Alaska Highway, approximately 7 km West of Watson Lake (see Figure 1-1).

The Liard River flows through the Yukon, into British Columbia, then into the Northwest Territories and joins the Mackenzie River at Fort Simpson. The Liard River at Upper Liard has a drainage area of approximately 32,600 km^2 and drains from the Pelly Mountains to the northwest and the Cassiar Mountains to the West (Government of Yukon, 2025). The area of interest for flood hazard mapping considered in this study covers about 19 km length of the Liard River, for a total area of approximately 44 km^2 (see Figure 1-1).

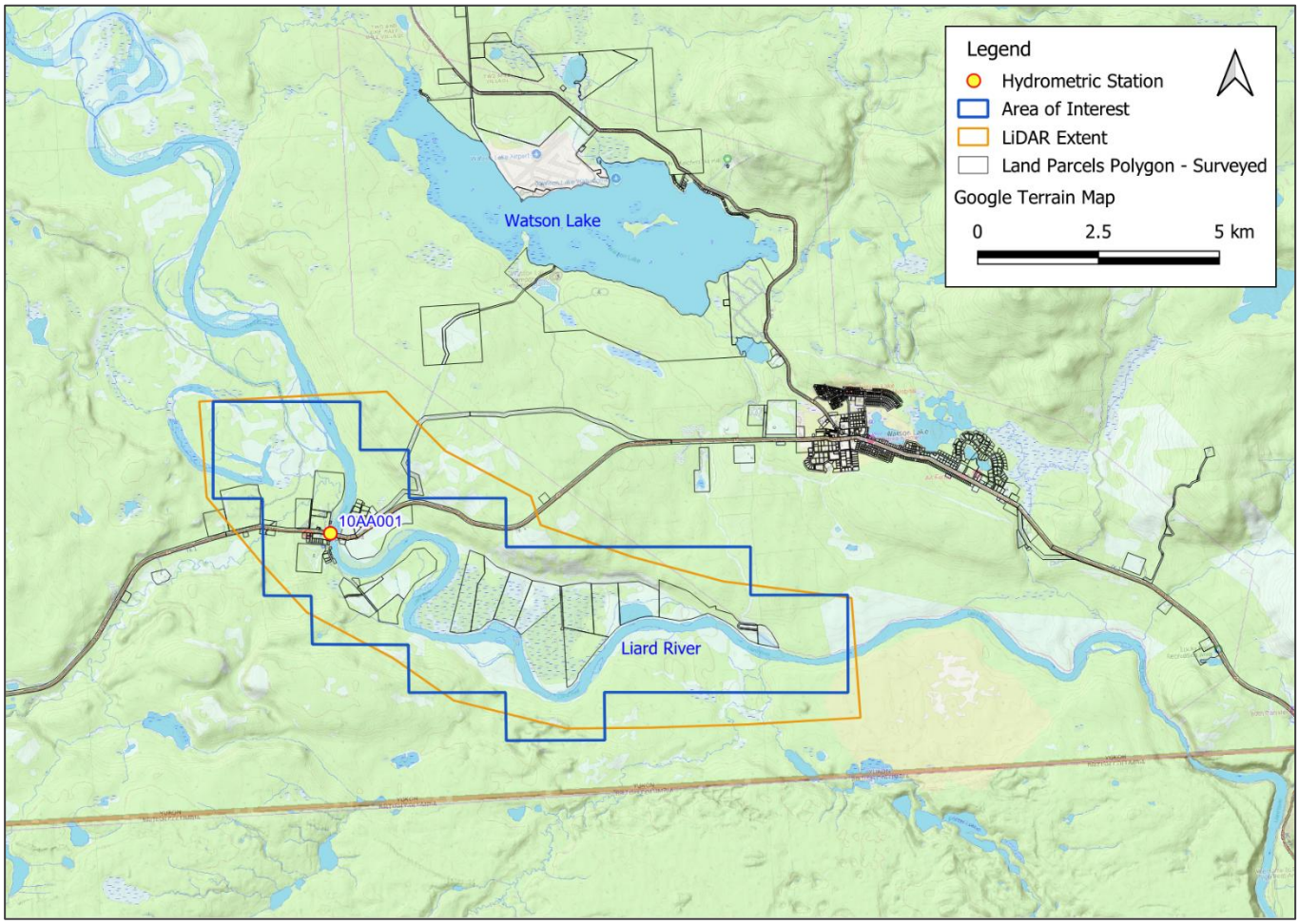

Figure 1-1 – Upper Liard Area of Interest for Flood Mapping Study

At Liard River at Upper Liard, the annual maximum water level usually occurs in early to mid-June during open water freshet. Peak annual water level can occasionally occur in May and is driven mainly by snowmelt runoff. While intense precipitation events are not common during freshet, they are frequent in the summer period. Intense localized downpours can exceed 50 mm in 24 hours and have generated washouts along the Alaska Highway on smaller water courses (Government of Yukon, 2025).

Regarding extreme flood events, the most recent event happened just a few years ago in 2022 with a peak discharge of 3010 m^3/s. The largest flood on record over the last 65 years occurred in 2012 with an instantaneous peak discharge of 3990 m^3/s caused by a rain-on-snow event. The flood led to the evacuation of multiple residents on the east bank of the river upstream of the Alaska Highway crossing, as well as flooding further downstream in the community of Lower Post, British Columbia.

It should be noted that it's not only the depth of the available snow cover that contributed to the extreme flow, but also the suddenness of the spring snowmelt. The basin wide snow water equivalent (SWE) estimated for the 2012 event was approximately 250 mm which is considerably lower than that of the 2022 event (i.e. approximately 330 mm). However, the peak discharge in 2012 was more than 30% higher than the peak discharge of the 2022 event (Government of Yukon, 2025). Note that the 2012 peak snowpack in the contributing basin only ranks as the eighth highest on record, based on Government of Yukon snow surveys.

Flood mapping can be used to support emergency preparation and response, and to inform the development planning to reduce community vulnerability to flooding in a changing climate. The primary purpose of the present study is to identify and map flood hazards, which will advance the goals of enhancing public safety and reducing future flood vulnerability for the community of Upper Liard.

1.2 Scope of Work

The study was carried out in accordance with the Federal Hydrologic and Hydraulic Procedures for Floodplain Delineation guideline (NRCan, 2023). The present report covers the following tasks:

- Hydrologic assessment: including preparation of data series, flood history documentation, flood frequency analysis.
- River ice assessment: containing ice flood history assessment and ice-affected flow frequency analysis.
- Climate change and land-cover assessment: involving the review of relevant climate change standards and practices, review of previous studies, calibration and validation of RAVEN hydrologic model, and quantitative assessment of potential impacts of climate and land-cover change.
- Fluvial erosion assessment: providing a qualitative assessment of fluvial erosion hazard.
- Hydraulic modelling: performing calibration and validation of the HEC-RAS model of Liard River, sensitivity analysis, and design flow modelling.

Other relevant tasks performed to support this study are outlined below:

- Site visit and survey: performing a site visit, preparing a survey plan, performing a river cross section survey, hydraulic structure and high-water mark surveys and photographic inventory.
- Flood hazard mapping: issuing flood hazard maps following the Government of Yukon Flood Hazard Mapping Basemap Guidelines (2024) and Federal Floodplain Mapping Guidelines and Specifications (2018).

2. Hydrologic Assessment

2.1 Procedure to Assess Design Flood Events

Following the Federal Hydrologic and Hydraulic Procedures for Floodplain Delineation guideline (NRCan, 2023), the hydrologic procedures that are required to develop reliable and realistic design flows are presented in Table 2-1 below.

Table 2-1 – Hydrologic Practices

Step	Description
1	Define hydrologic outcome according to the design flood event criteria of the jurisdiction.
2	Gather data: Identify all sources of relevant data and historical information in the defined hydrologic region. Include hydrologic and meteorological data that meet key data requirements. Document sources of historical information and data selected. Use the maximum flood record available.
3	Investigate non-stationarities and homogeneity: Conduct a quality assurance and quality control check of the hydrologic data including verification of stationarity and homogeneity. Identify the effects of flow regulation and diversion on hydrologic data to ensure it is appropriately addressed by the selected hydrologic procedure.
4	Select analytical approach.
5	Conduct a flood frequency analysis (FFA): Conducting a single station FFA if historical information and systematically collected flow data are available. Practitioners must be aware of the uncertainties of this approach and confirm that the data meets the underlying assumptions. When sufficient data are not available to support a single station FFA, conduct a regional FFA (RFFA) for a hydrologically homogeneous region having a sufficient number of streamflow records and adequate periods of record.
6	Conduct a deterministic hydrologic analysis: This is the preferred approach when design flows are based on a historical storm or synthetic design storm, a flood hydrograph is required, or where the watershed has experienced land use changes.
7	Incorporate the impact on design flood events of future non-stationarity caused by factors such as climate change, alternate land uses, regulation, and morphological changes.

The hydrologic outcomes (step 1) are the design flows for various annual exceedance probabilities (AEPs). They are clearly stated in Section 6.2.3 – Scope of Service, Consultant Services Agreement, from the Government of Yukon: "*The design flow estimation should use flow observations from the Liard River and (where appropriate) supplementary regional information and must reflect instantaneous peak flow conditions. Design flows for AEPs of 50%, 20%, 10%, 5%, 2%, 1%, 0.5% and 0.2% should be produced.*"

Collection of historical record data (step 2) is described in Section 2.2. The details of flood frequency analysis (step 3 to 5) are presented in Section 2.3. Effects of land use changes and climate changes (step 6 and 7) are provided in Section 3.

2.2 Historical Record Data

2.2.1 Gauge Data

All available recorded flow and flood peak data from five relevant hydrometric stations were collected from the Water Survey of Canada (WSC). These include the Station 10AA001 – Liard River at Upper Crossing located right in the study area of interest about 4 km from the upstream boundary of the AOI and four other stations located on the main upstream tributaries of the Liard River, such as Frances River, Rancheria River, and Big Creek. The Frances River is the largest tributary above Upper Liard and includes Frances Lake in the headwaters, which dampens the flow from that contributing area. The Rancheria River is the second largest tributary above Upper Liard. The locations of these stations and their corresponding watersheds are shown in Figure 2-1. The detailed information of these stations (including station IDs, names, coordinates, drainage areas, and record years) is provided in Table 2-2.

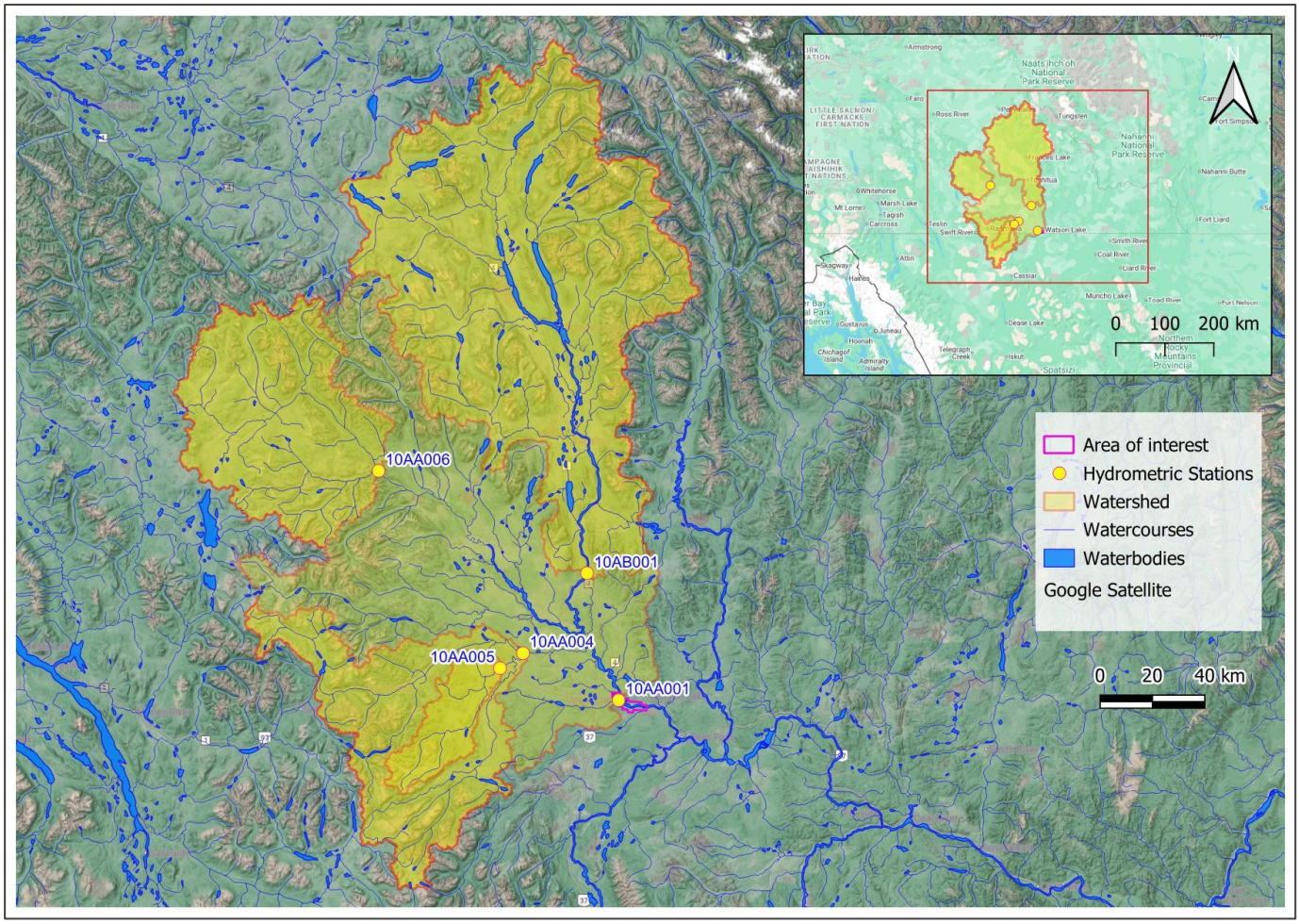

Figure 2-1 – Location of the Study Site: Station 10AA001 – Liard River at Upper Crossing

Table 2-2 – WSC Hydrometric Stations

Station ID	Station Name	Latitude	Longitude	Drainage Area (km²)	Record Year
10AA001	Liard River at Upper Crossing	60°03'03" N	128°54'24" W	32600	1960-2024
10AA004	Rancheria River Near the Mouth	60°12'29" N	129°32'58" W	5100	1985-2024
10AA005	Big Creek at Km 1084.8 Alaska Highway	60°09'28" N	129°42'14" W	1010	1989-2023
10AA006	Liard River below Scurvy Creek	60°48'38" N	30°31'15" W	n/a	2016-2024
10AB001	Frances River Near Watson Lake	60°28'26" N	129°07'08" W	12800	1962-2024

2.2.2 Data Series Preparation

The observed annual maximum daily mean and instantaneous peak flow record series were obtained directly from Water Survey of Canada (WSC, 2025). The data is provided in Table 2-3 below for Station 10AA001 – Liard River at Upper Crossing and in Appendix A1 for the remaining 4 stations. Note that instantaneous peak flows are required for the frequency analysis (see Section 2.3), however, they are not always available for each year of record, with only the corresponding daily mean values available. For example, for Station 10AA001 – Liard River at Upper Crossing, most of the instantaneous peak flows are missing for the 1960-1980 period. Therefore, a relationship between the daily and instantaneous peak flow was constructed for each station based on the available data.

The ratio of instantaneous to daily peak discharges is computed by estimating the slope of a linear regression model passing through the origin between the instantaneous and daily peak discharge data as shown in Figure 2-2 for Station 10AA001. For this station, the ratio is 1.02. The instantaneous peak flows are then computed by multiplying this ratio with the corresponding daily mean values.

A similar approach was applied to all other stations to derive the missing values, either the daily mean or instantaneous value if one of them was available. The ratios of all five study stations are summarized in Table 2-4 with ratios in the range between 1.01 and 1.08. As expected, stations with smaller watershed areas (i.e. 10AA004 and 10AA005) have higher ratios than those with larger watershed areas (i.e. 10AA001 and 10AB001).

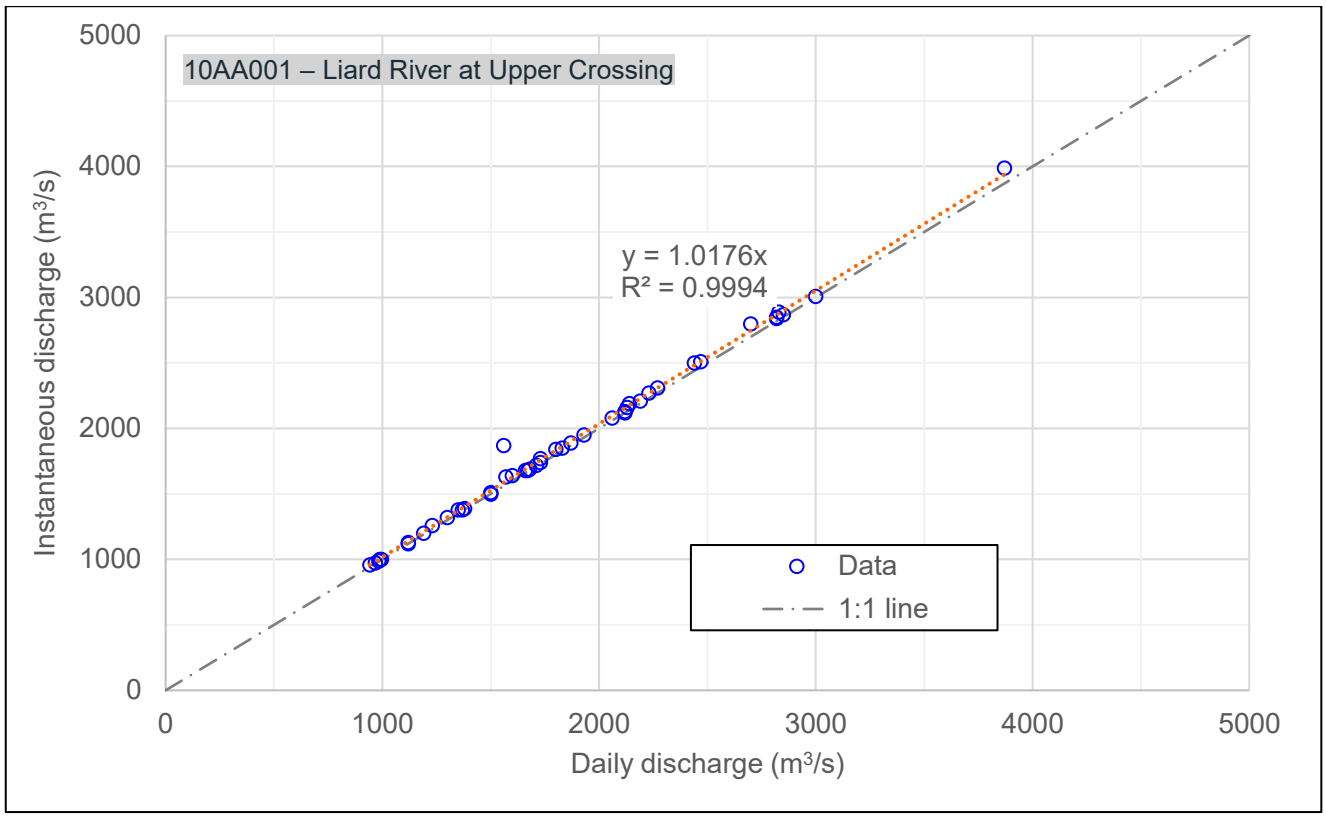

Figure 2-2 – Relationship between Instantaneous and Daily Peak Discharge of Station 10AA001

Table 2-3 – Annual Maximum Daily and Instantaneous Peak Discharge of Station 10AA001

No	Year	Q_{daily} (m^3/s)	Q_{inst} (m^3/s)	No	Year	Q_{daily} (m^3/s)	Q_{inst} (m^3/s)
1	1960	1600	**1632**	34	1993	1500	1510
2	1961	3030	**3091**	35	1994	1500	1500
3	1962	2790	**2846**	36	1995	989	1000
4	1963	1870	**1907**	37	1996	1040	**1061**
5	1964	2940	**2999**	38	1997	1570	1630
6	1965	1480	**1510**	39	1998	1730	1740
7	1966	1510	**1540**	40	1999	2140	2190
8	1967	1980	**2020**	41	2000	1370	1380
9	1968	1540	**1571**	42	2001	2120	2120
10	1969	1340	**1367**	43	2002	1350	1380
11	1970	1460	**1489**	44	2003	1120	1120
12	1971	2290	**2336**	45	2004	1660	1680
13	1972	3060	**3121**	46	2005	2830	2890
14	1973	1910	**1948**	47	2006	2130	2160
15	1974	1390	**1418**	48	2007	2820	2850
16	1975	1670	1680	49	2008	2470	2510
17	1976	2050	**2091**	50	2009	2120	2130
18	1977	1930	1950	51	2010	942	959
19	1978	943	**962**	52	2011	1800	1840
20	1979	1910	**1948**	53	2012	3870	3990
21	1980	1230	1260	54	2013	2820	2840
22	1981	2060	2080	55	2014	1380	1390
23	1982	1560	1870	56	2015	1600	1640
24	1983	1710	1720	57	2016	1300	1320
25	1984	1730	1770	58	2017	1120	1130
26	1985	2270	2310	59	2018	944	963
27	1986	1870	1890	60	2019	984	989
28	1987	2230	2270	61	2020	1680	1690
29	1988	2440	2500	62	2021	2190	2210
30	1989	996	1000	63	2022	3000	3010
31	1990	2700	2800	64	2023	1830	1850
32	1991	1190	1200	65	2024	968	974
33	1992	2850	2870				

Note: **Underlined** numbers are estimated values based on the relationship between daily and instantaneous discharge.

Table 2-4 – Ratio of Instantaneous to Daily Discharge

No	Station ID	Station Name	Watershed Area (km^2)	Ratio
1	10AA001	Liard River at Upper Crossing	32600	1.02
2	10AA004	Rancheria River near The Mouth	5100	1.08
3	10AA005	Big Creek at Km 1084.8 Alaska Highway	1010	1.08
4	10AA006	Liard River below Scurvy Creek	n/a	1.04
5	10AB001	Frances River near Watson Lake	12800	1.01

The annual maximum instantaneous discharge series of all five study stations are presented in Figure 2-3.

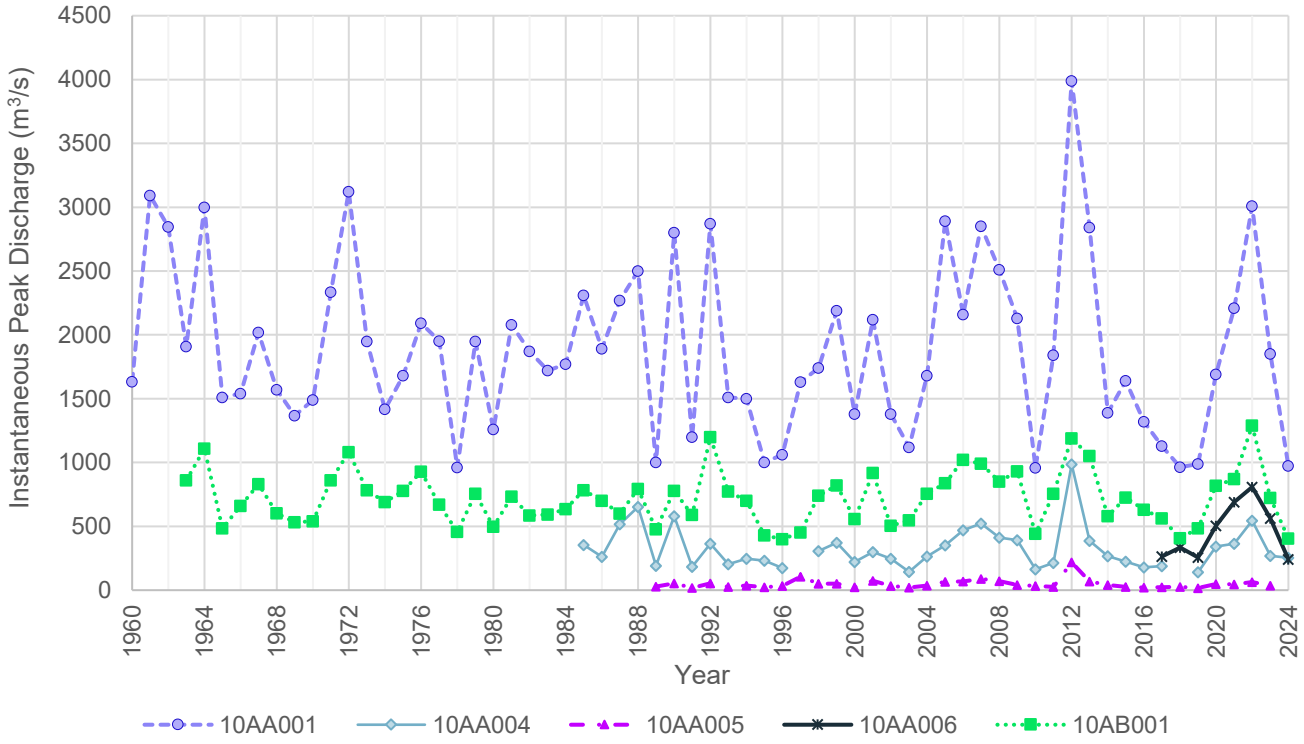

Figure 2-3 – Annual Maximum Series of Instantaneous Peak Discharge of Five Study Stations

2.2.3 Statistics of Annual Maximum Series

Sample statistics of the annual maximum instantaneous peak discharge series from the five study stations are provided in Table 2-5. These include: the sample length, the maximum and minimum record peak flows, as well as the mean, standard deviation, and skewness of the annual maximum series. For instance, for Station 10AA001 –

Liard River at Upper Crossing, the mean annual maximum peak flow recorded in 65 years is 1886 m^3/s and the maximum peak flow is 3990 m^3/s, which occurred in 2012.

Table 2-5 – Statistics of Annual Maximum Discharge Series of Five Study Stations

Statistics	Unit	Station				
		10AA001	10AA004	10AA005	10AA006	10AB001
Sample length	(year)	65	38	35	8	62
Max	(m^3/s)	3990	985	218	808	1290
Min	(m^3/s)	959	141	17	242	400
Mean	(m^3/s)	1886	329	48.4	458	722
Standard deviation	(m^3/s)	667	169	36.5	217	212
Skewness		0.73	1.88	3.16	0.55	0.60

2.2.4 Flood History Documentation

This section provides a detailed summary of the five major historical flood events that occurred in the area of interest (AOI). Since a very long record is available at the hydrometric station in the AOI (i.e. Station 10AA001 – Liard River at Upper Crossing) with data from Water Survey of Canada (WSC, 2025) and the Canadian River Ice Database (CRID, 2025), the most severe annual extreme hydrometric events were extracted and used for the study. The information includes the occurrence dates of extreme events, the daily and instantaneous peak discharge and water levels of the Liard River at Upper Crossing. Results are presented in Table 2-6.

It can be seen from this table that all five extreme events happened in the first half of June during the open-water period with a peak discharge between 3000 – 4000 m^3/s and caused an extreme water level between 609.00 – 610.50 m.

Table 2-6 – Top 5 Flood Events on Record Based on Hydrometric Data from Station 10AA001 – Liard River at Upper Crossing

No	Year	Daily Mean Hydrometric Record			Instantaneous Hydrometric Record		
		Date (mm-dd)	Discharge (m^3/s)	Water Level (m)	Date (mm-dd)	Discharge (m^3/s)	Water Level (m)
1	2012	06-10	3870	610.35	06-10	3990	610.47
2	1972	06-02	3060	609.25	n/a	**3121**	**609.31**
3	1961	06-12	3030	609.03	n/a	**3091**	**609.08**
4	2022	06-12	3000	609.46	06-13	3010	609.47
5	1964	06-11	2940	609.05	n/a	**2999**	**609.11**

Note: **Underlined** numbers are estimated values based on the relationship between daily and instantaneous records.

2.3 Flood Frequency Analysis

2.3.1 Method

The open water design flow for the Liard River is determined using the flood frequency analysis. This is Step 3 to Step 5 described in Table 2-1 above. Further details on how to carry out these steps are presented in Figure 2-4 below.

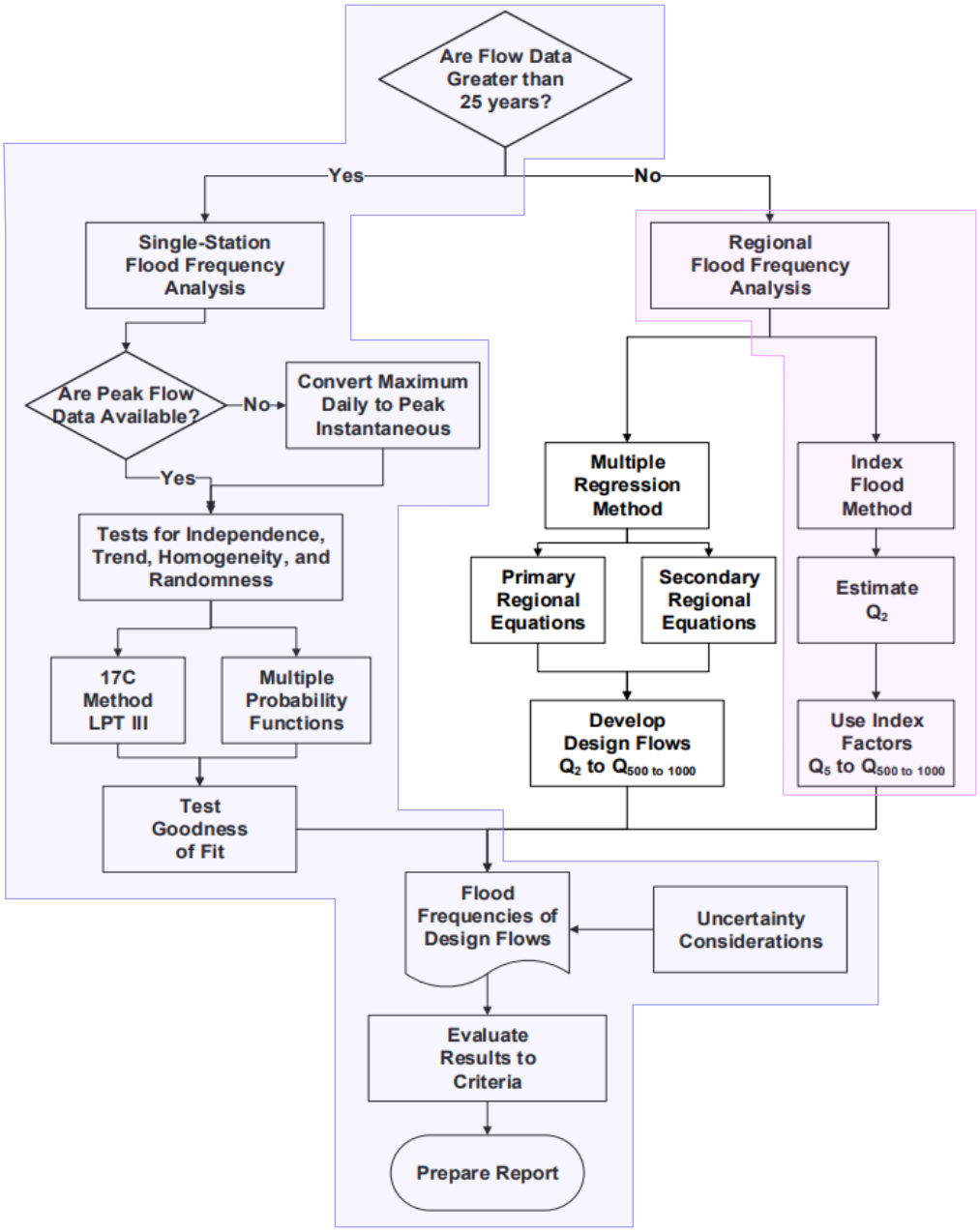

Figure 2-4. Procedure for Flood Frequency Analysis, Adapted from NRCan (2023)

Note that since Station 10AA001 – Liard River at Upper Crossing is located right in the study area and has a much longer data record than the minimum sample length requirement (i.e. 65 years vs. 25 years), only data from this station

will be used for the at-site (or single-station) flood frequency analysis. In addition, a regional flood frequency analysis is also not considered compulsory in this case. However, to have a better understanding and to quantify uncertainty of the estimation by relying on the regional information (i.e. pooled data by considering recorded information from other stations located within the same homogeneous region), a regional flood frequency analysis based on the index flood approach and the L-moment estimator was also performed (see section 2.3.4).

2.3.2 Hypothesis Testing

Before carrying out the single-station frequency analysis, three tests were performed on the annual maximum instantaneous peak discharge series of Station 10AA001 to verify the assumptions of independent and identically distributed samples. These include:

- Test for independence (Wald-Wolfowitz test): the null hypothesis (H_0) is the observations are independent, and the alternative hypothesis (H_a) is observations are dependent.
- Test for stationarity (Kendall test): the null hypothesis (H_0) is no trend is apparent in the observations, and the alternative hypothesis (H_a) is there is a trend in the observations.
- Test for homogeneity (Wilcoxon test): the null hypothesis (H_0) is the averages of the two samples are equal, and the alternative hypothesis (H_a) is the averages of the two samples are different.

The results are summarized in Table 2-7 with all the tests being accepted at the 5% significance level.

Table 2-7 – Hypothesis Testing of the Annual Maximum Flow Series

Station 10AA001	Hypothesis testing		
	Test for independence	Test for stationarity	Test for homogeneity
Test results	We accept H_0 at a significance level of 5 %.	We accept H_0 at a significance level of 5 %.	We accept H_0 at a significance level of 5 %.

2.3.3 Single-Station Frequency Analysis

To perform the single-station frequency analysis (SSFA), six different popular distribution models commonly used in the field of flood frequency analysis were selected for comparison. These include Gumbel (GUM), Generalized Extreme Values (GEV), Log-normal two-parameters (LN2), Log-normal three-parameters (LN3), Log-Pearson type-III (LP3) and Pearson type-III (PE3) distribution models. The method of L-moments (Hosking and Wallis, 1997) was utilized to compute the model parameters. Compared to the traditional method of moments, this method offers several advantages, including its robustness to outliers, improved estimation of parameters, and wider distributional coverage. Results of the single-station frequency analysis based on data from Station 10AA001 are presented in Figure 2-5.

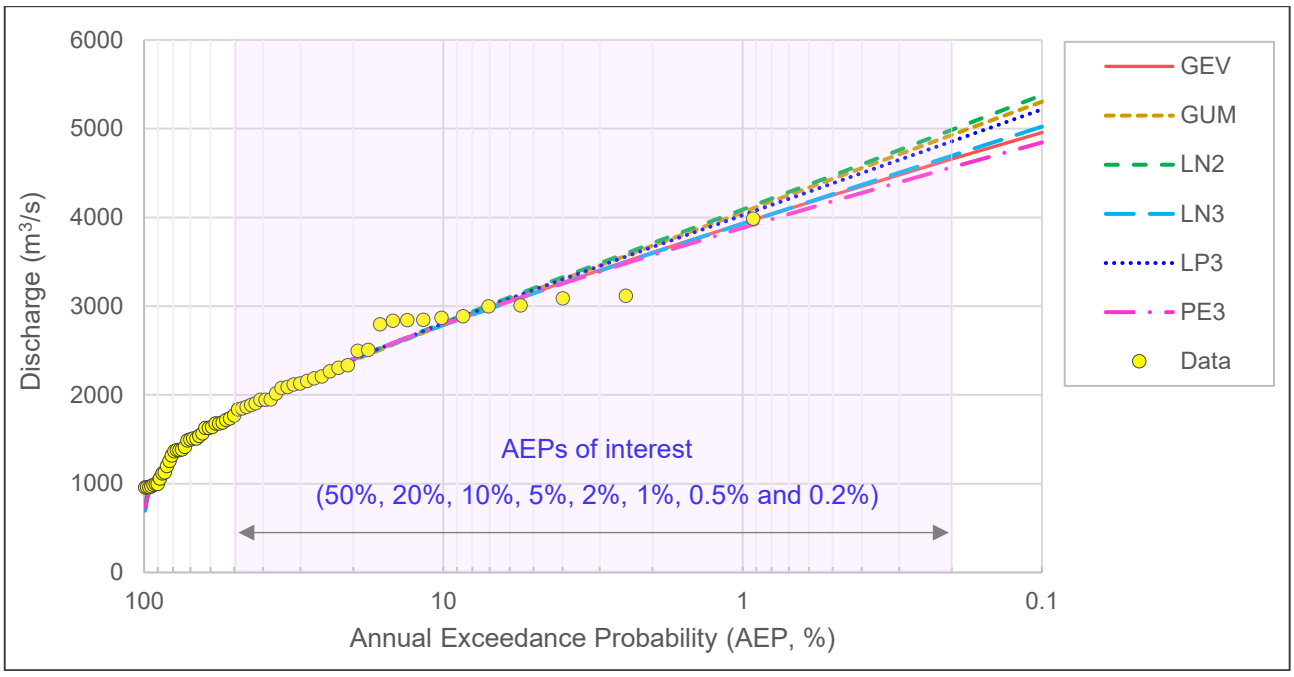

Figure 2-5 – Single-Station Frequency Analysis of Annual Maximum Discharge of Station 10AA001

To compare the performance of these models, four different numerical indices were used to measure the goodness-of-fit (GOF) between the estimated and observed data. These are: root mean square error (RMSE), root mean square relative error (RMSEr), Akaike Information Criterion (AIC), and Bayesian Information Criterion (BIC). The best models to be chosen are the ones with the lowest errors and consistent performance across different indicators. The results are summarized in Table 2-8.

Table 2-8 – Comparison of Model Performance Based on Different Goodness-of-Fit Criteria

Model	Goodness-of-Fit (GOF) Measure			
	RMSE	RMSEr	AIC	BIC
GUM	101.6	0.053	874.5	878.4
GEV	95.6	0.055	867.8	873.6
LN2	101.3	0.051	874.0	877.9
LN3	94.2	0.054	865.8	871.7
PE3	89.9	0.049	859.8	865.6
LP3	97.4	0.051	870.1	876.0

Results indicated that the PE3 distribution model yields the best performance followed by the LN3 distribution model. The GUM and LN2 produce much larger errors and are considered the worst performance models for this station. In addition, by comparing the ensemble results of all six distribution models, it is likely that the estimated design flows from the PE3 model tend to be less conservative compared to those from the LN3 and GEV distribution models which are almost similar for AEPs higher than 0.5% and less than 1% different for design flows of smaller AEPS of interest. Comparing between the LN3 and PE3 estimated design flows for the AEPs of interest, the differences are up to 3% with PE3 on the less conservative side (see Table 2-9). Hence, as a result, the LN3 is considered the most appropriate

model for representing the distribution of the annual maximum peak discharge of the study site, i.e. Station 10AA001 – Liard River at Upper Crossing.

Table 2-9 – Summary of Single-Station Flood Frequency Analysis Results

Model	Annual Exceedance Probability (AEP, %)							
	50	20	10	5	2	1	0.5	0.2
LN3	**1789**	**2401**	**2786**	**3145**	**3598**	**3931**	**4261**	**4695**
PE3	1788	2411	2796	3146	3577	3886	4184	4565
Difference (%)	0.1	-0.4	-0.3	0.0	0.6	1.2	1.8	2.8

2.3.4 Regional Frequency Analysis

In addition to the single-station frequency analysis above, a regional frequency analysis (RFA) was carried out to quantify uncertainty of the design flow estimation using all available neighboring hydrometric data from all five study stations in the region of interest. The hypothesis testing results of these stations are provided in Appendix B. All stations passed the three tests at the 5% significant level.

The regional frequency analysis approach is based on the combination of the L-moment and the index flood method as described in Hosking and Wallis (1997). The main idea of the regional method is to "trade space for time" by using the pooled data from different stations which are considered not discordant from each other and are located within the same homogeneous region to develop a regional growth curve. This regional distribution is then used to compute the recurrence quantiles at a site of interest located within the same homogeneous region.

For the discordancy measure, a critical value D^* based on the number of study sites is provided by Hosking and Wallis (1997). For a region with 5 sites, the critical value D^* = 1.33. If the computed discordance value for a specific site, D_i, is higher than the critical value, this site will be removed from the defined region. The computed discordance values are presented in Table 2-10 along with the index flood and several useful L-moment statistics (i.e. coefficient of L-variation L-CV, L-skewness, L-kurtosis) for each site. Results indicate that no site is considered discordant.

Table 2-10 – Summary of L-moment statistics, discordancy measure, and index flood for each station

Station	Area (km^2)	Length (year)	Index flood (m^3/s)	L-CV	L-skewness	L-kurtosis	Discordancy measure
10AA001	32600	65	1886.3	0.20	0.14	0.10	0.54
10AA004	5100	38	328.6	0.26	0.31	0.19	1.23
10AA005	1010	35	48.4	0.34	0.39	0.27	1.26
10AA006	n/a	8	457.6	0.28	0.23	-0.11	1.32
10AB001	12800	62	721.9	0.17	0.11	0.11	0.65

For the heterogeneity measure, a critical heterogeneity value H^* is defined in Hosking and Wallis (1997) to justify the homogeneity of a region. The study region is considered as "acceptably homogeneous" if $H^* < 1$, "possibly heterogeneous" if $1 \leq H^* < 2$, and "definitely heterogeneous" if $H^* \geq 2$. Generally, if the computed H value is greater than 1.0 and the number of investigated sites is sufficiently large (i.e. more than 20 sites), then it is suggested that the

study region should be further refined (i.e. divided into sub-regions) to improve the accuracy of the quantile estimates for the location of interest. For this study, a heterogeneity measure based on different numbers of stations in the region was investigated. The elimination of a station was based on the drainage area (i.e. the site with the smallest watershed will be removed first). Results are shown in Table 2-11. The last two cases in the table are retained for the regional frequency analysis and sensitivity of the results since there are only three sites remaining and the heterogeneity values are not far from the upper limit of a homogeneous definition.

Table 2-11 – Cluster Analysis and Heterogeneity Measure Based on Number of Stations

Number of Stations	List of stations	Heterogeneity measure	Retain for RFA
5	10AA001, 10AB001, 10AA006, 10AA004, 10AA005	5.44	No
4	10AA001, 10AB001, 10AA006, 10AA004	5.30	
3	10AA001, 10AB001, 10AA004	3.46	
3	10AA001, 10AB001, 10AA006	2.13	Yes
2	10AA001, 10AB001	1.18	

Several distributions were fitted to the regional data, including the GEV model (and its special case, the GUM model), the Generalized Logistics (GLO) model, the LN3 model, and the PE3 model. Note that the LN2 and LP3 models are not available for the regional analysis since it involves a much more complex process rather than simply transforming the station data to the log domain, performing the fit and transforming it back to the real domain like a single-station frequency analysis.

For the goodness-of-fit (GOF) measure, a critical value Z^* is provided by Hosking and Wallis (1997) to evaluate whether a distribution model is considered acceptable. Provided that the region is acceptably close to homogeneous, the fit may be judged acceptable if the calculated absolute Z value is less than $Z^* = 1.645$ at the 10 % significance level. The GOF results are presented in Table 2-12 for both cases (i.e. a region of two and three stations respectively). The regional growth curves based on different distribution models are plotted in Figure 2-6 along with the observed data normalized by the index flood of each site.

Table 2-12 – Goodness-of-Fit Measure for Different Regional Distribution Models

Distribution Model	Goodness-of-Fit Measure	
	2-station RFA	3-station RFA
GLO	2.75	3.22
GEV	1.11	1.63
LN3	1.11	1.61
PE3	0.82	1.3

Similar to the SSFA, the GOF results indicate that the PE3 distribution is the best model followed by the LN3 and the GEV model. The estimated quantiles based on these three models are quite similar. In detail, the PE3 tends to be less conservative compared to the LN3 and the GEV models with the LN3 tending to be more conservative to the estimated quantiles of small AEPs of interest. Figure 2-6 also shows that the RFA using data from 3 stations provides slightly higher values, but not significantly different from those based on data from 2 stations. This is because the record data of Station 10AA006 is very short (i.e. only 8 years) and does not play a significant weight in the estimation. Results of the 3-station RFA based on the LN3 model are then retained to compare with those of the SSFA.

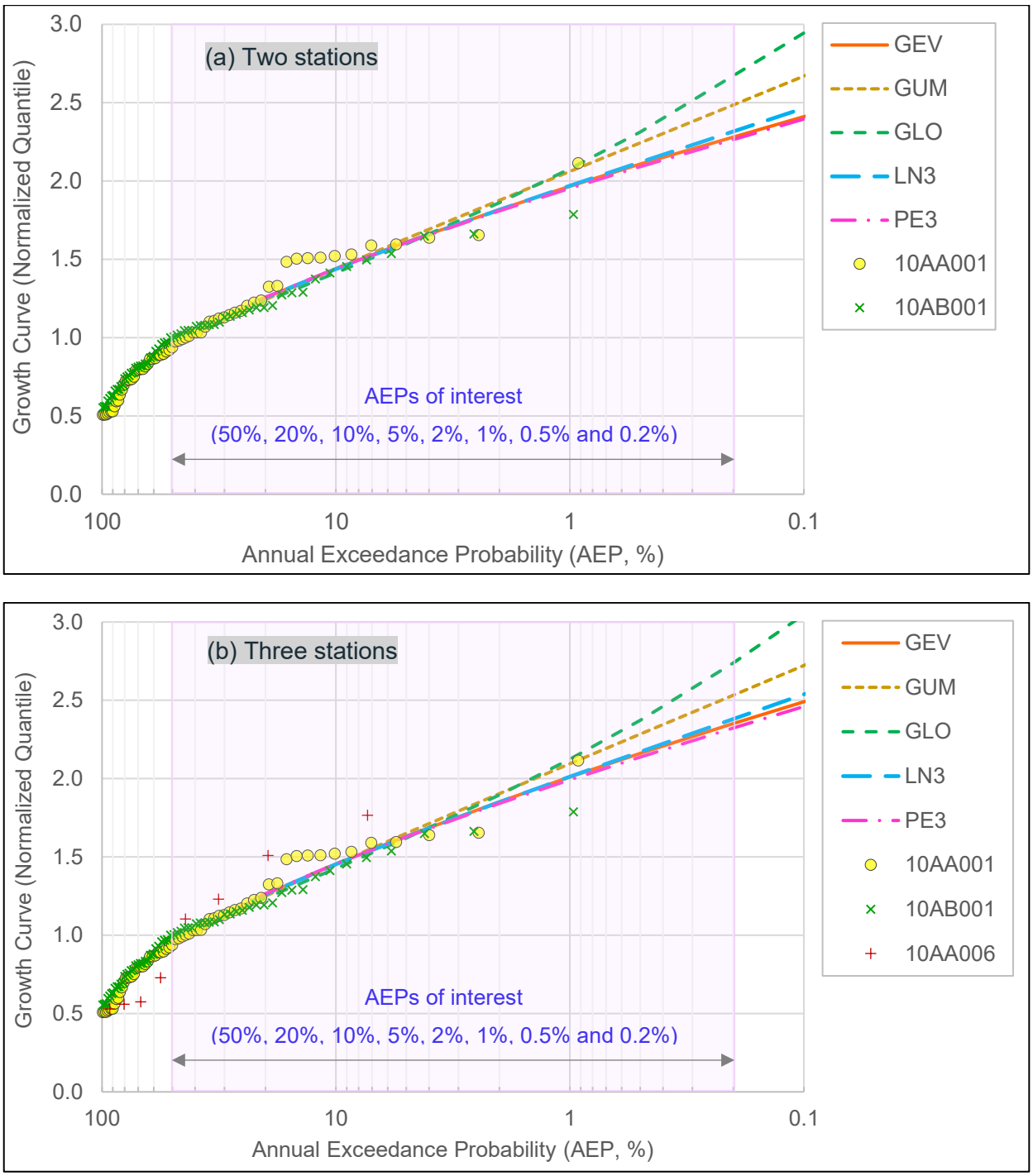

Figure 2-6 – Regional Frequency Analysis Based on Regional Data from (a) Two and (b) Three Stations

2.3.5 Single Station VS. Regional Frequency Analysis

This section compares the estimated design flow for various AEPs of interest based on both the single-station and regional frequency analysis approaches. Note that the quantiles corresponding to various AEPs of interest based on the RFA are computed for Station 10AA001 by multiplying the regional growth curve obtained from the LN3 model with the index flood of this site. Estimated quantiles of the two methods are visually compared in Figure 2-7 and summarized in Table 2-13.

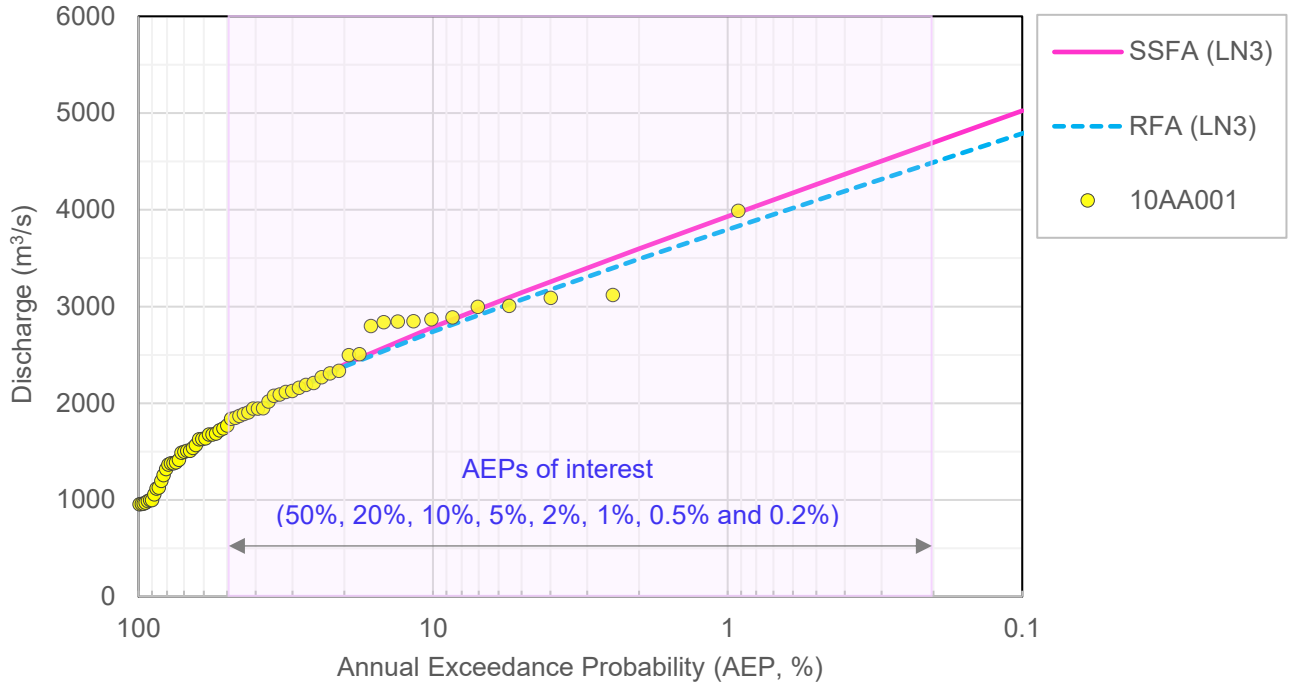

Figure 2-7 – Comparison of Single-Station and Regional Frequency Analysis Results

Comparison of the relative difference in the design flow estimation between the two methods shows that the SSFA produced between 1-5% higher values for the quantiles of AEPs of interest. In addition, the SSFA is based on a very long flow record (i.e. 65 years compared to the minimum requirement of 25 years). Hence, it is recommended to use the estimated design flow values from the LN3 (SSFA) as the input for the hydraulic modelling and flood hazard mapping study. Finally, the largest historical flood event in 2012 with a peak discharge of 3990 m^3/s is considered lower than the design flow of an event corresponding to an AEP of 0.5% which is 4260 m^3/s. Therefore, it is concluded that mapping of the 2012 event is not necessary.

Table 2-13 – Estimated Design Flows Based on Single-Station and Regional Frequency Analysis

Method	Annual Exceedance Probability (AEP, %)								Remark
	50	20	10	5	2	1	0.5	0.2	
LN3 (SSFA)	**1789**	**2401**	**2786**	**3145**	**3598**	**3931**	**4261**	**4695**	**Retained for mapping**
LN3 (RFA)	1800	2379	2740	3073	3490	3796	4097	4490	
Difference (%)	-0.6	0.9	1.7	2.3	3.0	3.4	3.9	4.4	

2.3.6 Comparison with Previous Studies

The estimated design flows obtained from the LN3 (SSFA) method above are compared to the values from previous studies. Note that the most recent frequency analysis studies from Morrison Hershfield (2022) and Yukon University (2022) were directly conducted on the water level data and not on the flow data. There is an older study from EBA (2008) which provides the design flow estimation for comparison. The comparisons of the flow and water level estimations of different studies are presented in Table 2-14 and Table 2-15 respectively.

For the flow frequency analysis, this study utilized a much longer extreme flow series for the analysis compared to the EBA (2008) study which did not cover the largest extreme event that occurred in 2012. The estimated design flow in the current study yields more conservative results between 1-10 % depending on the AEP of interest.

Table 2-14 – Comparison of Flow Estimations from the Current and Previous Studies

Study	Present Study	EBA (2008)	
Data	1960-2024	n/a-2007*	
Record (year)	65	n/a	
Model	LN3	LP3	
AEP (%)	**Flow Estimation (m^3/s)**		Difference (%)
50	1789	1830	-2.3
20	2401	2370	1.3
10	2786	2690	3.5
5	3145	2980	5.2
2	3598	3340	7.2
1	3931	3590	8.7
0.5	4261	3840	9.9
0.2	4695	n/a	n/a
Note: * the start year is not mentioned in EBA (2008)**.**			

For the water level analysis, to be comparable with previous studies, the water levels of various AEPs of interest are converted from the estimated design flow by using the rating curve (i.e. relationship between stage and discharge) provided by WSC (2025) for Station 10AA001. Note that a comparison of water level estimation for Upper Liard between Morrison Hershfield (2022) and Yukon University (2022) study was already done by Stantec (2023). The estimated levels from Morrison Hershfield (2022) were higher for different AEP of interest and were considered more conservative for the designs.

A comparison between water levels estimated in this study and Morrison Hershfield (2022) was carried out. Results indicate that the current study provides similar (but slightly lower) values to those in Morrison Hershfield (2022). The difference is from 0.00 to 0.15 m for different AEPs. To estimate the relative difference, the average depths were calculated for each study using surveyed cross-section data at the location of Station 10AA001. The average bed elevation is 602.50 m. The corresponding relative differences in water depths are between 0 to 2% for different AEPs.

Table 2-15 – Comparison of the Water Level Estimations from the Current and Previous Studies

Study	Present Study	Morrison Hershfield (2022)	Yukon University (2022)*		
Data	1960-2024	1990-2022	1972-2022		
Record (year)	65	33	51		
Model	Rating curve	LP3	LN3		
AEP (%)	Water Level Estimation (m)			Difference (Present VS Morrison Hershfield) (cm)	Difference (% of flow depth)
50	607.83	607.80	607.70	0.03	0.5
20	608.70	608.70	n/a	0.00	0.0
10	609.20	609.22	n/a	-0.02	-0.4
5	609.64	609.69	609.40	-0.05	-0.8
2	610.15	610.24	n/a	-0.09	-1.2
1	610.51	610.63	n/a	-0.12	-1.5
0.5	610.86	611.01	610.70	-0.15	-1.8
* These results are extracted from the Stantec (2023) report.					

These limited differences might be explained by one, or a combination, of the following factors:

1. The sample length used for the frequency analysis (i.e. 65 vs. 33 years).
2. The selection of the most appropriate distribution model (LN3 vs. LP3 model).
3. The use of direct frequency analysis on water level data vs. indirect estimate from the discharge-water level relationship.

3. River Ice Assessment

Riverine flooding on the Liard River at Upper Liard has historically been observed in the open water period. However, flooding events could also occur in ice-affected seasons (both freeze-up and breakup periods). Therefore, an ice analysis is required to compare ice-affected water levels and open water flooding.

The complete detail of the river ice assessment is presented separately as a technical memorandum in Appendix C. For flood hazard mapping scenarios corresponding to different AEPs of interest (i.e. 5%, 1%, and 0.5%), it was concluded that potential flooding is controlled by open-water conditions, and that it is not necessary to model ice-jam conditions.

4. Climate and Land-Cover Change Assessment

4.1 Literature Review

4.1.1 Review of Relevant Standards and Practices

This section presents a review of relevant standards and practices applied to flood frequency analysis and flood mapping in a changing climate following Federal and Provincial/Territorial guidelines.

The Federal Hydrologic and Hydraulic Procedures for Floodplain Delineation guideline (NRCan, 2023) presents the details of the climate change practices through seven steps as summarized in Table 4-1 below.

Table 4-1 – Practices to Incorporate Climate Change into Flood Hazard Studies

Step	Description
1	Select emissions scenarios from possible representative concentration pathways (RCPs).
2	Select general circulation model (GCMs) for either statistical downscaling or regional climate approach.
3a	Statistical downscaling approach: Screen the climate models, spatially disaggregate and compare with historical data to determine any bias correction needed to establish a weather generator of meteorological factors that impact extreme high stream flows and lake water levels. The weather generator components may be linked to future stream flows and water levels by linear regression. Canadian Centre for Climate Services (CCCS) may develop some components of a weather generator downscaled when a need is justified for regional studies.
3b	Regional climate approach: CCCS may be approached to produce some bias-adjusted water supply sequences from dynamically downscaled models available from its website.
4	Compare with the historical series and other global climate change models to ensure the results are reasonable as a check of the plausibility of occurrences.
5	Evaluate flood hazard delineation with the stream flows that result from the sequences of climate factors and a verified hydraulic model.
6	Consider a range of values from an ensemble of results to quantify uncertainty.
7	Map the flood hazard delineation and report on the process.

For emissions scenarios, in general, the higher the RCP, the greater the greenhouse gas and aerosol concentrations in Earth's future atmosphere. Thus, the Federal guideline (Natural Resources Canada, 2023) suggests that the consideration of the scenario RCP8.5 in any analysis would be prudent given the current global greenhouse gas production.

The Technical Guidelines for Flood Hazard Mapping Studies – Issued for 2025-26 from the Government of Newfoundland and Labrador (2025) provides further details on the selection of emission scenarios and the timeframe for the most recent development of global climate models (GCMs) to be used in developing provincial flood maps as follows:

- Global climate model: Coupled Model Intercomparison Project Phase 5 (CMIP5) or CMIP6
- Climate change assessment report: Intergovernmental Panel on Climate Change - Fifth Assessment Report (IPCC AR5) or IPCC AR6
- Scenario: Representative concentration pathways (RCP) 8.5 or Shared Socioeconomic Pathways (SSP) 5-8.5 (median values)
- Timeframe: 2100 (or late century period ─ from 2071 to 2100).

For steps 3 and 4, the regional climate data (which is available at a much finer resolution compared to those of GCM data) can come from different approaches, either based on a statistical downscaling method or from using Regional Climate Models. For the Yukon in general, and the region of Upper Liard in particular, the Pacific Climate Impacts Consortium (PCIC) has offered statistically downscaled, daily climate scenarios, at a gridded resolution of approximately 10 km (equivalent to 300 arc-seconds or 1/12°) for both the historical period of 1950-2014 and the projected period of 2015-2100. In general, these downscaled scenarios were constructed from 26 GCMs and 3 SSPs from CMIP6, using either the Univariate Downscaling approach (referred to as CanDCS-U6) or the Multivariate Downscaling method (known as CanDCS-M6). However, for a single region of interest, users are advised to use the corresponding regional subset data. For Northern Canada, the list of subset models and their developers are presented in Table 4-2 (Curry et al., 2023; ClimateData, 2025):

Table 4-2 – List of CMIP6 Global Climate Models Used in the CanDCS-M6 Ensemble

No	Institution	Model Name	Realization
1	Canadian Centre for Climate Modelling and Analysis (Canada)	CanESM5	r1i1p2f1
2	Institute for Numerical Mathematics (Russia)	INM-CM5-0	r1i1p1f1
3	Norwegian Climate Center (Norway)	NorESM2-LM	r1i1p1f1
4	Max Planck Institute for Meteorology (Germany)	MPI-ESM1- 2-HR	r1i1p1f1
5	Meteorological Research Institute (Japan)	MRI-ESM2-0	r1i1p1f1
6	CSIRO (Australia)	ACCESS-ESM1-5	r1i1p1f1
7	Research Center for Environmental Changes (Taiwan)	TaiESM	r1i1p1f1
8	Euro-Mediterranean Centre for Climate Change (Italy)	CMCC-ESM2	r1i1p1f1
9	Beijing Climate Center (China)	BCC-CSM2- MR	r1i1p1f1
10	EC-Earth-Consortium (Europe)	EC-Earth3- Veg	r1i1p1f1

Once the downscaled precipitation and temperature series are obtained for the region of interest, they can be injected into a hydrologic model to assess the impact of climate change on stream flow data (Step 5). Then, the flood frequency analysis of the historical and projected annual maximum peak discharge can be carried out to estimate the design flows for various timeframes. An ensemble of relative changes in design flows for various AEPs from different downscaled datasets can be assessed and used for the flood hazard mapping (Step 6 and 7).

4.1.2 Review of Previous Studies

This section presents the main findings of impacts of climate change on several important hydro-meteorological variables from several relevant studies for both Northern Canada in general and the Yukon in particular to gain a qualitative understanding of the potential impacts of climate change on flood hazard in the study areas from the present day to 2100.

For changes in temperature in Northern Canada, Chapter 8 - Changes in Canada's Regions in a National and Global Context of the Canada's Changing Climate Report (Bush and Lemmen, 2019) states that the "*annual mean temperature has increased by 2.3°C from 1948 to 2016, roughly three times the warming rate of global mean temperature. This increase has been strongest during winter (4.3°C), and weakest during summer (1.6°C), over the same time period."* In addition, the annual mean temperature for Canada's North is projected to increase up to 2.7°C for the period of 2031–2050 and up to 7.8°C for 2081–2100 with a high emission scenario (RCP8.5); all values are relative to the 1986–2005 mean value. Data from the Watson Lake station, located near the study site, shows an average increase of 1.7 ^{o}C over the last 64 years (1950-2013). This is consistent with the analysis from Perrin and Jolkowski (2022), which shows an average increase of 2^{0}C in the Yukon.

For long-term changes in total precipitation over Northern Canada, Bush and Lemmen (2019) mentioned that they are difficult to accurately quantify because of the sparse observing network. Nonetheless, "*all available sites in the region reveal large percentage increases in precipitation, both annual and seasonal, with precipitation having increased in every season*". Particularly, "*during the summer, snowfall has decreased and is being replaced by rain. However, on an annual basis, snowfall has increased, since total precipitation has increased and temperatures during the cold part of the year are still low enough for precipitation to fall as snow*". Furthermore, *"in association with warming temperatures and resulting changes to snow and permafrost, winter streamflows have increased, and the timing of spring freshet has shifted earlier."* Hence, it is expected that *"precipitation is projected to increase in all seasons, and daily extreme precipitation is also projected to increase"* with high confidence based on the results of multiple climate models and can also be explained by the expected increase in atmospheric moisture induced by warming. In association with these increases, *"annual streamflow in the North is also projected to increase, along with continuing earlier spring freshets due to rising temperatures"* (Bush and Lemmen, 2019).

For the Yukon specifically, the Climate Change Adaptation Plan – 2024 Summary Report from Yukon Energy (2024) states that, in the last 50 years, Yukon's average temperatures and rainfall have both increased, and climate change events are becoming more frequent and intense, particularly in the North. To arrive at the conclusion, Yukon Energy utilized the climate change models and results developed by leading Canadian climate scientists to understand impacts of climate change on the two weather parameters of interest: temperature and precipitation.

- *"Over the last 50 years, temperature in the territory has increased by 2 °C with winter temperatures warming more significantly than summer temperatures. Climate models predict continued temperature increase over the next 50 years with estimates of temperature increases between 0.7 and 3.7 °C. Most of this temperature increase is predicted to occur in winter months."*

- *"Over the past 50 years, precipitation has increased around 3 to 12%, mostly in summer months, and this trend is continuing. Climate models predict precipitation will increase by 4 to 17% over the next 50 years. The degree to which precipitation is changing in the territory depends on the geographic region."*

In addition to the upward trends in the historic and projected temperature and precipitation, the variability of the Yukon climate is also expected to increase according to the report from Yukon University (Perrin and Jolkowski, 2022). This will mean an increase in extreme weather events and greater fluctuations in precipitation. The report also states that *"climate change is affecting and will continue to affect the hydrological regime"* as various hydrological processes such

as glacial melt, permafrost thaw, snowmelt and so on are driven by changes in temperature and precipitation. As a consequence, *"flood risk is expected to increase in some locations in the Yukon, while it may decrease in others"*.

The Government of Yukon (2022), in their report Assessing Climate Change - Risk And Resilience in the Yukon, also points out various potential impacts due to more frequent extreme weather events associated with climate change on flood hazards, such as: flooding in communities is more frequent and severe; extreme winter precipitation leads to transportation interruptions or failures; extreme precipitation increases the erosion of and damage to riverbanks; extreme precipitation and flash flooding cause physical and chemical instability at mine sites, and so on.

Effects of climate change impacts on the Liard River basin are analyzed in Shrestha et al. (2019) using the Variable Infiltration Capacity hydrologic model and the multivariate bias correction/downscaling climate change dataset of RCP 4.5 and 8.5 available at 1/16° gridded resolution. The results showed that for temperature changes, the *"ensemble median annual temperature increasing from −2.4°C in 1976–2005 to about +0.9°C (RCP4.5) and +3.7°C (RCP8.5) by the end of century (2071–2100)"*. For precipitation changes, *"strong precipitation increases are projected in the basin under both RCPs, with annual increases for the GCMs ranging from +4% to +18% for RCP4.5 and from +9% to +30% for RCP8.5 (2080s versus 1976–2005)"*. For streamflow changes, *"the projected increases in monthly and annual mean flows by the end of century (2080s) compared to the baseline period for the subbasins of the Liard River basin are consistent with the higher precipitation input to the basin"*. In addition, *"the annual maximum flow Q_{max}, which occurs primarily as a result of snowmelt, is projected to increase in 2080s for most GCM ensemble members"*. The results also indicate that *"mechanisms other than snowpack storage, such as rainfall and possibly rain-on-snow, play increasingly important roles in the generation of future Q_{max}"*. For change in timing of Qmax, the authors state that *"a generally consistent pattern of progressively earlier Q_{max} timing emerges with greater warming scenarios. Specifically, compared to the historical period, the median timings are projected to shift by about 10 days under RCP4.5 and a further 10 days under RCP8.5."*

With the increased climate variability associated with climate change, a rain on snow event like 2012 is likely to occur again. As climate change continues to drive more extreme weather, the frequency and magnitude of peak water level on the Liard River is likely to change (Government of Yukon, 2025). The next section presents in detail the methodology used to investigate the effects of climate change impacts on flooding at Upper Liard.

4.2 Methodology

The methodology used for studying climate change impacts on flood hazards in this study follows the seven steps described in Table 4-1 and is presented as a flowchart in Figure 4-1. In particular, the multivariate-downscaled precipitation and temperature data series (CanDCS-M6) of the emission scenario SSP5-8.5 from ten selected global climate models presented in Table 4-2 were obtained for four locations corresponding to the four meteorological stations used in the hydrologic simulation described in Section 4.3. For each station and each model, 3 daily time series of precipitation, maximum and minimum temperatures were obtained. As a result, for all 4 climate stations and 10 GCMs, a total of 120 daily time series were obtained to assess the climate change impacts using the ensemble approach.

For the hydrologic simulation, the Raven software developed by the University of Waterloo (Craig et al., 2020) was used to simulate the hydrologic processes in the Upper Liard watershed. Details of the Raven model and the validation are presented in Section 4.3.

The validated Raven model was then used to study climate change impacts on daily stream flow using 10 projected climate data series (corresponding to the SSP8.5 emission scenario) for each run. Note that the PCIC data are available at a regional scale (i.e. each grid cell) of approximately 6 x 10 km. However, the Raven model is built using inputs at weather stations. Therefore, the series were extracted at the locations corresponding to the meteorological

stations used in the hydrological model (see section 4.3.2). To do so, a scaling factor of precipitation was used to transfer this regional value (i.e. grid cell) to each station (i.e. point data). The scaling factor was computed based on the observed, long-term, multiple-year mean value so that precipitation for the historical period of the model inputs matched as much as possible observed precipitation at the stations. Calculation of the scaling factor also acted as a good check to verify the consistency between different downscaled GCM datasets and to assess how similar the downscaled GCM data is to reproduce one of the important statistics (i.e. the mean) of the station data. In addition, Raven also requires the projected mean temperature series which is not directly available for download from PCIC. This series is therefore derived by averaging the projected maximum and minimum temperature series.

The annual maximum peak discharges were then extracted for three different timeframes, including: (i) historical reference period from 1986-2015, (ii) mid-century period from 2041-2070, and (iii) end of century from 2071-2100. Flood frequency analyses of different AEPs were conducted for these timeframes respectively using the same frequency distribution model selected for the single-station frequency analysis presented in Section 2.3 above. The relative changes (%) between the historic (reference) period and projected periods were computed for each AEP as follows:

$$Relative\ change\ (\%) = \frac{Design\ flow(Projected\ period) - Design\ flow(Baseline\ period)}{Design\ flow(Baseline\ period)} \times 100\% \qquad (1)$$

A positive value of relative change (%) signifies an increase in the design flow of an AEP of interest compared to that of the reference period. The median value of the relative change (%) based on the ensemble of 10 model results was retained as the change in the design flow due to climate change. These values were applied to the original single-station flood frequency analysis of observed data at station 10AA001 presented in Section 2.3 above and were used for mapping the flood hazards for different AEPs of interest.

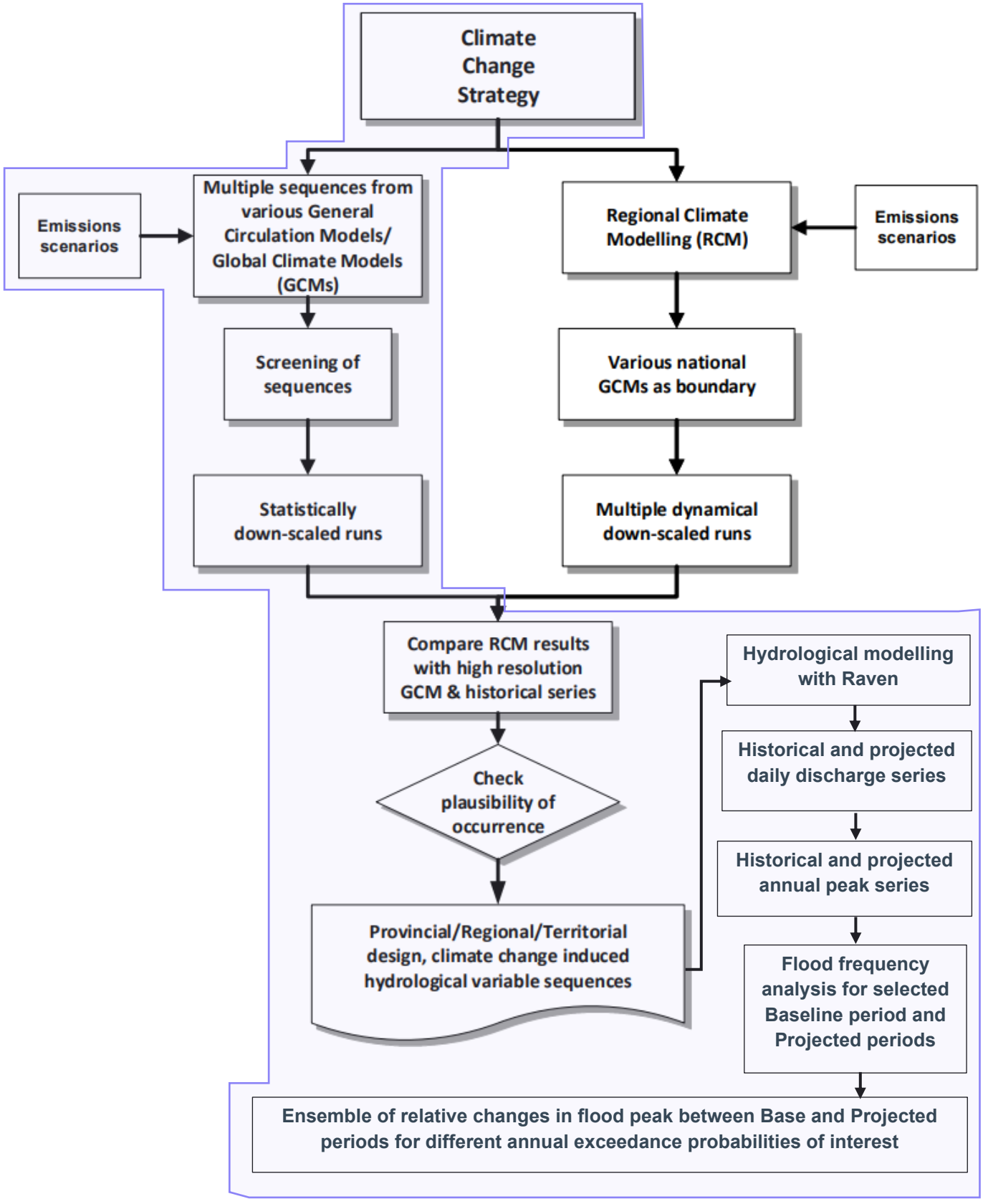

Figure 4-1 – Climate Change Impact Assessment Approach (Adopted from NRCan, 2023)

4.3 Climate Change Impact on Flood Hazards

4.3.1 PCIC Downscaled Climate Projections

In this section, an example of the SSP5-8.5 downscaled projected precipitation and maximum temperature series obtained from PCIC for the BCC-CSM2-MR model are presented for the four locations (i.e., Dease Lake, Hour Lake, Tuchitua, and Watson Lake) in the study region (see Figure 4-2 and Figure 4-3). In general, with this model and this emission scenario, it can be seen from the graphs that both the precipitation and temperature are showing increasing trends, especially for the period between 2050-2100. This is in line with the main findings of climate change impacts on Northern Canada and the Yukon from previous studies presented in Section 4.1 above.

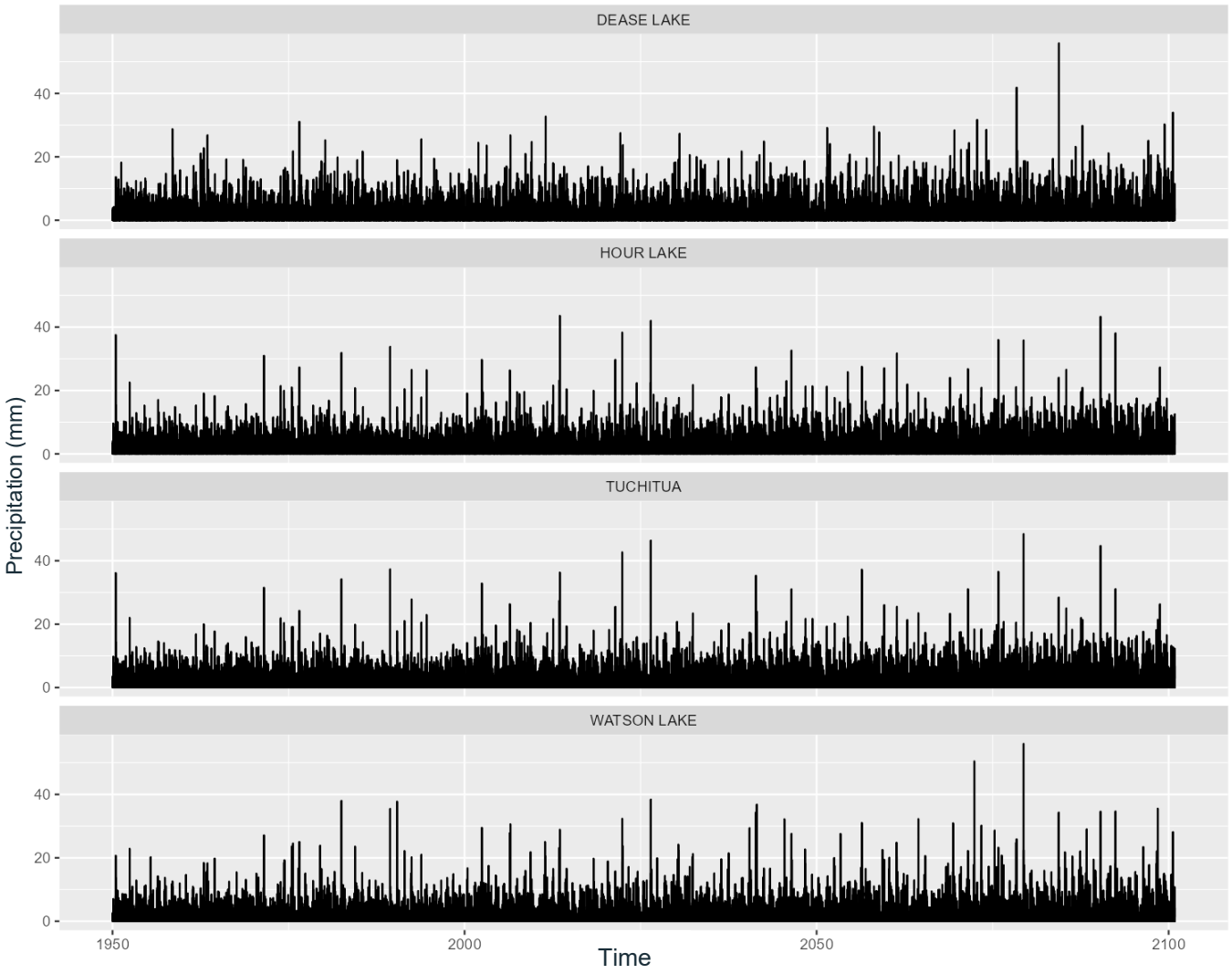

Figure 4-2 – Example of PCIC SSP5-8.5 Downscaled Precipitation Series from BCC-CSM2-MR Model

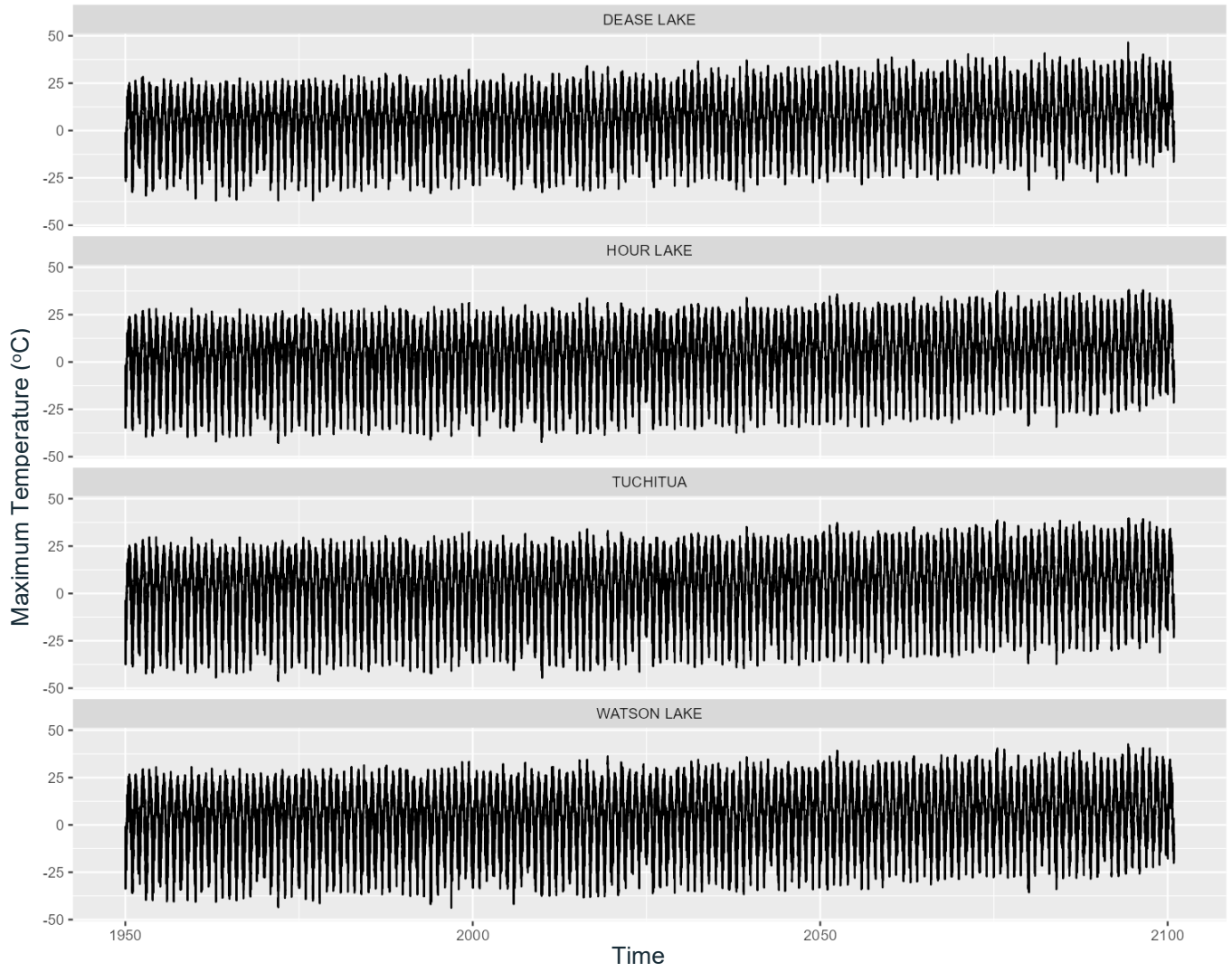

Figure 4-3 – Example of PCIC SSP5-8.5 Downscaled Maximum Temperature Series from BCC-CSM2-MR Model

Note that the downscaled precipitation series downloaded directly from PCIC are available at a grid-cell resolution of approximately 6 x 10 km. To adjust this series for a station of interest located within the same grid-cell, it is multiplied by the scaling factors presented in Figure 4-4 below. The scaling factor is the ratio of the mean of observed daily data available between the period of 1960-2014 at a specific station to the mean of the downscaled data over the same period and length. In general, the scaling factors are consistent among these downscaled GCM data and close to 1. The simulated mean precipitation series is well captured for Hour Lake, Watson Lake, and Tuchitua with less than 5% difference, but about 10% higher for Dease Lake.

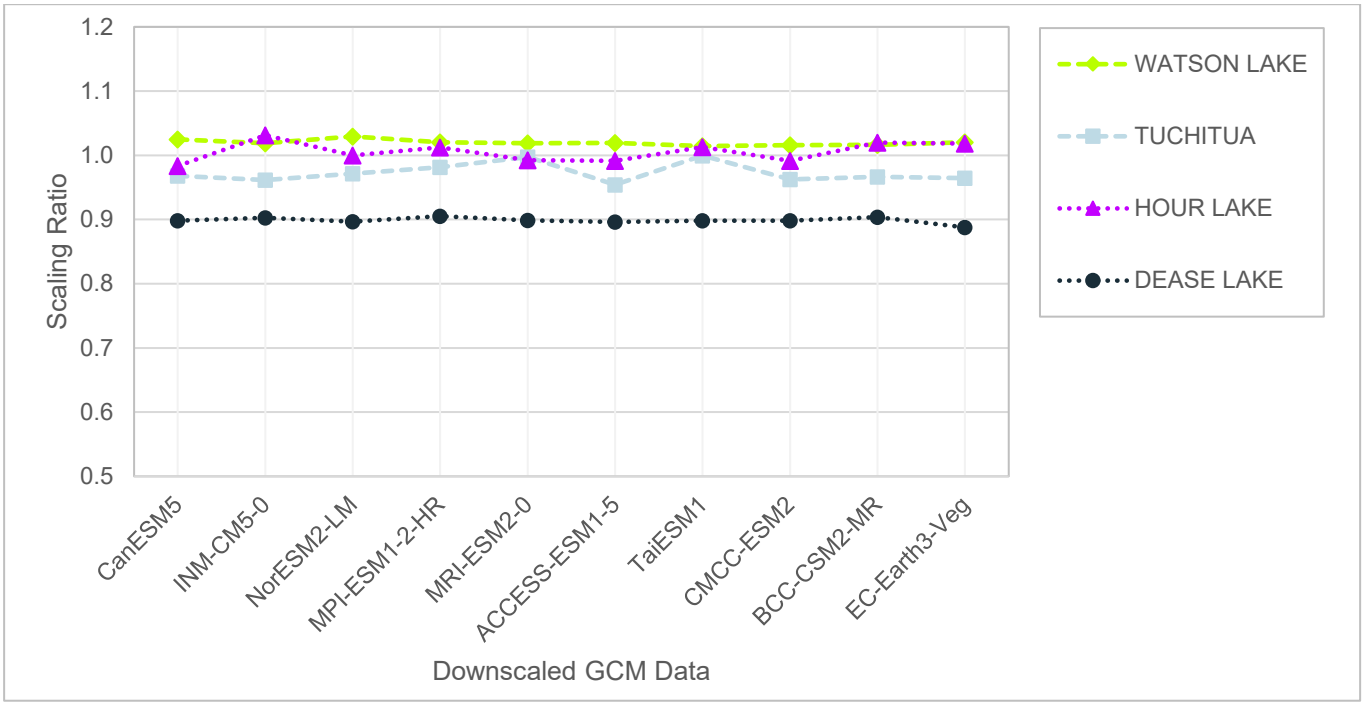

Figure 4-4 –Scaling Ratios for Adjusting the Downscaled GCM Precipitation Series

4.3.2 Hydrological Modelling Using Raven Software

Extensive hydrological modelling of the Liard River was undertaken by researchers at the University of Waterloo using Raven, a hydrological modelling software (Craig et al., 2020). The calibration process and results are presented in their 2020 publication titled "*Structural calibration of a semi-distributed hydrological model of the Liard River basin*" (Brown and Craig, 2020). Model files are available online as the final example project for the open-source Raven model.

Raven offers a flexible framework supporting a wide range of modelling options. The software is based on a distinct discretization method, where sub-watersheds are made of *Hydrological Response Units* (HRUs), relatively homogeneous land parcels with a unique hydrologic signature. The Liard River model is a continuous model, where the complete annual hydrologic cycle of snow accumulation and snowmelt is represented. The complete model schematic is presented in Figure 4-5.

The Raven model was used to assess the impact of climate change and change in land cover on flood hazards, following the methodology outlined below:

1. The complete Liard River model was trimmed down so the downstream limit of the model corresponds to Station 10AA001 – Liard River at Upper Crossing. The trimmed-down model allows for faster runtimes.

2. The model calibration was further validated by extending the modelled period to cover the most severe event on record at Station 10AA001 – Liard River at Upper Crossing (see section 4.3.3).

3. The model was used to model historical and future climate scenarios based on downscaled climate modelling results (see section 4.3.4).

4. The model was used to assess the impact of a change in land cover on flood hazard (see section 4.4).

The trimmed-down model schematic is presented in Figure **4-5**.

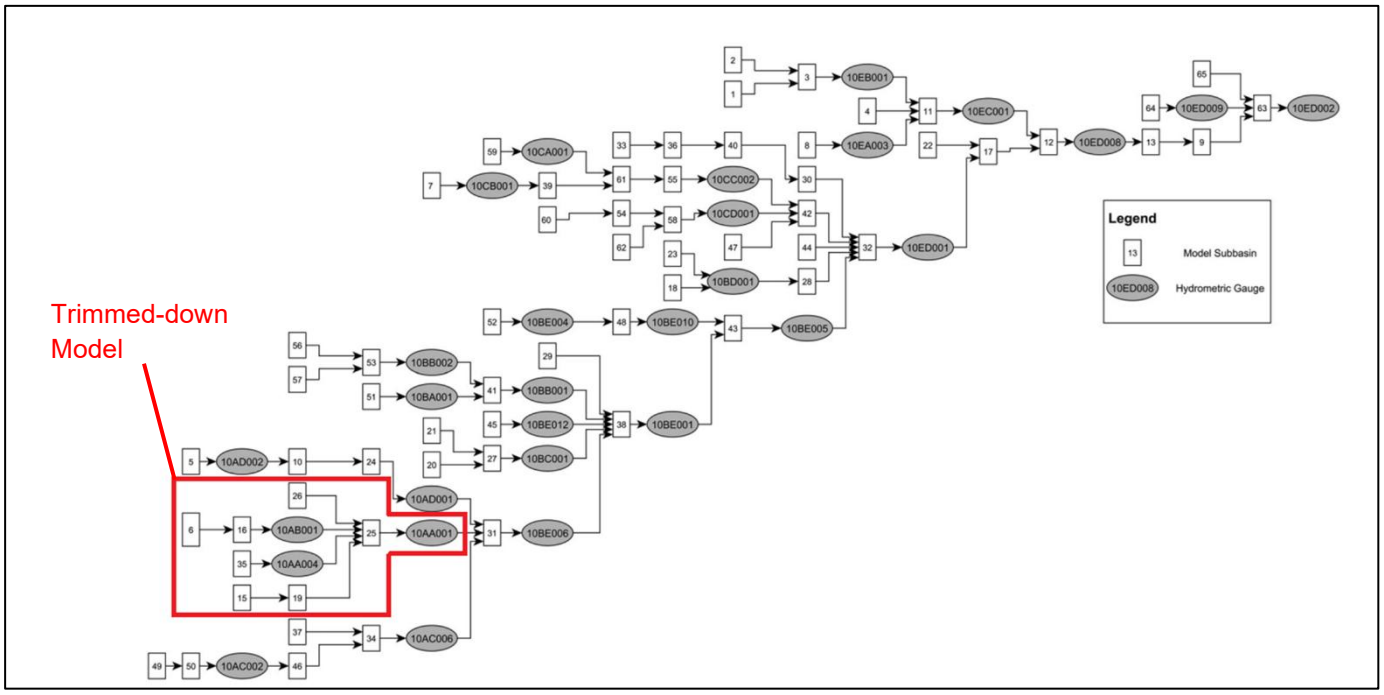

Figure 4-5 – Original and Trimmed-down Liard River Raven Model Schematic

The trimmed-down version of the model is influenced by data from only four climate stations. Their climate identifiers (ID), names, coordinates, and elevations extracted from Environment and Climate Change Canada (ECCC, 2025) are listed in Table 4-3. The corresponding station IDs utilized for the description of the *.rvt files of the Raven model are also provided.

Table 4-3 – Climate Stations used in the Trimmed-down model

CLIMATE ID	STATION ID	NAME	LATITUDE (°)	LONGITUDE (°)	ELEVATION (m)
1192340	1454	DEASE LAKE	58.43	-130.01	806.6
2100FCG	1511	HOUR LAKE	61.18	-129.13	890.0
2101135	1613	TUTCHITA	60.93	-129.22	723.9
2101200	1615	WATSON LAKE A	60.12	-128.82	687.4

4.3.3 Model Validation

The 2020 publication presented calibration and validation results from 1986 to 2005. The modelling period was extended to 2014, the main objective being to capture the June 2012 flood, the most severe event on record at Station 10AA001 – Liard River at Upper Crossing. This additional period was already covered in the input data forcing files

made available by the Raven team (*.RVT). These inputs files were reviewed to ensure that they were coherent with published data at the climate stations. Figure 4-6 shows a comparison between the modelling results and observations at Station 10AA001 – Liard River at Upper Crossing.

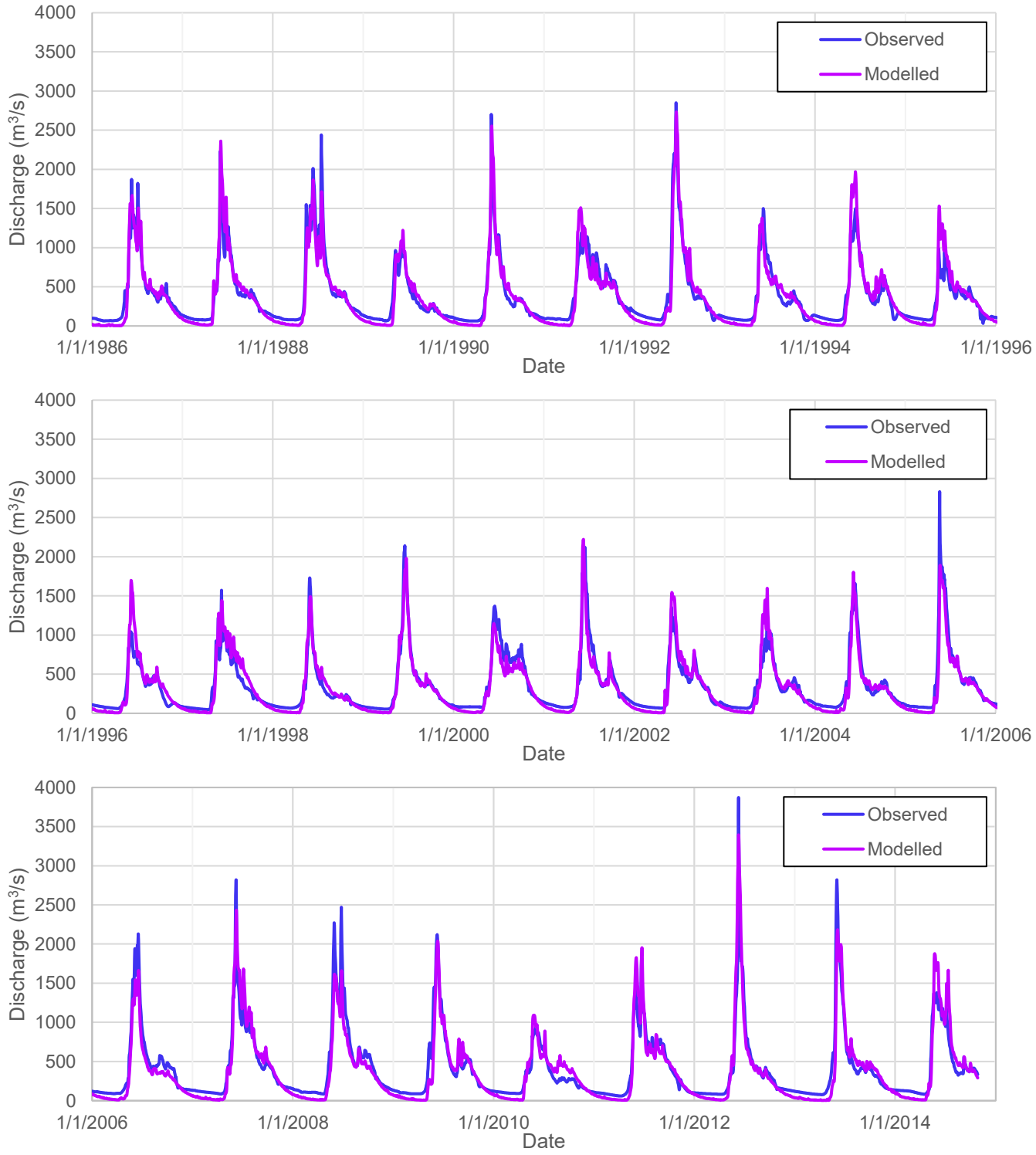

Figure 4-6 – Liard River Trimmed-down Raven Model Validation Results

The goodness-of-fit was assessed using the Nash-Sutcliffe criteria:

$$NSE = 1 - \frac{\sum_{t=1}^{T}(Q_0^t - Q_m^t)^2}{\sum_{t=1}^{T}(Q_0^t - \bar{Q}_0)^2} \quad (2)$$

where :

$\bar{Q}_0$ = Average observed discharge; Q_m^t = Modelled discharge at time t; and Q_0^t = Observed discharge at time t.

The Nash-Sutcliffe criteria calculated over the complete modelled period is 0.90, showing a generally excellent fit between observed and modelled discharge values. Freshet and peak flood timing is very well represented. The timing of the recession is generally well represented, but baseflow values are underestimated during the summer months.

Annual peak flows, however, are underestimated for the six most severe events. The 2012 peak discharge, the highest on record, is underestimated by 12% (3 394 vs 3 870 m^3/s). While these results undermine the confidence in the model regarding the absolute value of peak discharge estimates, the model is deemed adequate for the present study purpose, which is to identify the directionality and the order of magnitude of the impact of climate change on peak flow values associated with given AEPs.

4.3.4 Future Climate Hydrological Modelling

To assess the impact on stream flow, the downscaled projection precipitation and temperature series from different climate models were injected into the validated Raven model. Each run/simulation spans the full available time series (1950-2100).

Figure 4-7 shows an example of the simulated daily flow series obtained using downscaled data from the BCC-CSM2-MR model. Note that the simulated results for the historical reference period (1986-2015) do not always match the observed data. This is to be expected, as a difficulty to precisely represent historical climate is a known limitation of downscaled climate models. The objective of the modelling being the identification of climate trends, each projected period output is compared to the reference period results obtained with the same climate model.

Projected results obtained with each climate series generally show the same trends:

- A general increase in the annual runoff volume
- An earlier freshet
- An earlier date of occurrence of the peak discharge
- A general increase in peak annual flows

These trends are illustrated in Figure 4-8, which shows the average discharge modelled over the reference period and the end-century period obtained using downscaled data from the BCC-CSM2-MR model.

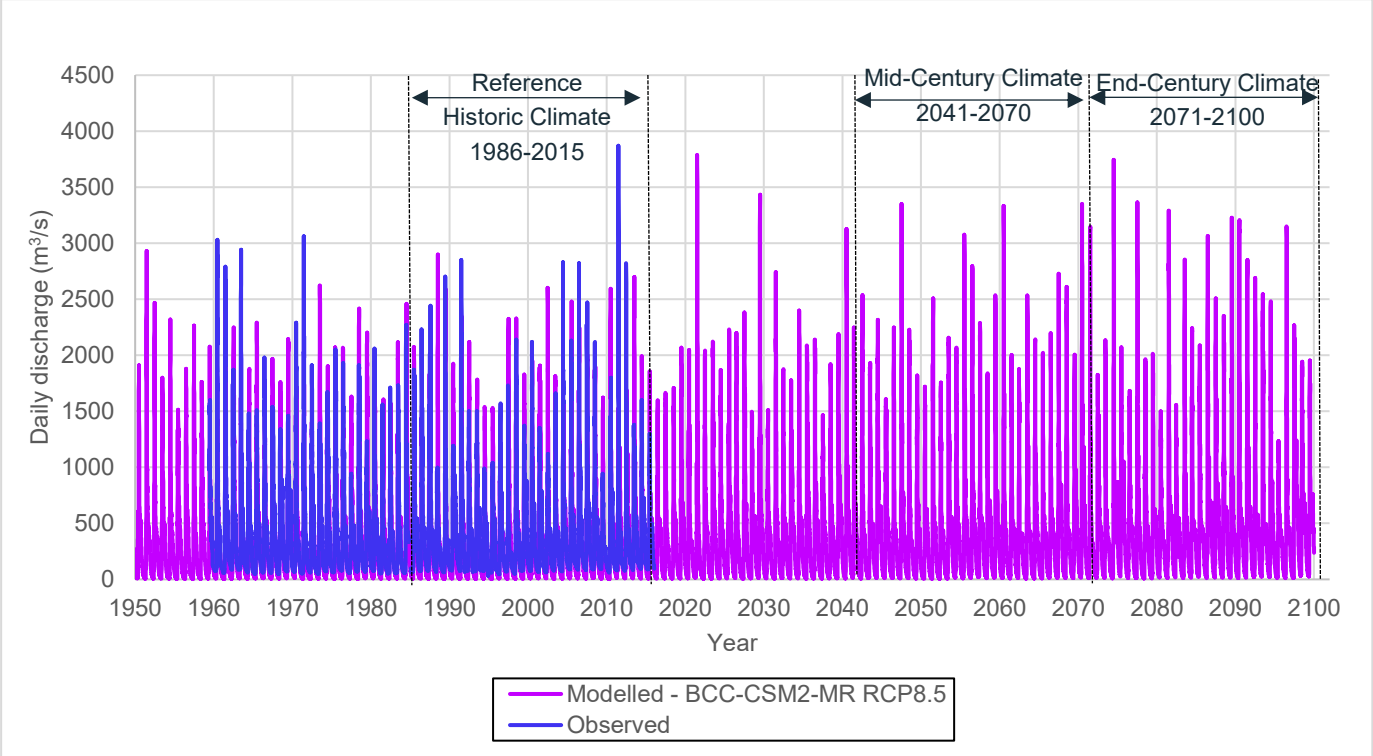

Figure 4-7 – Example of Simulated Daily Flow Series Using Downscaled BCC-CSM2-MR RCP8.5 Model Data

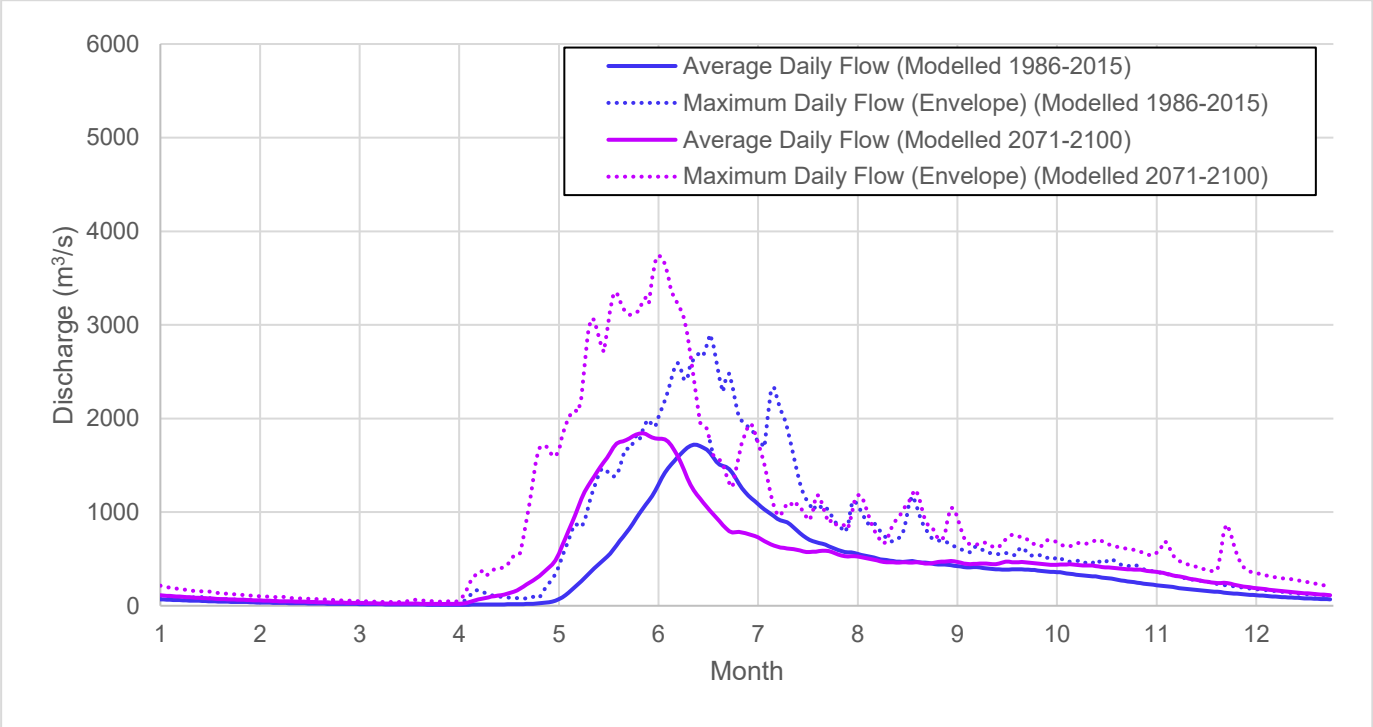

Figure 4-8 – Example of Average and Maximum Envelope Flow Modelled for the Historical (1986-2015) and End-Century (2071-2100) Periods Using Downscaled BCC-CSM2-MR RCP8.5 Model Data

4.3.5 Design Flow Change Considering Climate Change Impacts

The simulated annual peak flow series were extracted for the flood frequency analysis corresponding to three different timeframes: (i) Reference 1986-2015, (ii) Mid-Century 2041-2070, and (iii) End-Century 2071-2100. The same flood frequency analysis procedure was carried out for each data series. The resulting envelopes of all 10 downscaled GCMs are presented in Figure 4-9 for all three timeframes for comparison. It can be seen from the graph that the estimated design flows vary significantly between the 10 downscaled GCMs. Even for the historical (reference) period, the results are not consistent between these downscaled GCM models. In addition, there is a wide range of uncertainty in the estimation of design flow for each period. The uncertainty is much higher (i.e., a much wider interval) for the projected periods compared to that of the reference period.

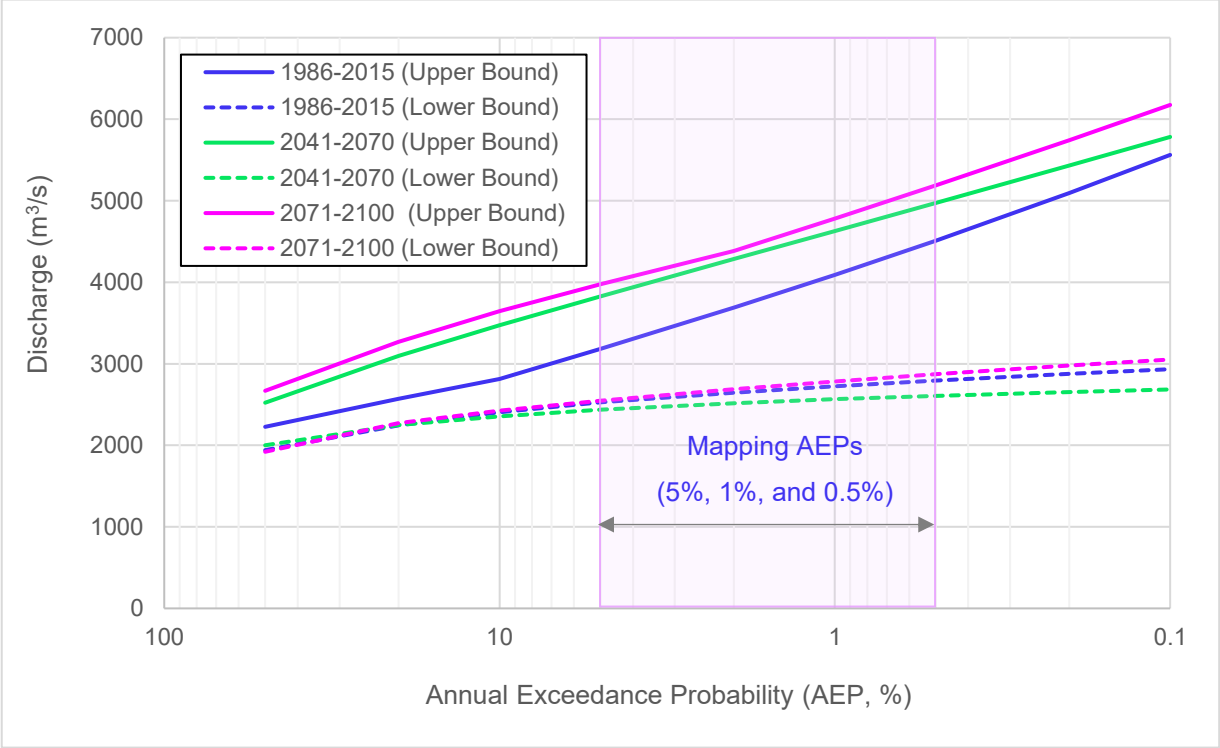

Figure 4-9 – Comparison of the Envelopes of the Flood Frequency Analysis Results for the Reference and Projected Periods

To compute the change in design flow for different periods and for each GCM, Equation (1) described in Section 4.2 was used. The results of relative change between the historic and the mid-century as well as the end-century periods are presented in Table 4-4 and Table 4-5 respectively.

It can be seen from the ensemble results of 10 models that, for the mapping AEPs, the relative change (%) in the design flow can be negative (i.e. a reduction of the design flow), can be close to zero (nothing changes in the design flow), or can be very positive (i.e. a significant increase of the design flow). For the difference between the historic and mid-century periods, the relative changes are between -18 to 32% for the 5% AEP, -23 to 40% for the 1% AEP, and -25 to 44% for the 0.5% AEP. For the end-century period, the corresponding ranges are -4 to 35%, 0 to 38%, and -1 to 39%, respectively.

Table 4-4 – Relative Change (%) between Historic (1986-2015) and Mid-Century (2041-2070) Periods

Annual Exceed. Prob. (%)	Downscaled GCM Data and Relative Change (%)									
	CanESM5	INM-CM5-0	NorESM2-LM	MPI-ESM1-2-HR	MRI-ESM2-0	ACESS-ESM1-5	Tai-ESM1	CMCC-ESM2	BCC-CSM2-MR	EC-Earth3-Veg
50	9.8	21.1	19.8	-7.0	22.5	1.3	2.1	-2.2	12.6	7.3
20	15.8	24.4	16.1	-12.6	14.4	9.6	7.2	5.9	12.9	7.9
10	19.2	27.9	12.8	-15.8	6.7	14.6	12.1	12.1	14.5	7.6
5	22.1	31.5	9.5	-18.5	-0.7	19.0	17.3	18.3	16.4	7.2
2	25.5	36.5	5.3	-21.5	-9.8	24.4	24.6	26.2	19.3	6.6
1	27.9	40.4	2.1	-23.5	-16.0	28.2	30.2	32.1	21.7	6.1
0.5	30.1	44.3	-0.9	-25.3	-21.7	31.7	36.1	37.9	24.1	5.5

Table 4-5 – Relative Change (%) between Historic (1986-2015) and End-Century (2071-2100) Periods

Annual Exceed. Prob. (%)	Relative Change (%) between Historic (1986-2015) and End-Century (2071-2100) Periods									
	CanESM5	INM-CM5-0	NorESM2-LM	MPI-ESM1-2-HR	MRI-ESM2-0	ACESS-ESM1-5	Tai-ESM1	CMCC-ESM2	BCC-CSM2-MR	EC-Earth3-Veg
50	22.8	28.1	27.2	-10.7	29.3	7.2	8.4	1.1	23.8	2.0
20	29.3	22.1	34.3	-8.5	26.1	13.0	13.0	7.6	28.2	1.2
10	32.2	18.4	35.6	-6.4	23.8	17.3	17.5	12.3	29.5	0.8
5	34.4	15.2	35.5	-4.2	21.6	21.3	22.3	16.7	30.0	0.4
2	36.7	11.4	34.1	-1.4	18.9	26.4	28.9	22.2	30.1	-0.1
1	38.1	8.8	32.6	0.8	16.9	30.1	34.0	26.1	30.0	-0.4
0.5	39.4	6.4	30.8	2.9	15.0	33.7	39.4	29.9	29.7	-0.6

The median value of the ensemble change (%) for both projected periods are computed in Table 4-6 and plotted on Figure 4-10a. It can be seen from the graph that both projected periods indicate a significant increase in the design flow for the three mapping AEPs. In particular, for the period of 2041-2070, the relative increases based on the ensemble-median value are approximately 17%, 25%, and 27%. Similarly, for the period of 2071-2100, the corresponding values are 22%, 28%, and 30%. Thus, the relative changes corresponding to the end-century period are between 3-5% higher than those of the mid-century timeframe for the mapping AEPs. In addition, the end-century (or late-century) period is also recommended for use in the Technical Guidelines for Flood Hazard Mapping Studies – Issued for 2025-26 from the Government of Newfoundland and Labrador (2025). Therefore, it was concluded that the relative change (%) based on the median value of the ensemble results of 10 GCM models using the SSP5-8.5 scenario for the end-century timeframe should be used for updating the design flow values considering the potential

impacts of climate change. Note that the whole procedure was also repeated for the same type of downscaled GCM data but of the SSP2-4.5 scenario. The median value of the ensemble change (%) for this scenario is presented in Figure 4-10b. The result indicates that the relative increase from this scenario is less significant than that of the SSP5-8.5 scenario.

Table 4-6 – Ensemble-Median Relative Change (%) of the Design Flows for Different AEPs and Periods

Timeframe and Relative Change (%)	Annual Exceedance Probability (AEP, %)						
	50	20	10	5	2	1	0.5
2041-2070	8.5	11.2	12.5	16.9	21.9	24.8	27.1
2071-2100	15.6	17.6	17.9	21.5	24.3	28.0	29.8

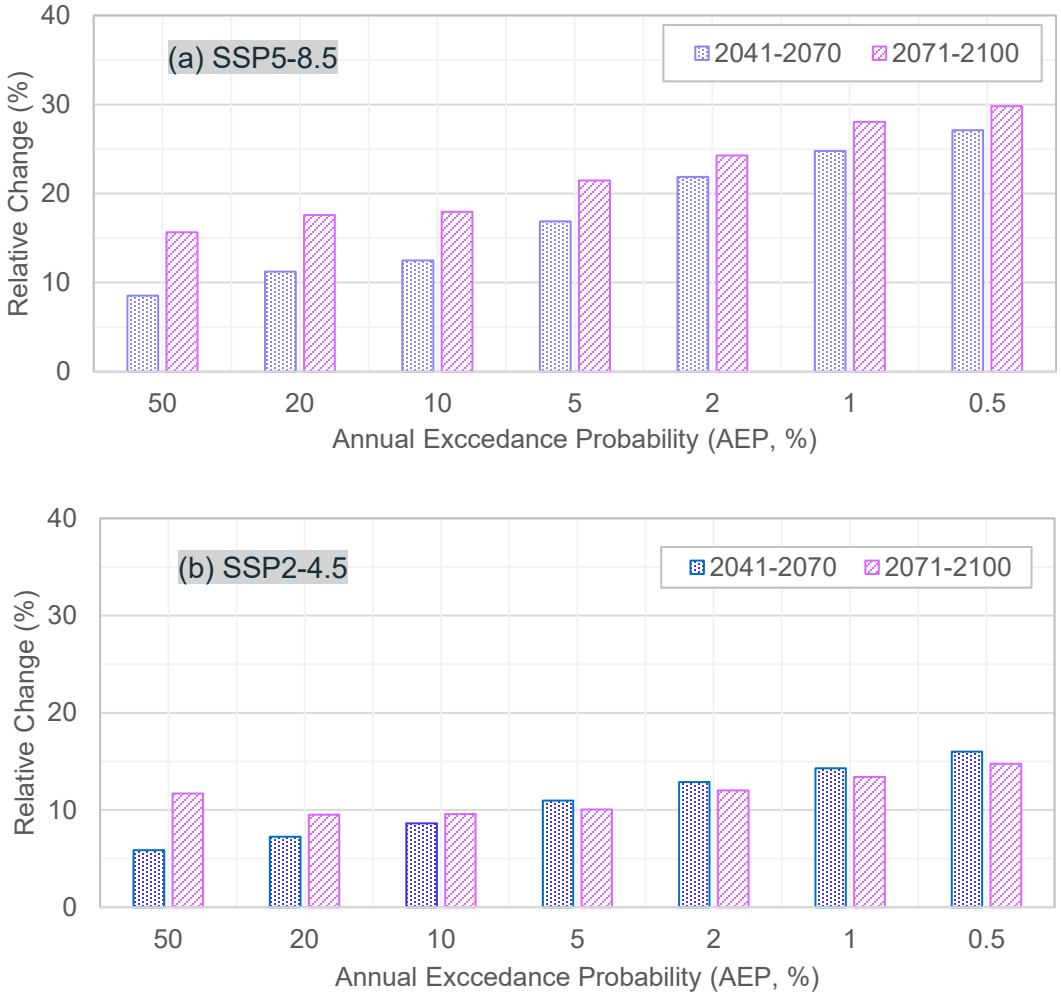

Figure 4-10 – Ensemble-Median Relative Change (%) of Design Flows for Different Projected Periods

4.4 Effect of Change to Land-Cover on Flood Hazards

Land-use and land-cover have a large impact on the hydrological processes at play over a watershed. For instance, land-cover can influence evapotranspiration rates, canopy storage, concentration time, infiltration rates, etc. Therefore, a significant change in land-use or land-cover can have an impact on the hydrological response of a catchment.

However, there is no clear justification for projecting a significant modification of the land-cover over the 32 600 km^2 catchment of the Liard River at Upper Crossing Station (10AA001) that could lead to an increase of flood hazards, as outlined below:

Anthropic Change in Land-Use

There is no significant urbanized area or arable land in the catchment. It is unlikely that future anthropic development (for instance urbanization) could significantly impact the land use over the 32 600 km^2 area.

Climate Change Impact on Wildfires

An increase in the number or magnitude of wildfires could lead to changes in land-cover. More frequent or larger burns could lead to a reduction of forested area, which could change the hydrological response of the watershed.

A study conducted by AECOM in 2021 (AECOM, 2021) for the Government of Yukon modelled the potential impact of climate change on wildfire risk. The assessment was done on two scales, a Yukon-wide scale and a regional scale. The Yukon wide assessment showed no projected increase in wildfire risk in the Yukon. While some indicators point to higher wildfire risk, such as a rise in temperatures, they are balanced by other indicators such as projected increases in precipitation and relative humidity. The regional assessments showed similar conclusions.

It is therefore not appropriate to assume a significant change in land-cover driven by an increase of the wildfire risk over the watershed.

Climate Change Impact on Permafrost

The watershed includes areas of both widespread and scattered permafrost. Permafrost areas are expected to recede due to climate change. The impact of permafrost thawing on the hydrological processes can be complex to assess (Walvoord, M.A., Barret, 2016). However, it is understood that permafrost is impermeable. Therefore, permafrost thawing is expected to increase the permeability of soil, which can lead to an increase in subsurface storage and a slower rain-runoff response. These changes would be associated with a potential reduction in flood hazard.

None of the elements listed above suggest a significant modification in land-cover that would lead to an increase of flood hazard. In addition, the magnitude of the potential impact of a modification of land-cover is dependant on the hydrological mechanism driving the flood hazard. Large, recorded floods at the study site are driven by the freshet. Therefore, the flood peak magnitude is more influenced by the snow cover and the melt rate than by the rain-runoff response of the basin. Therefore, it is assumed that the flood peak magnitude would not be very sensitive to a modification of the land-cover.

A sensitivity analysis was performed using the Raven hydrological model. The model relies on *Hydrological Response Units* (HRUs), which are defined in part by the nature of the land-cover. The validation period was re-run after modifying the land-cover type of random HRUs. The total area with the "Forest" classification was reduced by 10 points, and the area with the "Barren" classification was conversely increased, as shown in Figure 4-11. This is a very conservative representation of a significant deforestation of the watershed.

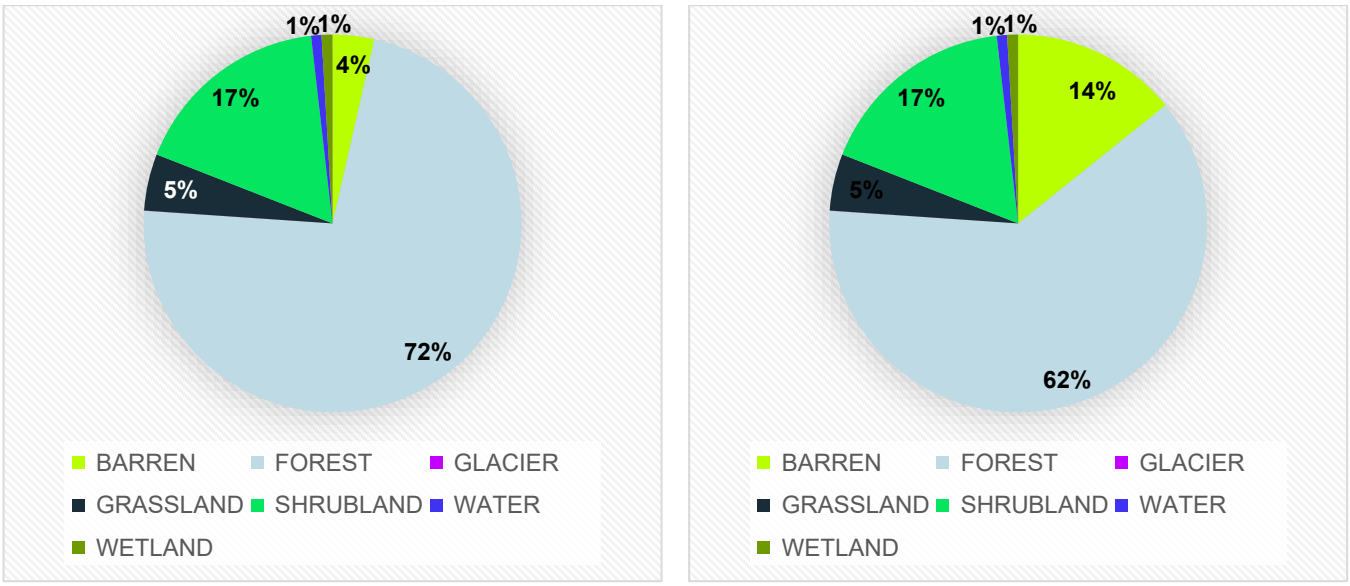

Figure 4-11 – Land Cover Sensitivity Analysis – Original (Left) and Modified (Right) Land Cover Distribution

Results show that such a modification to the land-cover would have a limited impact on flood peak discharges, with an average increase in the annual flood peak over the validation period of 6%.

Considering the limited justifications for projecting a significant modification of the land-cover and the limited sensitivity of the hydrological modelling to significant alteration of the land-cover, it is recommended not to increase the discharge of the mapped flood scenarios to account for future change in land-use and land-cover.

5. Fluvial Erosion Assessment

The study scope also included a qualitative Fluvial Erosion Hazard assessment. This assessment is presented separately as a technical memorandum in Appendix D.

The assessment shows that the study reach is characterized by a highly dynamic regime. Field observations, LiDAR analysis and historical imagery indicate that the river exhibits active lateral migration, significant bank erosion and ongoing floodplain reworking. The reach presents high erosion susceptibility, driven by non-cohesive bank materials and high stream power.

Following this assessment, the following recommendations were made:

- Conduct a detailed quantitative analysis to assess channel migration rates, bank erodibility, and sediment transport dynamics. This should include modelling under various hydrological scenarios to predict future channel adjustments and erosion hazards.
- Implement a long-term monitoring strategy to track morphological evolution and identify emerging erosion hotspots.
- Evaluate the need for targeted bank stabilization near critical infrastructure (bridge, houses), while considering nature-based solutions that maintain floodplain connectivity and hydrogeomorphic integrity.
- Integrate findings into land-use planning strategies for Upper Liard, particularly in areas adjacent to active meander bends and abandoned channels prone to reactivation during high flows.

6. Hydraulic Modelling

6.1 Digital Elevation Model

6.1.1 Topographic and Bathymetric Data Acquisition

To support the flood hazard assessment, McElhanney Ltd. conducted a LiDAR and aerial photography survey on August 2 and 8, 2024. The survey covered a low-relief valley near Watson Lake and included post-processing and quality control. The final deliverables—referenced to NAD83(CSRS) UTM Zone 9N and CGVD28-HTv2/CGVD2013 vertical datums—included classified LiDAR point clouds (bare-earth and non-bare-earth), key elevation points, an index map, and 20 cm-resolution RGB orthophotos in both tiled and mosaic formats. The average bare-earth point density was approximately 9.98 points/m², with a spacing of 0.32 m, providing sufficient detail for terrain analysis and flood modelling. These data were used by AtkinsRéalis to produce high-resolution elevation models for the present study.

To address gaps in bathymetric coverage, AtkinsRéalis conducted a complementary field survey from June 4 to 18, 2025. The survey collected bathymetric data over a 19 km stretch of the Liard River and topographic data along the riverbanks, including water levels, infrastructure, and high-water marks. Bathymetric data were acquired using a single beam echosounder (SBES) integrated with GNSS positioning and processed using Xylem Hypack and Qinertia software to ensure high positional accuracy. All data were referenced to NAD83(CSRS) UTM Zone 9 (epoch 2002) and CGVD2013. Deliverables included bathymetric and topographic datasets in CSV format, along with a technical report.

The extent of the LIDAR-derived DEM and the location of the bathymetric survey data are presented in Figure 6-1.

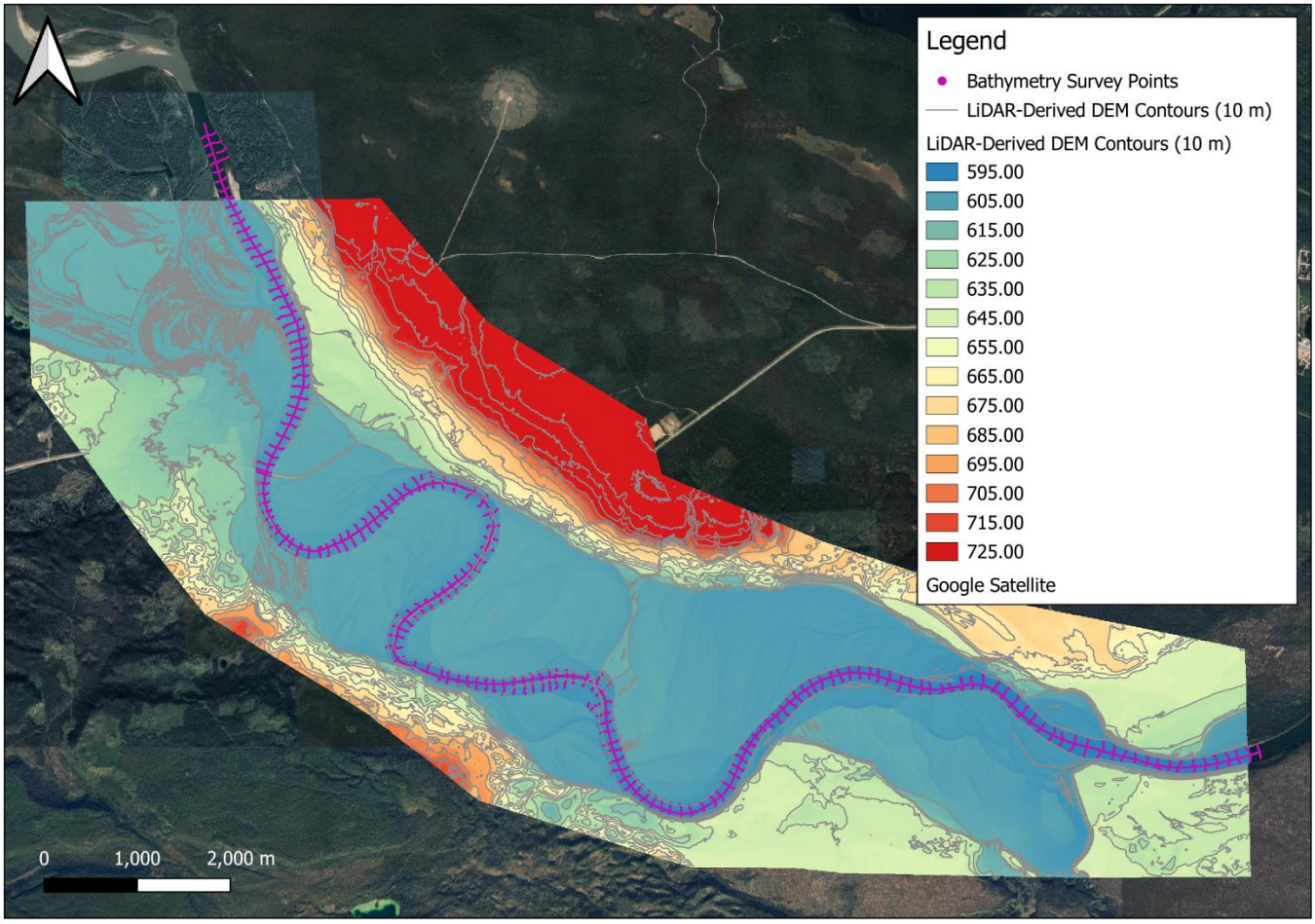

Figure 6-1 – Topographic and Bathymetric Datasets

6.1.2 Continuous DEM Generation for Hydraulic Modelling

To support 2D hydraulic modelling, a continuous digital elevation model (DEM) integrating both terrestrial and riverbed topography was developed for the Upper Liard study area. This seamless DEM is critical for accurately representing surface elevations across the floodplain and wetted channel, enabling reliable hydraulic analysis.

The terrestrial DEM was derived from LiDAR data, while bathymetric points were projected to EPSG:3156 (NAD83(CSRS) / UTM Zone 9N). To integrate these datasets, the wetted channel was first delineated and used to clip the LiDAR DEM, producing a land-only surface. Contour lines at 1 m intervals were generated from this surface and used, along with bathymetric points, to interpolate the riverbed using ESRI ArcMap's Topo to Raster tool.

During interpolation, artifacts such as unrealistic elevation gradients, abrupt transitions, and spurious depressions or peaks can occur—especially in areas with sparse bathymetric data, complex channel geometry, or where contour lines intersect irregularly. These artifacts can compromise the hydraulic model by misrepresenting flow paths, water surface profiles, and inundation extents. To address this, the initial interpolated raster was used to generate a new set of contours, which were manually reviewed and edited to remove anomalies and ensure topographic continuity.

A refined raster was then generated from the corrected contours and validated against surveyed bathymetric and topographic points to confirm accuracy. Finally, the interpolated channel DEM was clipped to the wetted extent and

merged with the LiDAR-derived land DEM, resulting in a seamless, continuous elevation surface. An example of the interpolation result is presented in Figure 6-2.

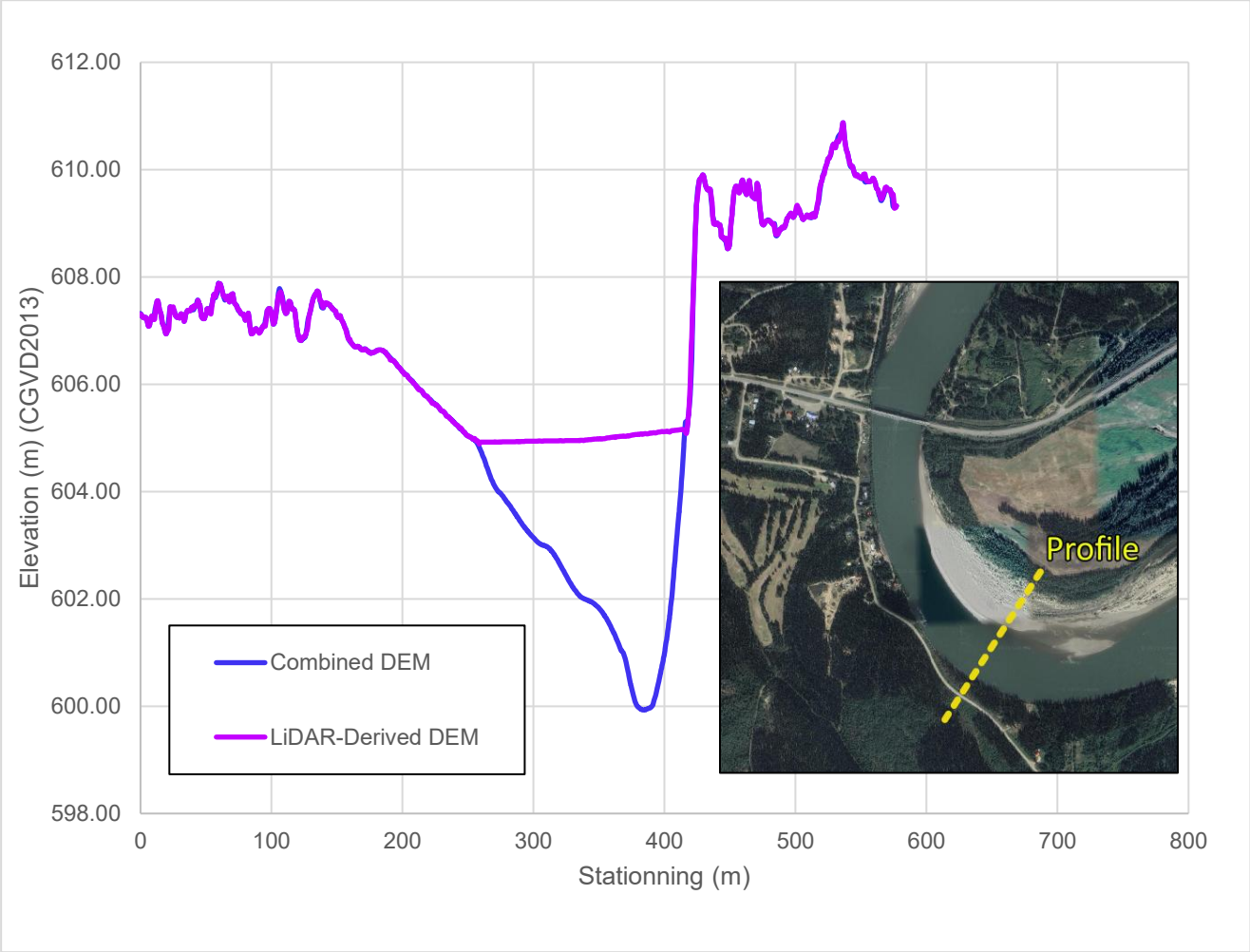

Figure 6-2 – Example of DEM Interpolation Results on a River Cross Section

6.2 Hydraulic Model

6.2.1 Model Development

6.2.1.1 Software

The hydraulic model was built using the software HEC-RAS (version 6.6), developed by the US Army Corps of Engineers (USACE, 2016). HEC-RAS is a computer program that models the hydraulics of water flow through natural rivers, and it is widely used to model flood events. Since the release, in 2016, of the version 5.0, HEC-RAS also provides a 2D modelling module. HEC-RAS 2D uses a Finite Volume Scheme to solve the two-dimensional Saint-Venant equations.

6.2.1.2 Model Extent and Boundary Conditions

The model extent is identical to the LiDAR elevation dataset extent, as shown in Figure 6-3. The upstream boundary condition is a fixed discharge, while the downstream boundary condition is a normal depth, calculated based on the provided energy slope (see section 6.2.2.1).

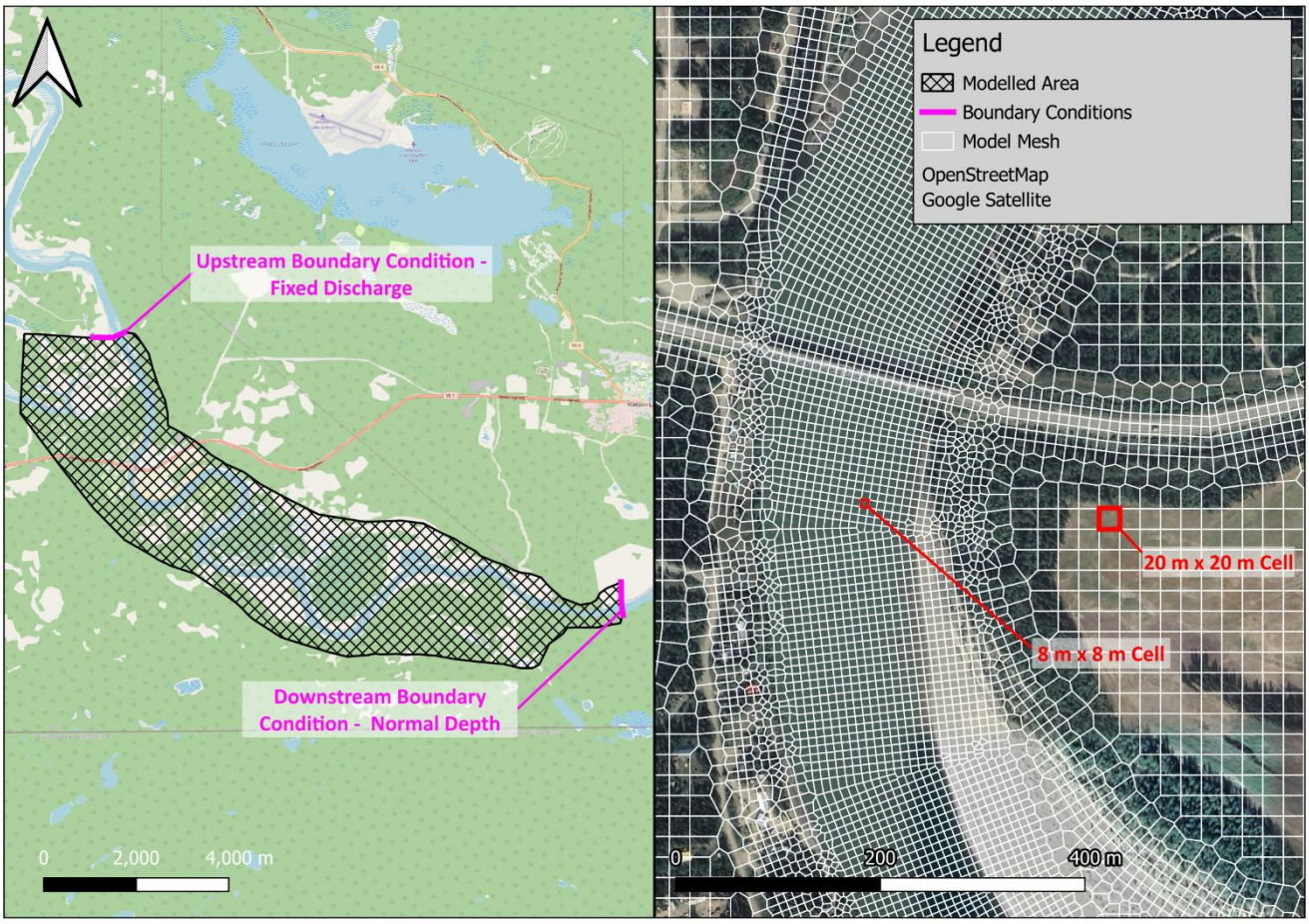

Figure 6-3 – Model Extent and Mesh Sample

6.2.1.3 Mesh

The model mesh is built using mostly square cells of different dimensions:

1. 8 x 8 meters over the riverbed, oriented in the direction of the flow.
2. 10 x 10 meters along roadways.
3. 20 x 20 meters over the floodplain,

Breaklines are used to align the mesh around sharp features terrain features, like roadways. The final mesh size was selected after performing a mesh independence analysis.

6.2.1.4 Hydraulic Structures

The Liard Crossing Bridge and the culverts under the Alaska Highway were modelled using a SA-2D Connection. The geometry of the bridge was modelled using available drawings and validated using survey data. The culverts were modelled based on surveyed dimensions.

6.2.2 Model Calibration and Validation

6.2.2.1 Calibration Parameters

Two model parameters were calibrated:

1. The roughness parameter (Manning's roughness).

2. The energy slope applied at the model's downstream boundary conditions.

The roughness parameter was calibrated over two distinct zones, the riverbed and the floodplain, as shown in Figure 6-4. This simplified approach was chosen over the use of a more detailed land cover map for the following reasons:

1. The floodplain land cover is relatively uniform, with heavy vegetation covering most of the modelled area.

2. The available land cover data, such as the 2020 Land Cover of Canada dataset published by Natural Resources Canada (NRC, 2022), does not provide a sufficiently precise representation of the land cover over the modelled area, with a large section of the area being unclassified.

3. The floodplain roughness being a critical calibration parameter, the use of a unified Manning's roughness value over the floodplain allowed for a more efficient calibration process.

The initial and final calibration parameters are presented in Table 6-1. Both final roughness parameters are in the range of expected values (Chow, 1959).

Table 6-1 – Initial and Final Calibration Parameters

Parameter	Initial Value	Final Value
Riverbed Roughness	0.035	0.030
Floodplain Roughness	0.080	0.180
Downstream Boundary Normal Depth Energy Slope (m/m)	0.0010	0.00028

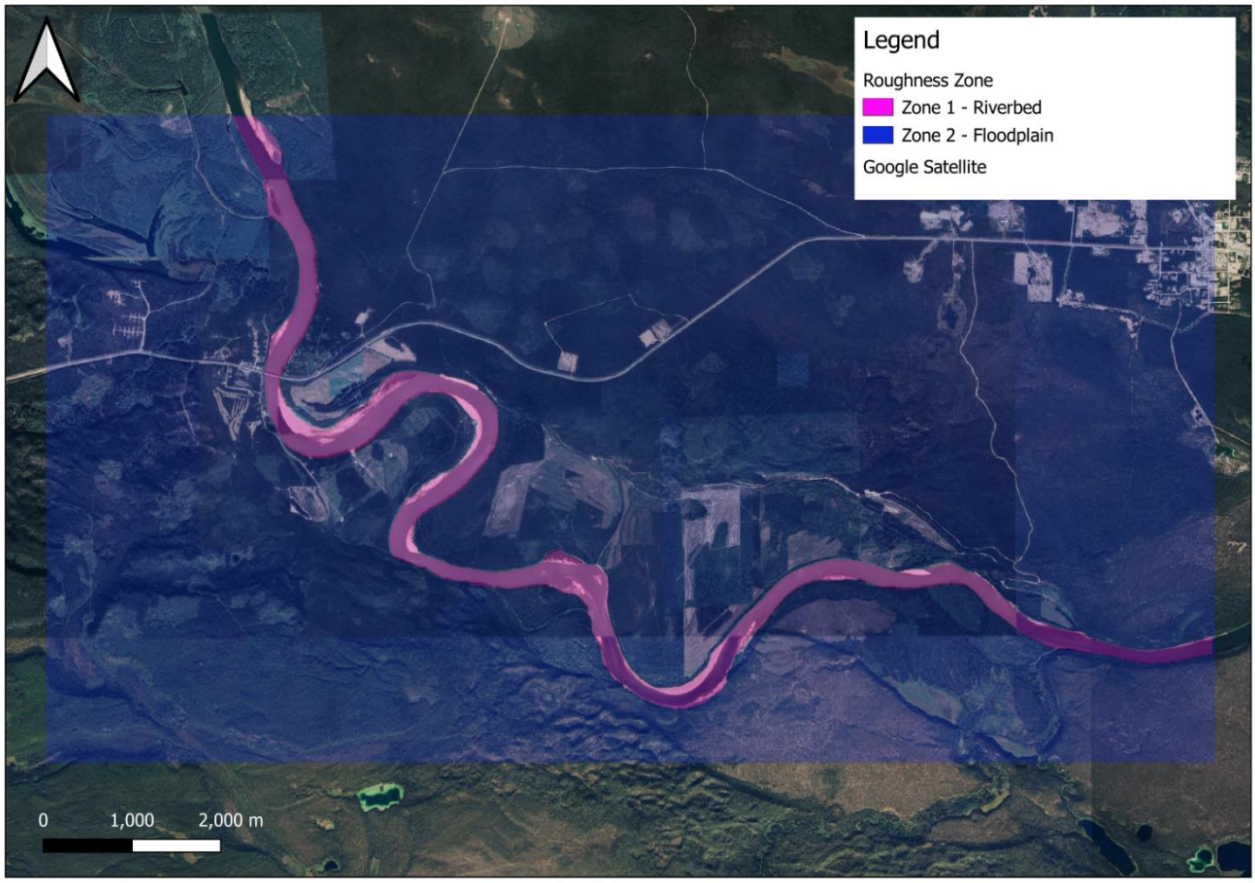

Figure 6-4 – Modelled Roughness Zones

Note that a flow roughness factor curve is also added to the model to be able to capture accurately the water level for flow values below 1500 m^3/s. The Manning's roughness factor is different from an absolute roughness value, which would be expressed using a unit of length (e.g. mm). It is expected that the Manning's roughness of the riverbed would be higher for lower flow depths, because of the ratio between the wetted perimeter and the flow section. The use of a roughness factor curve allows for the representation of the relationship between flow depth and the Manning's roughness parameter and is common for calibrating a model made to represent a large range of flow values (USACE, 2025).

Table 6-2 – Flow Roughness Factor

Parameter	Value					
Flow (m^3/s)	0	500	750	1000	1250	1500
Roughness Factor	1.17	1.17	1.13	1.10	1.03	1.00

6.2.2.2 Calibration – LiDAR Water Profile

The water surface profile captured by the 2024 LiDAR Survey was reproduced as part of the calibration process. While LiDAR does not directly capture the water surface, the interpolation of the lowest ground points captured next to the water allows for a generally good representation of the water surface.

This scenario allowed for a calibration over the complete modelled area and provided data at the downstream limit of the model.

The discharge at the time of the LiDAR survey was estimated by comparing water level measured by the LiDAR survey to the rating curve at Station 10AA001. This method provided a discharge of 450 m^3/s, which was used to model the flow conditions at the time of the survey. This discharge is coherent with the daily discharge published at Station 10AA001 for the day of the LiDAR survey (430 m^3/s on August 2, 2024).

Final modelling results with the calibrated model are presented in Figure 6-5. The fit between the modelled water profile and the profile captured by the LiDAR survey is good, with an average difference of 0.06 m and an average absolute difference of 0.09 m, sampling every 5 m. It should be noted that the LiDAR surface is noisy, which complicates the quantitative analysis of the goodness of fit. A moving-average water profile based on the LiDAR data (with a distance of 50 m and sampling every 50 m) is used to reduce the noise and to have a better visual comparison.

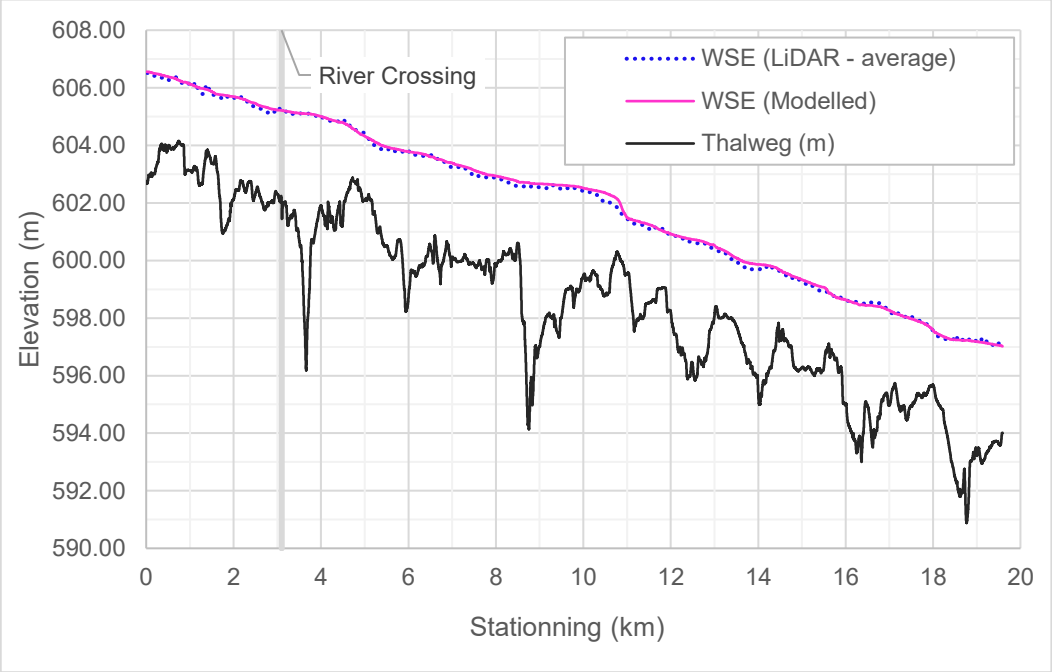

Figure 6-5 – Model Calibration Results – LiDAR Survey Water Profile

6.2.2.3 Calibration – Rating Curve at Station 10AA001

The model was also calibrated using the measured discharge values and water levels at Station 10AA001 - Liard River at Upper Crossing. All available published discharge values for open-water conditions were plotted against the water level data at the station to produce a discharge-water level relation (i.e., a rating curve). It should be noted that the resulting rating curve is distinct from the one published by WSC. While the station only provides water level at one location, the comparison of modeled levels with the rating curve extracted from the measurements allow for a calibration over the complete range of observed discharges. This reduces the risk of overfitting the calibration to a single event and increases the confidence in the predictive power of the model.

Figure 6-6 shows the modelling results for a wide range of discharges. The fit with the observed data is excellent for the entire curve, from low to very high discharges. For instance, the water level measured under the peak flow of the June 2012 flood is reproduced within 5 cm (i.e., 610.42 m as simulated vs. 610.47 m as observed).

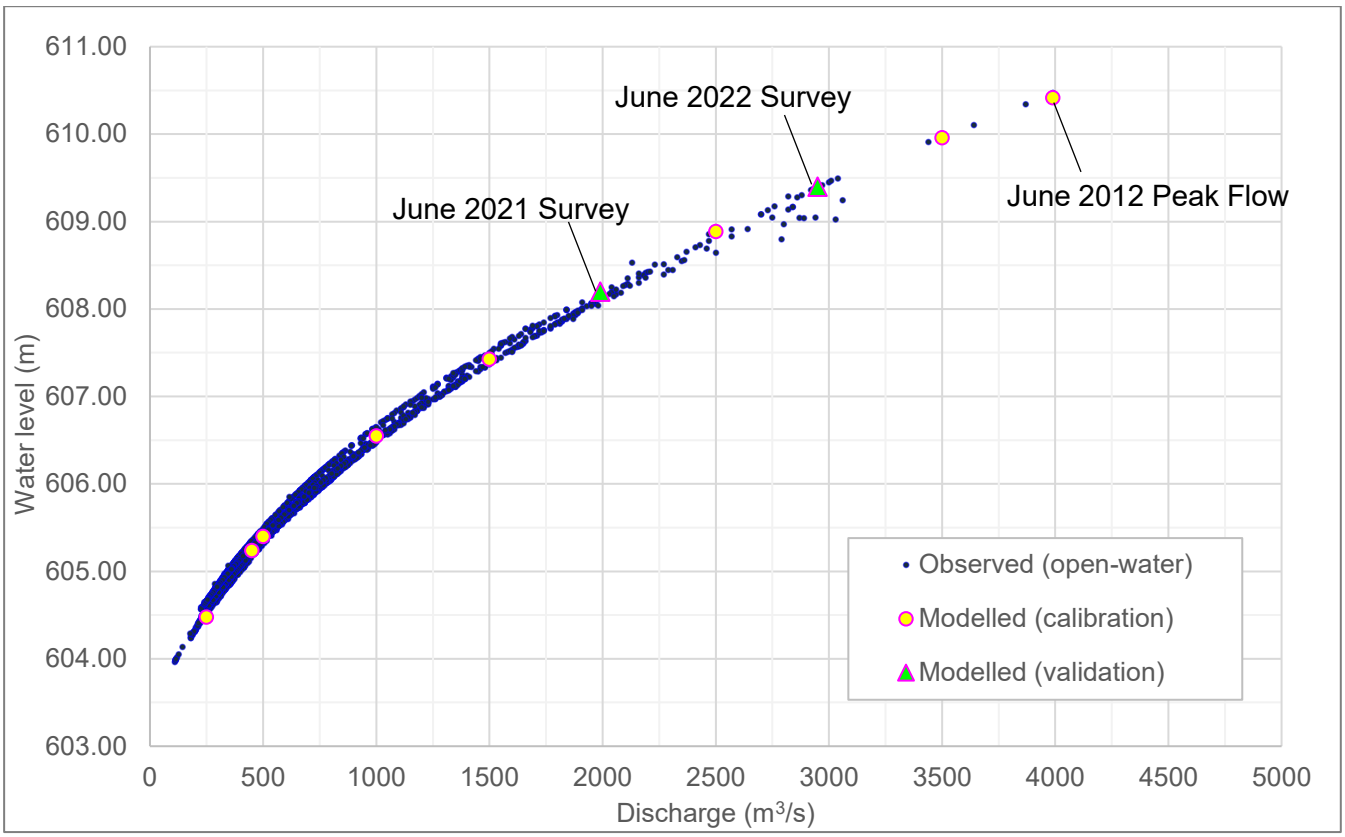

Figure 6-6 – Model Calibration Results – Rating Curve at Station 10AA001 Liard River at Upper Crossing

6.2.2.4 Validation – 2022 Flood Event

The water level on June 11, 2022, was surveyed at multiple points upstream and downstream of the Upper Liard crossing. Modelling results for the daily discharge measured on that day at Station 10AA001 (2950 m^3/s) were compared to the survey results, as summarized in Figure 6-7 and Table 6-3.

The model generally agrees with the measured water levels, with an average difference of 0.00 m. This is consistent with results presented in Figure 6-6.

The average absolute difference between modelled and surveyed data is 0.08 m. The root mean square error (RMSE) is 0.11 m. As shown in Figure 6-7 and Figure 6-8, these differences are fairly consistently distributed along the river reach, which shows that the model provides a good representation of the surface slope and does not miss any significant hydraulic controls in the surveyed area. The absolute maximum difference between modelled and surveyed data is 0.36 m. It should however be noted that there might be some uncertainty related to the precision of the surveyed water levels. For instance, some nonphysical values seem to have been captured by the survey, which shows an inverted energy slope in the southwest section of the surveyed area, showed in Figure 6-9.

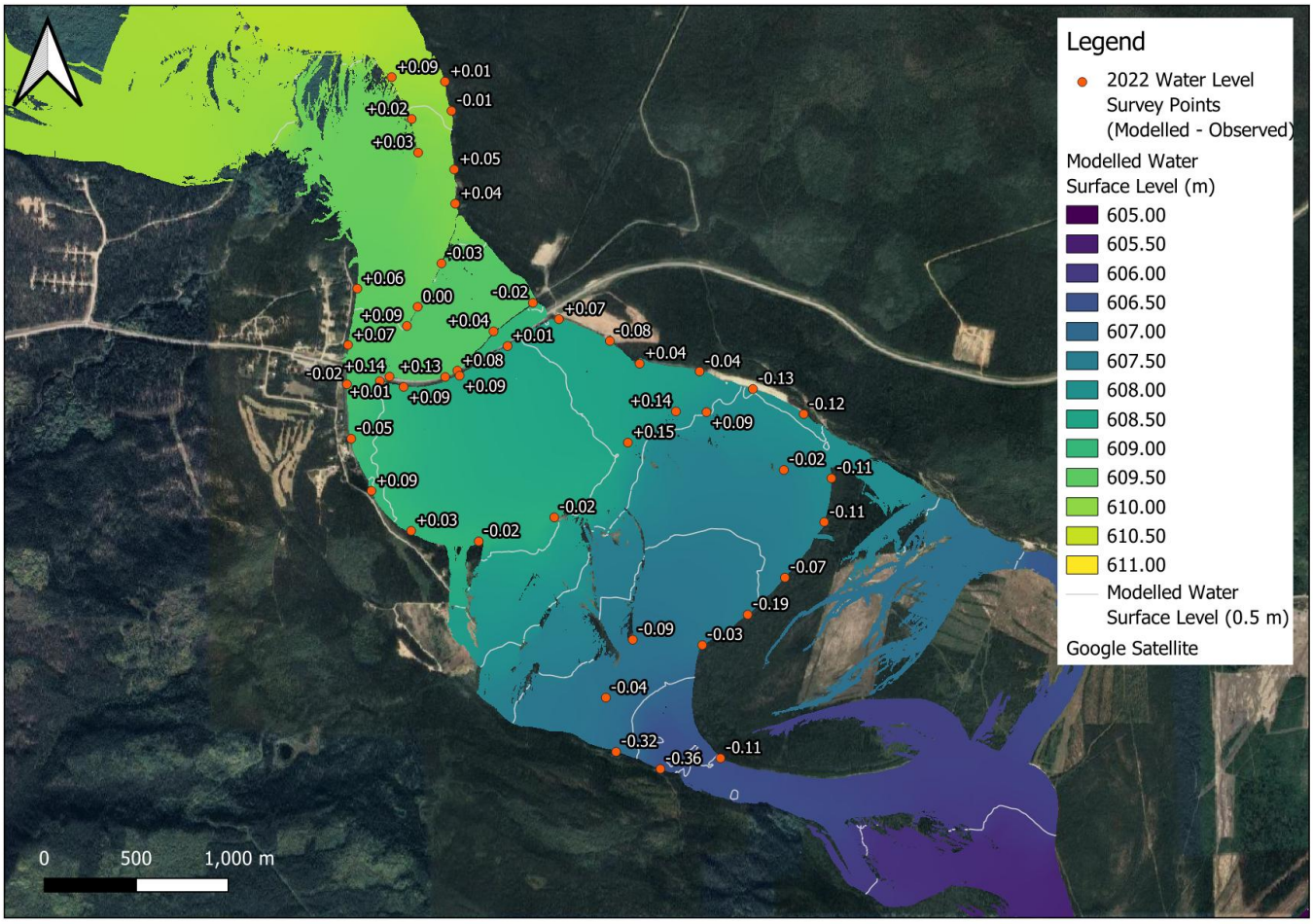

Figure 6-7 – Model Validation Results – 2022 High-Water Survey

Table 6-3 — Model Validation Results – 2022 High-Water Survey

Northing (m)	Easting (m)	Description	Measured Level (m)	Modelled (m)	Difference (m)
6658619.55	505726.34	Right Side	610.14	610.15	0.01
6658643.89	505436.61	Left Side	610.06	610.15	0.09
6658416.18	505545.49	Left Side	609.91	609.93	0.02
6658460.52	505761.74	Right Side	610.05	610.04	-0.01
6658141.88	505776.42	Right Side	609.78	609.83	0.05
6658233.42	505580.36	Left Side	609.77	609.80	0.03
6657955.77	505781.87	Right Side	609.76	609.80	0.04
6657631.14	505707.24	Right Side	609.72	609.69	-0.03
6657395.33	505577.80	Right Side	609.53	609.53	0.00
6657494.29	505249.60	Left Side	609.47	609.53	0.06
6657188.14	505199.45	Left Side	609.36	609.43	0.07
6657291.00	505519.12	Right Side	609.42	609.51	0.09
6656973.87	505193.41	Left Side	609.27	609.25	-0.02
6656677.96	505216.63	Left Side	609.19	609.14	-0.05
6656394.63	505326.54	Left Side	608.91	609.00	0.09
6656177.13	505542.39	Left Side	608.96	608.99	0.03
6656119.81	505909.53	Left Side	608.86	608.84	-0.02
6656250.59	506320.09	Left Side	608.70	608.68	-0.02
6656656.79	506720.08	Left Side	608.26	608.41	0.15
6656826.28	506980.98	Left Side	608.04	608.18	0.14
6656822.32	507147.26	Left Side	607.94	608.03	0.09
6656508.18	507567.69	Left Side	607.70	607.68	-0.02
6655585.39	506746.55	Left Side	607.37	607.28	-0.09
6655270.50	506600.55	Left Side	607.27	607.23	-0.04
6654975.78	506655.76	Left Side	607.51	607.19	-0.32
6654882.56	506896.75	Left Side	606.94	606.58	-0.36
6654941.12	507223.41	Right Side	606.60	606.49	-0.11
6655555.95	507124.63	Right Side	607.39	607.36	-0.03
6655721.41	507371.10	Right Side	607.67	607.48	-0.19
6655922.74	507573.54	Right Side	607.63	607.56	-0.07
6656225.11	507787.03	Right Side	607.86	607.75	-0.11
6656462.93	507826.32	Right Side	607.99	607.88	-0.11
6656811.95	507675.67	Right Side	608.13	608.01	-0.12
6656948.22	507399.33	Right Side	608.14	608.01	-0.13
6657043.89	507109.81	Right Side	608.33	608.29	-0.04
6657086.34	506784.03	Right Side	608.36	608.40	0.04
6657015.60	505424.90	Right Side	609.21	609.35	0.14
6657013.72	505727.41	Right Side	609.27	609.40	0.13
6657048.09	505793.79	Right Side	609.32	609.40	0.08
6657416.76	506203.93	Right Side	609.41	609.39	-0.02
6657261.61	505990.05	Right Side	609.36	609.40	0.04
6657209.48	506622.20	Right Side	608.54	608.46	-0.08
6657327.88	506345.60	Right Side	608.41	608.48	0.07
6657181.65	506066.23	Right Side	608.52	608.53	0.01
6657020.80	505805.74	Right Side	608.54	608.63	0.09
6656959.69	505501.35	Right Side	608.77	608.86	0.09
6656991.09	505372.31	Right Side	609.06	609.07	0.01
			Average		0.00
			Average (absolute)		0.08
			RMSE		0.11

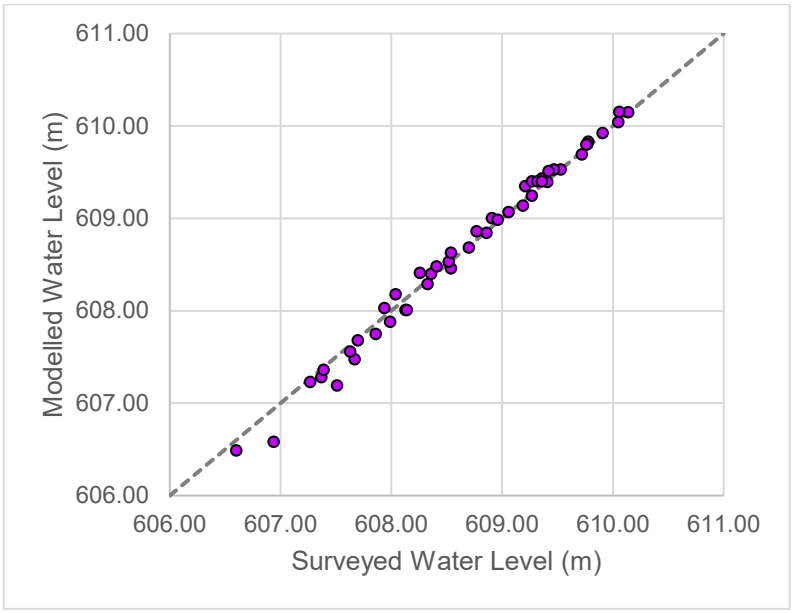

Figure 6-8 – Model Validation Results – 2022 High-Water Survey – Modelled VS Surveyed Water Levels

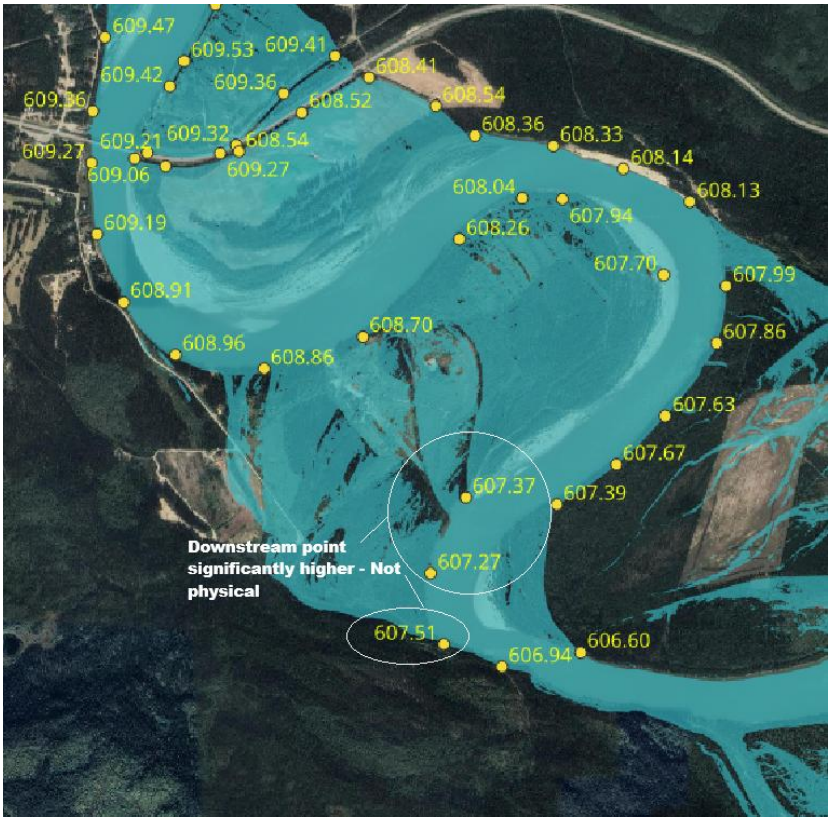

Figure 6-9 – Potential Inconsistencies in the 2022 High-Water Survey

A satellite imagery-derived estimation of the flooded area in June 2022 was provided by the Government of Yukon. This dataset was produced by Natural Resources Canada using Radarsat Constellation Mission imagery, captured during the peak flow period. This estimation does not look very accurate and shows a few oddly shaped features. Multiple reason might explain these limitations, such as the timing of the satellite imagery capture or the presence of a cloud cover. A comparison with modelling results (see Figure 6-10) still shows a somewhat good fit, especially around the community of Upper Liard.

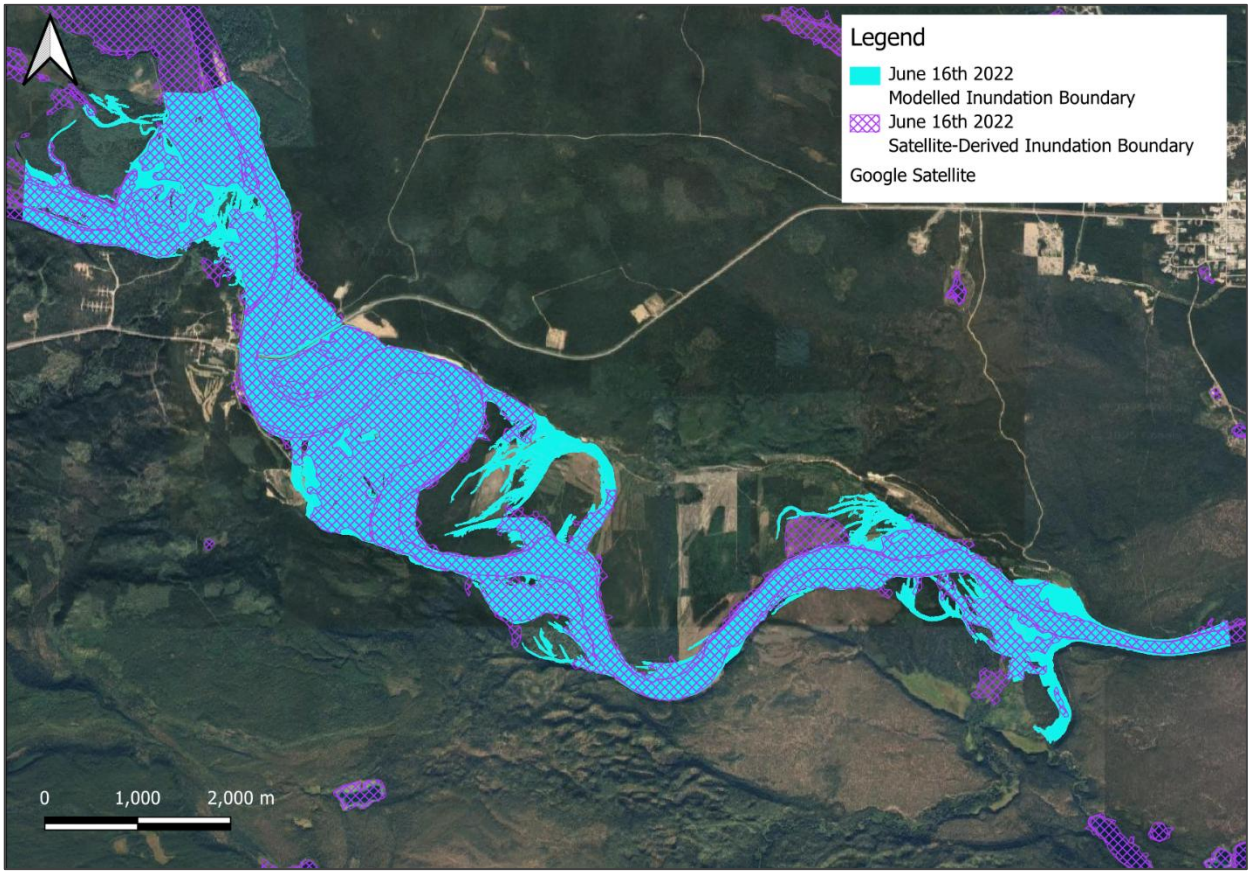

Figure 6-10 – Model Validation Results – 2022 Estimated Flooded Area

6.2.2.5 Validation – 2021 Flood Event

The water level on June 14, 2021, was surveyed at multiple points upstream and downstream of the Upper Liard crossing. Modelling results for the daily discharge measured on that day at Station 10AA001 (1990 m^3/s) were compared to the survey results, as summarized in Figure 6-11 and Table 6-4.

The model slightly overestimates water levels by an average of 0.14 m. The root mean square error (RMSE) is 0.16 m. Around the Upper Liard residential area, the results are more conservative between 0.10-0.28 m. As shown in Figure 6-11 and Figure 6-12, the difference is fairly consistent along the river reach, which shows that the model provides a good representation of the surface slope and does not miss any significant hydraulic controls in the surveyed area.

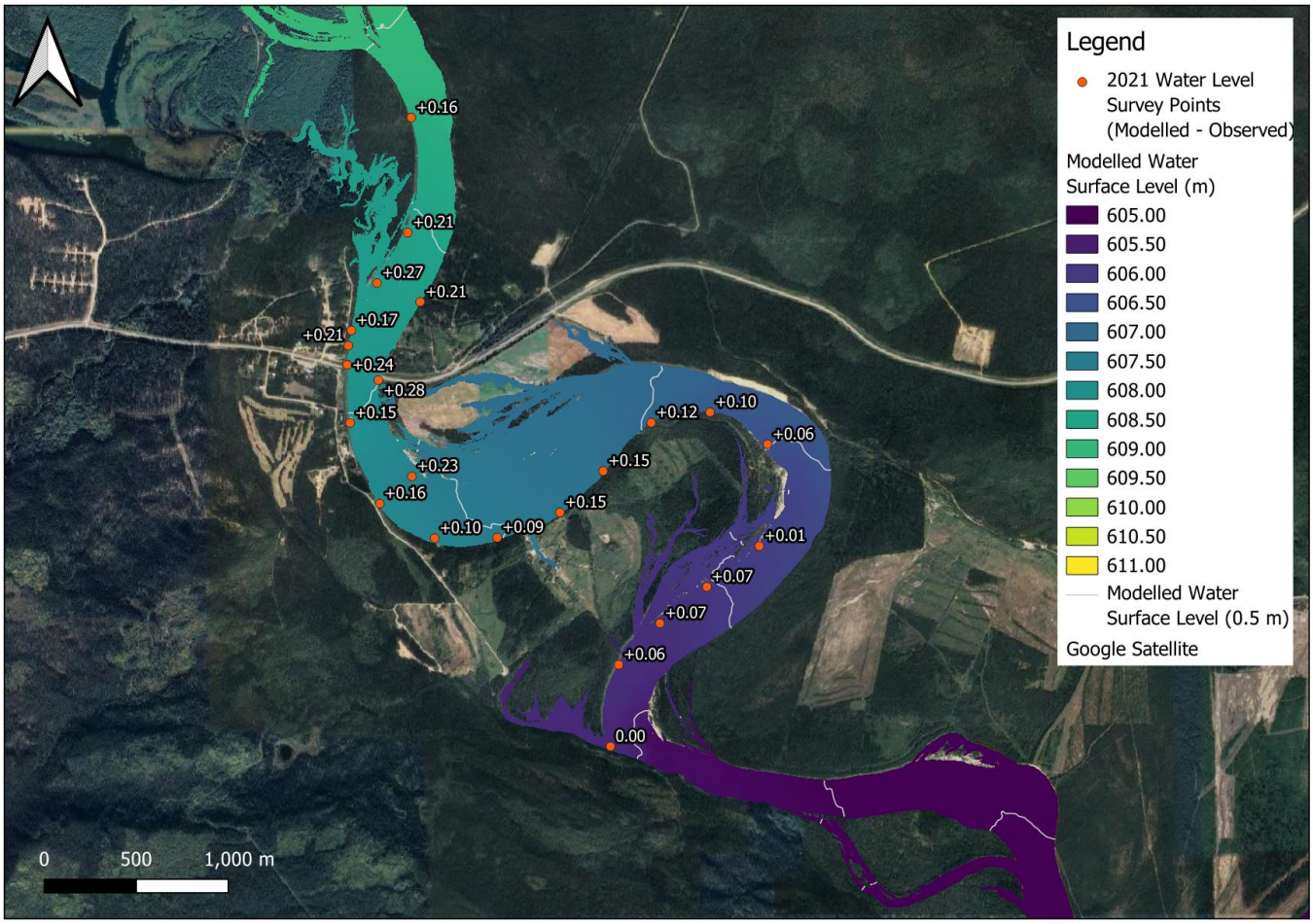

Figure 6-11 – Model Validation Results – 2021 High-Water Survey

Table 6-4 — Model Validation Results – 2021 High-Water Survey

Northing (m)	Easting (m)	Description	Measured Level (m)	Modelled (m)	Difference (m)
6657082.15	505195.20	Right Side	607.95	608.20	0.24
6656998.53	505364.32	Left Side	607.77	608.04	0.28
6658424.94	505543.44	Right Side	608.57	608.72	0.16
6657799.81	505523.75	Right Side	608.23	608.44	0.21
6657526.04	505356.54	Right Side	608.05	608.32	0.27
6657423.94	505592.25	Left Side	608.13	608.33	0.21
6656766.87	505210.17	Right Side	607.82	607.97	0.15
6656328.10	505371.93	Right Side	607.67	607.83	0.16
6656476.23	505546.70	Left Side	607.45	607.68	0.23
6656139.78	505670.17	Right Side	607.61	607.71	0.10
6656143.57	506010.39	Right Side	607.46	607.55	0.09
6656279.44	506350.83	Right Side	607.24	607.39	0.15
6656504.66	506585.97	Right Side	607.11	607.26	0.15
6656767.30	506846.71	Right Side	606.84	606.95	0.12
6656824.09	507166.65	Right Side	606.62	606.72	0.10
6656650.66	507479.26	Right Side	606.45	606.51	0.06
6656097.54	507434.22	Right Side	606.09	606.10	0.01
6655875.76	507149.66	Right Side	605.89	605.95	0.07
6655677.97	506894.23	Right Side	605.78	605.85	0.07
6655452.75	506670.44	Right Side	605.74	605.80	0.06
6655009.47	506625.68	Right Side	605.72	605.72	0.00
6657186.34	505200.82	Right Side	608.02	608.23	0.21
6657268.57	505217.50	Right Side	608.06	608.22	0.17
6657082.15	505195.22	Right Side	608.02	608.20	0.17
			Average		0.14
			Average (absolute)		0.14
			RMSE		0.16

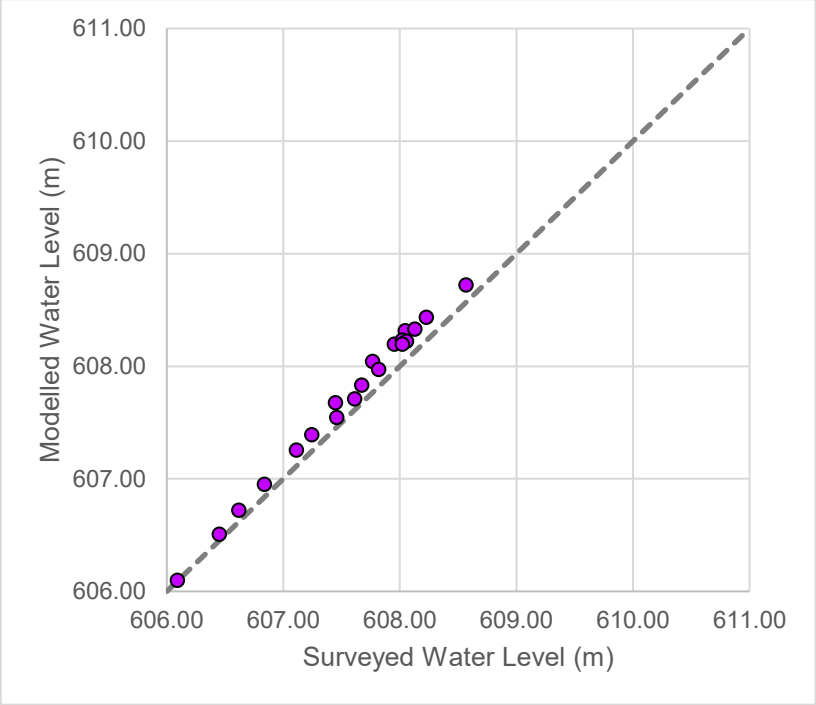

Figure 6-12 – Model Validation Results – 2021 High-Water Survey – Modelled VS Surveyed Water Levels

6.2.3 Sensitivity Analysis

6.2.3.1 Effect of Changing Mesh Size

A sensitivity analysis using different mesh sizes was carried out to establish if the 2D model solution is “independent” from the mesh resolution (see Figure 6-13). It is necessary to know that no model is inherently completely "mesh independent". The main purpose is to demonstrate that refining the mesh resolution would not significantly modify the modelling results. This indicates that the solution is robust and not just an artifact of the mesh size.

The current (original) mesh used in the model calibration process has the resolution of 8 m in the main river channel and 20 m in the floodplain area. This mesh was refined to the resolution of 6 m in the main channel and 15 m in the floodplain area. Due to this refinement, the total number of cells on the refined mesh increased by 63 % compared to the current mesh which significantly increase the computational cost.

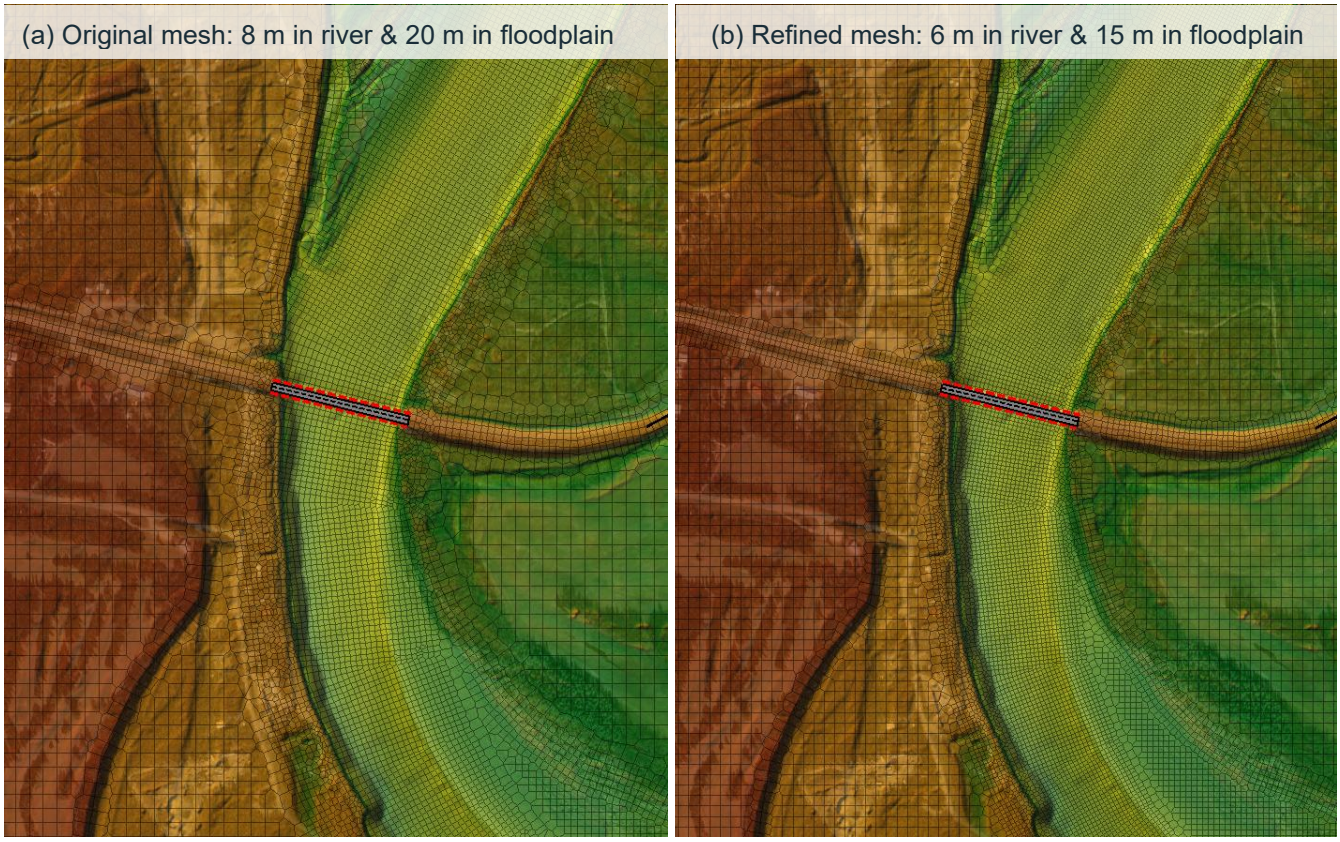

Figure 6-13 – Comparison of (a) Original and (b) Refined Mesh Used for Hydraulic Modelling

The sensitivity analysis results of changing the mesh size for the 0.5% AEP event are plotted in Figure 6-14. The two water level profiles are almost identical with an average difference of about 2 cm (current mesh is on the conservative side). The largest difference of about 5 cm mainly occurs at the complex zone between PK 8 to PK 10. This result demonstrates that the simulation results can be considered “mesh independent”.

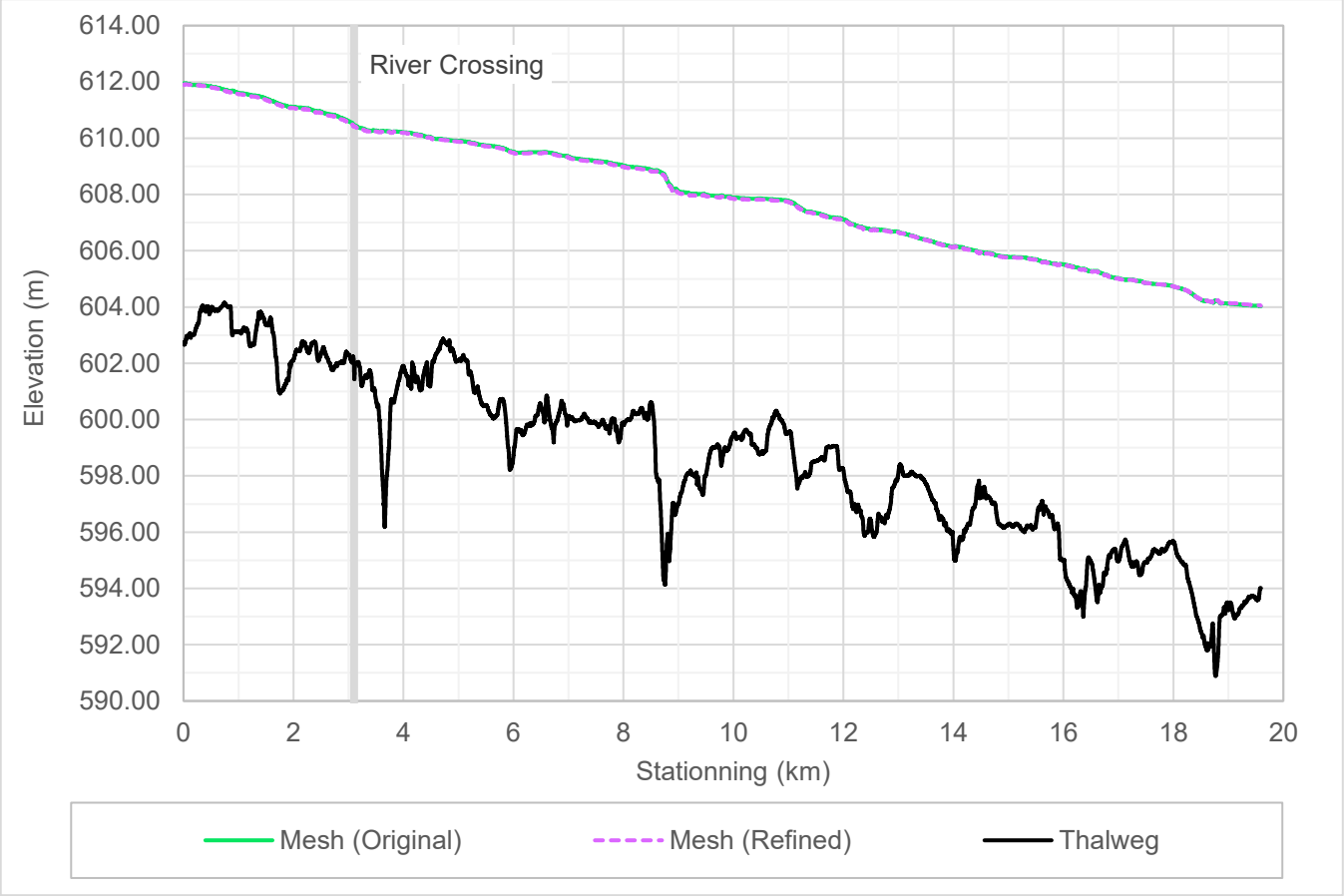

Figure 6-14 – Sensitivity Analysis Result of Changing Mesh Size

6.2.3.2 Changing Downstream Energy Slope

To assess the impact of using different downstream energy slope values on water level and inundation extents, another sensitivity analysis was carried out for the 0.5% AEP event. A relative change of ±15% compared to the calibrated value S_o = 0.00028 was used as shown in Table 6-5.

Table 6-5 – Range of Downstream Energy Slope used for Sensitivity Analysis

Model Parameter	Calibrated Value	Uncertainty Range	Relative Change
Downstream slope	0.00028	0.00024 - 0.00032	±15%

Figure 6-15 shows a comparison of water level profiles between the original result and the downstream-slope-modified results. Results indicate that for a lower downstream energy slope, water level between PK 8.5 to the downstream boundary can increase between a few cm and up to 45 cm. On the other hand, for a higher downstream energy slope, water level at the points located downstream of PK 8.5 can decrease between a few cm to 36 cm. The change in the flood extents induced by these changes in slope are shown in Figure 6-16.

Figure 6-15 – Sensitivity Analysis Result of Changing Downstream Energy Slope

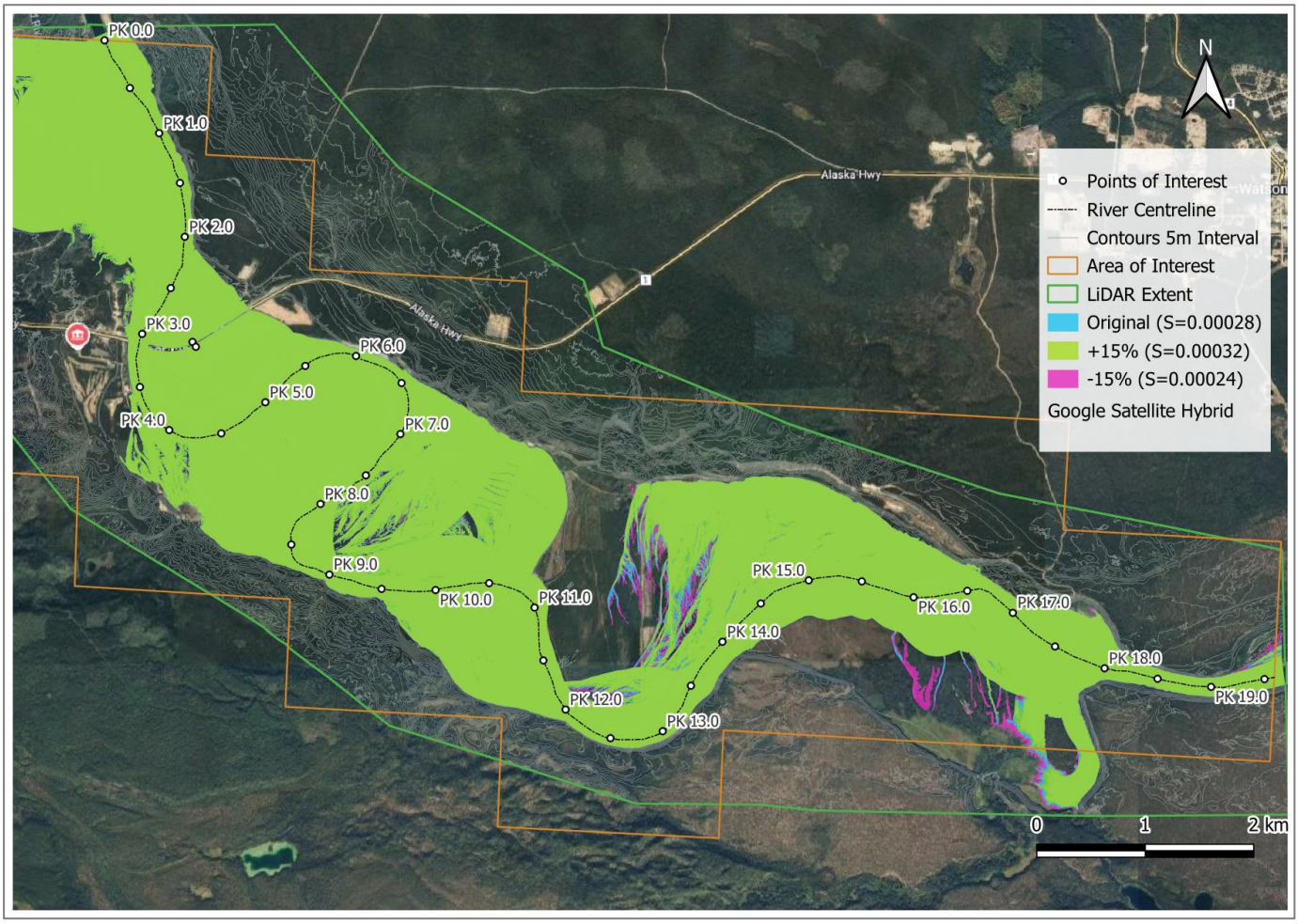

Figure 6-16 – Change in Flood Extent Induced by Changing Downstream Energy Slope

While the sensitivity analysis shows that results in the downstream section of the model are sensitive to the energy slope applied to the boundary condition, this parameter was successfully calibrated using the LiDAR-captured water surface from 2024 (Figure 6-5).

It should also be noted that the impact of changing the downstream energy slope on the water levels around the community of Upper Liard itself is negligible.

6.2.3.3 Effect of Changing Roughness Coefficient (Manning's n)

To assess the uncertainty of using different roughness coefficient (Manning's n) values on water level and inundation extents, a sensitivity analysis was conducted on the highest design flow for the current condition (i.e. 0.5% AEP event). The range of Manning's n considered for this uncertainty assessment was 0.02 – 0.04 which was selected to represent a standard range of expected riverbed roughness typically used for riverine modelling. Two separate scenarios of downstream boundary conditions were considered, including (i) using the downstream energy slope, where the manning roughness influences the calculated normal depth, and (ii) using a fixed downstream water level corresponding to the calibrated roughness value.

Table 6-6 presents the manning's n value and the downstream boundary condition for the first scenario.

Table 6-6 – Summary of Manning's n and Downstream Condition used for Sensitivity Analysis (Scenario i)

Model Parameter	Calibrated Value	Uncertainty Range	Relative Change	Downstream BC
Manning's n	0.03	0.02 - 0.04	±33%	Energy slope

The sensitivity analysis results of the simulated water profiles along the river are plotted in Figure 6-17.Increasing the roughness coefficient will increase the entire water profile, and vice versa. A relative change of 16% of Manning's n value would result in a change of water level by 0.4 to 1.0 m depending on the location. A 33% change of Manning's n value would change the water level between 0.7 to 2 m. Directly upstream of the river crossing, the change in modelled flood level ranges from -0.9 m to +0.7 m, in comparison with the calibrated model results.

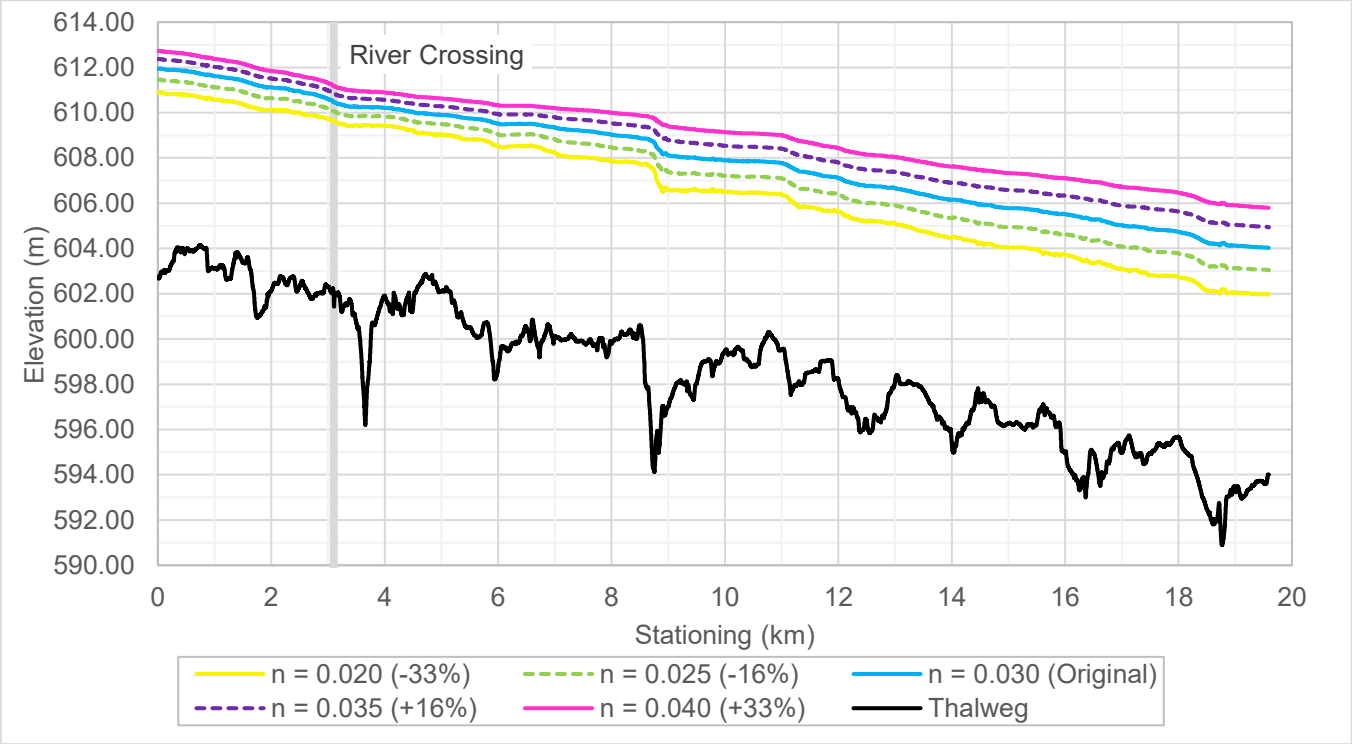

Figure 6-17 – Sensitivity Analysis Result of Changing Roughness Coefficient (Maning's n) – Energy Slope Downstream Boundary Condition (Scenario i)

Figure 6-18 illustrates the change in the flood extent induced by changing the roughness coefficient.

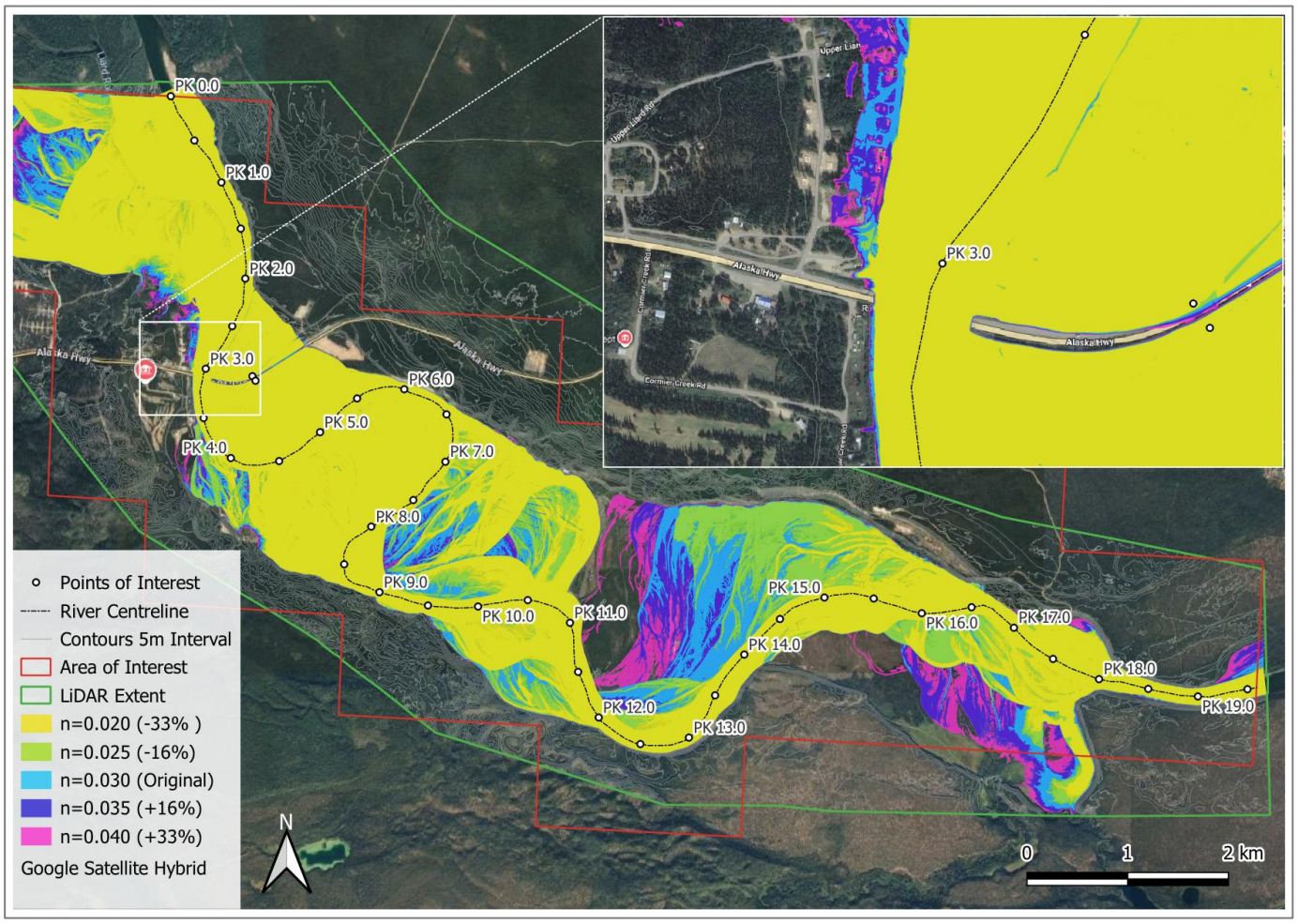

Figure 6-18 – Change in Flood Extent Induced by Changing Roughness Coefficient (Scenario i)

Table 6-7 presents the manning's n value and the downstream boundary condition for the second scenario.

Table 6-7 – Range of Manning's used for Sensitivity Analysis (Scenario ii)

Model Parameter	Calibrated Value	Uncertainty Range	Relative Change	Downstream BC
Manning's n	0.03	0.02 - 0.04	±33%	Fixed water level (Z = 604.03 m)

The sensitivity analysis results of the simulated water profiles along the river are plotted in Figure 6-19. The modelled change in water levels near the community of Upper Liard are of similar magnitude to those of scenario (i), with a range of -0.8 to +0.6 m directly upstream of the river crossing, in comparison with the calibrated model results. Further downstream, all three water profiles converge to the fixed downstream boundary water level.

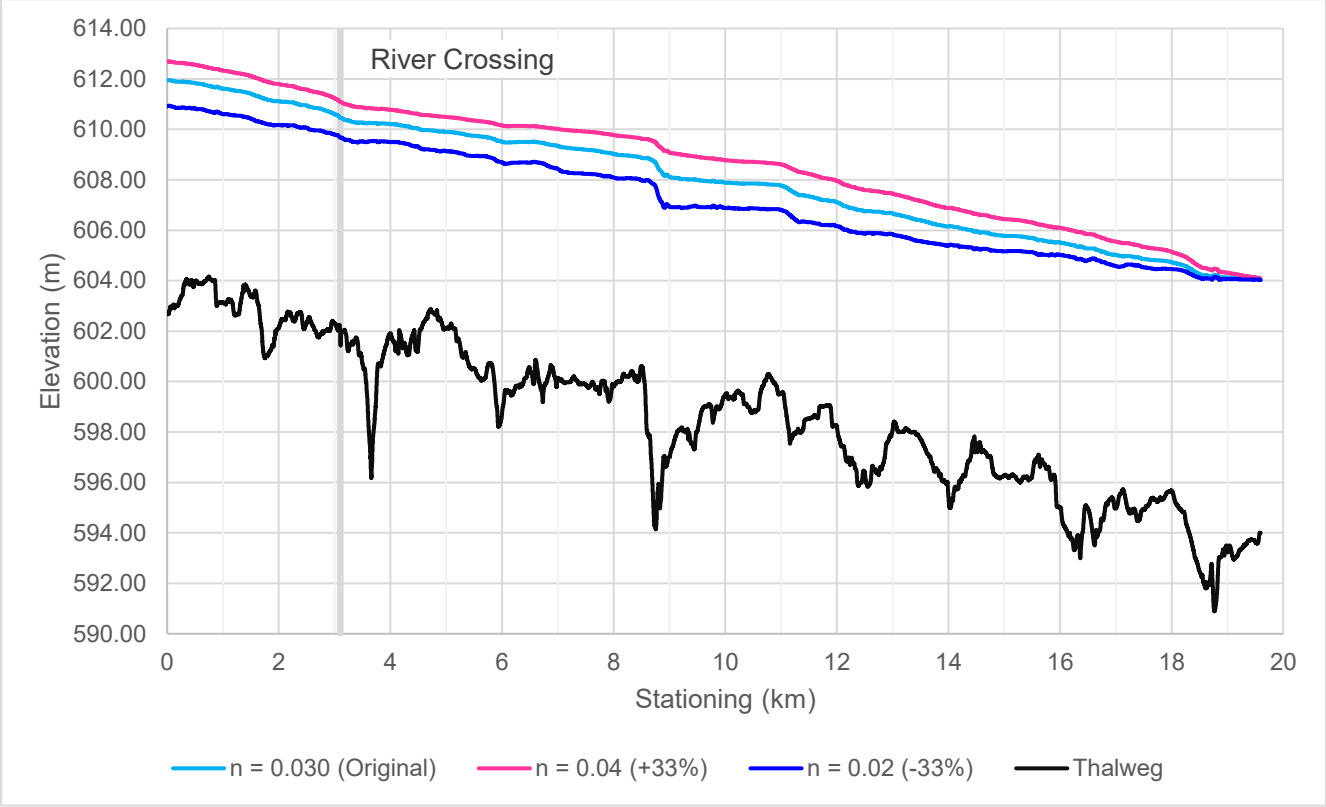

Figure 6-19 – Sensitivity Analysis Result of Changing Roughness Coefficient (Maning's n) – Fixed Downstream Boundary Condition (Scenario ii)

Note that based on the field survey photos (see appendix D), a Manning's n value of 0.04 is not realistic for the study reach of the Liard River at Upper Liard as this value is often used for rivers with vary large cobbles or with boulders (USGS, 1989). While modelling results are quite sensitive to the roughness coefficient, this parameter was extensively calibrated on a broad range of flow values. Calibration and validation results show that the model can reproduce with good accuracy water levels around the community of Upper Liard. Therefore, the Manning's n value of 0.03 was used for the modelling and mapping results.

7. Flood Hazard Mapping

7.1 Mapping Scenarios

Following the results and conclusions presented in Sections 2 to 6, this section summarizes the design flow values used for five mapping scenarios corresponding to different AEPs and different climate conditions. Note that the 5% AEP scenario for future climate is omitted, as it provides a discharge close to the 1% AEP current climate scenario. The five scenarios and the corresponding flows are summarized in Table 7-1 below:

Table 7-1 – Mapping Scenarios and Design Flows

Mapping Conditions and Flow (m^3/s)	Mapping AEPs (%)		
	5	1	0.5
Current Climate	3150	3930	4260
Climate Adjusted	-	5030	5530

7.2 Flood Modelling Results

Using the calibrated HEC-RAS model presented in Section 6.2 and the design flows in Section 7.1 as model inputs, the inundation boundary of each mapping scenario was computed. Figure 7-1 presents the inundation limits of all five flood mapping scenarios. Note that the base layer (or reference water level) corresponding to the average annual peak of 1790 m^3/s (i.e., design flow of 50% AEP event) is also simulated and added to the figure (in yellow in the figure).

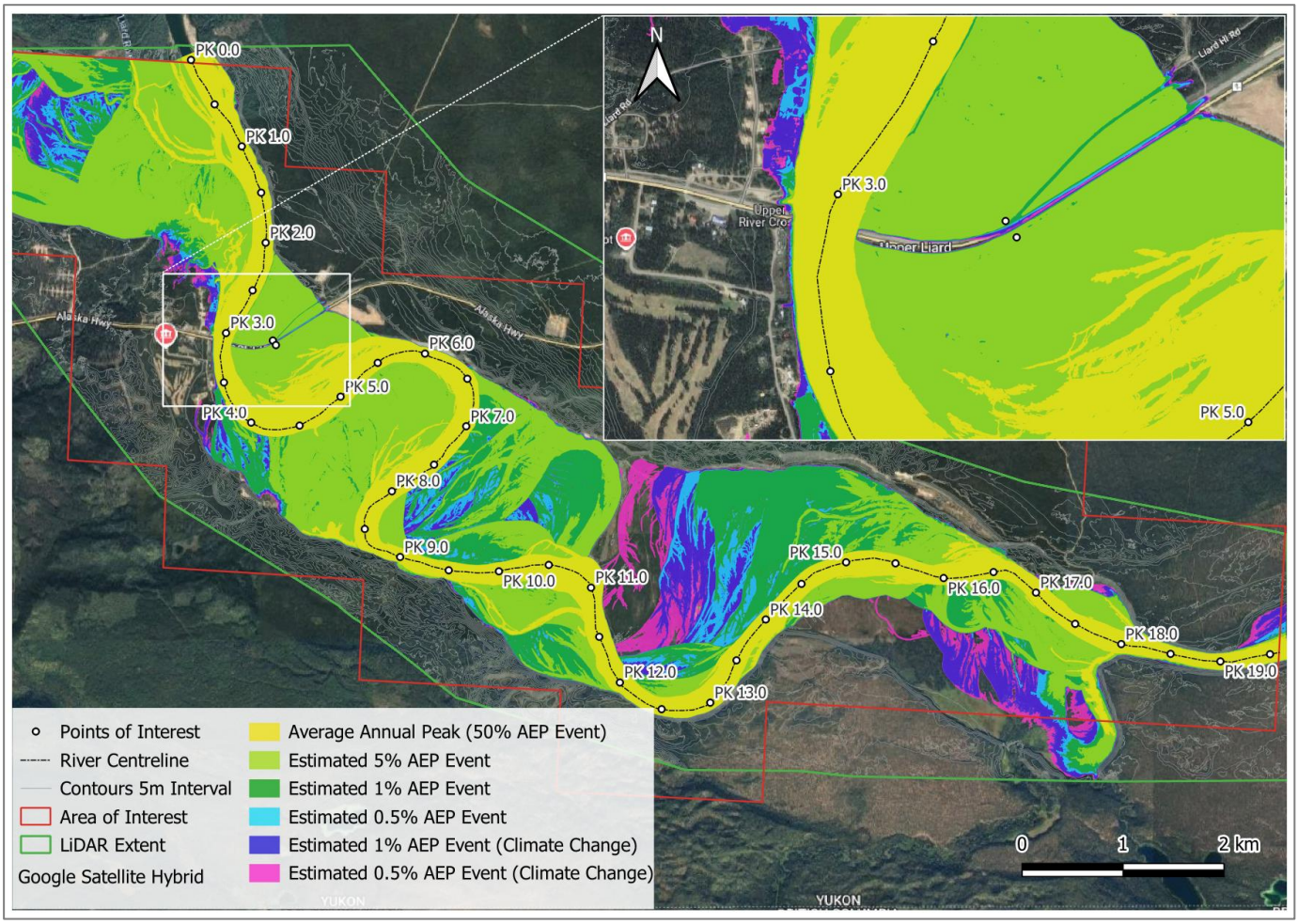

Figure 7-1 – Inundation Extents of All Five Mapping Scenarios

The modelled water levels along the river centreline are presented in Figure 7-2 below for the five mapping scenarios and the average annual peak scenario.

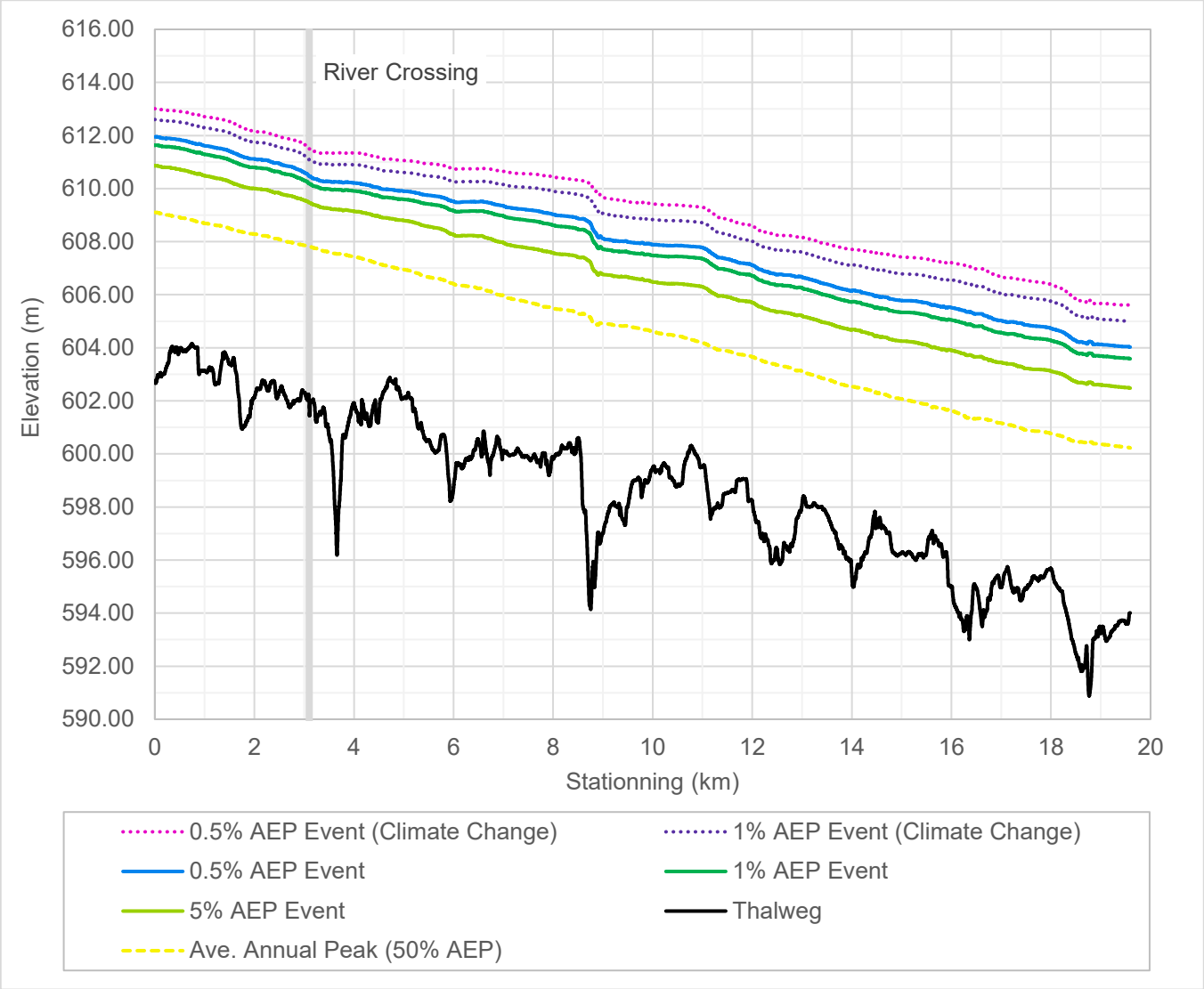

Figure 7-2 – Water Level Profiles of Reference and Mapping Scenarios

The distance between the water surface and the bridge low chord and deck elevation is presented in Table 7-2. The bridge deck elevation was surveyed by AtkinsRéalis personal during the June 2025 field survey. The bridge low chord was estimated using the surveyed elevation of the middle of the H-shaped beam (see Figure 7-3). The road deck is levelled, as confirmed by the drawing and the survey results (maximum 14 cm variation in the survey). The lowest surveyed points were nonetheless used for the vertical clearance estimation as a conservative hypothesis (see Figure 7-4).

There are multiple meters of vertical clearance available between the modelled water levels and the bridge low chord, for each of the mapping scenario.

Table 7-2 – Modelled Vertical Clearance at Upper Liard Crossing

Feature	Scenario	50% AEP	5% AEP	1% AEP	0.5% AEP	1% AEP (Climate Change)	0.5% AEP (Climate Change)
	Water Level (m)	607.86	609.56	610.31	610.61	611.26	611.67
	Elevation	Distance from the Soffit to Water Surface (Vertical Clearance) (m)					
Bridge Deck	616.24	8.4	6.7	5.9	5.6	5.0	4.6
Bridge Low Chord	615.09*	7.1	5.4	4.7	4.4	3.7	3.3

*Estimated, see Figure 7-3

Figure 7-3 –Estimated Bridge Low Chord

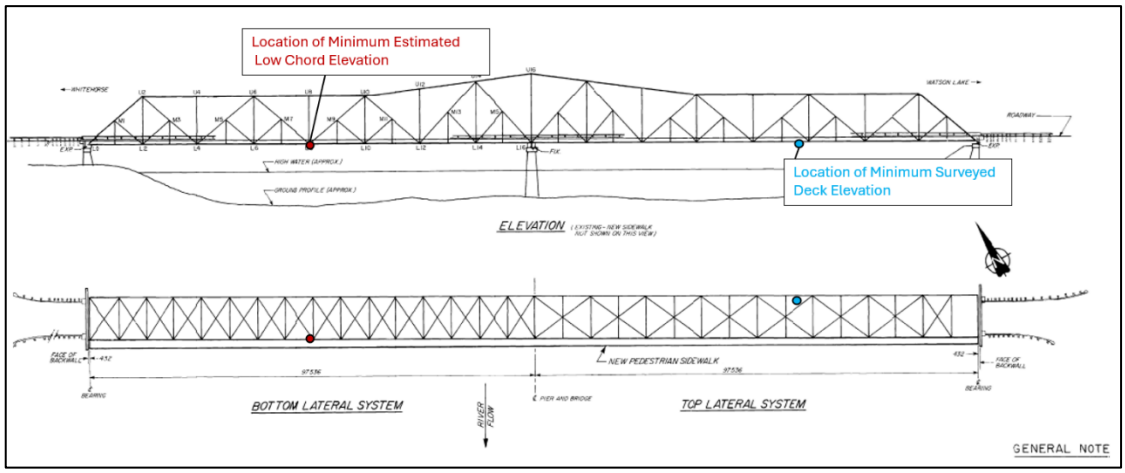

Figure 7-4 – Location of Bridge Deck and Low Chord Low Points

7.3 Flood Hazard Maps

For each mapping scenario, a map book of 16 maps was produced as shown in Figure 7-5. This includes 13 maps at 1:7 500 scale (numbered #1 to #13) and four zoomed maps at 1:2 500 scale (numbered #14 to #17) for the residential areas in the vicinity of Liard River at Upper Crossing. The set of maps can be found in Appendix E.

The flood hazard maps are prepared according to the Government of Yukon Flood Hazard Mapping Basemap Guidelines (2024) and the Federal Floodplain Mapping Guidelines and Specifications (2018). Each map is prepared using ArcGIS software. The horizontal datum is North American Datum of 1983 (NAD83) of the Canadian Spatial Reference System (NAD83 CSRS UTM Zone 9N Epoch 2002). The vertical datum is Canadian Vertical Geodetic Datum of 2013 (CGVD2013). The Geoid model is Canadian Gravimetric Geoid Model of 2013 (CGG2013a). Map projection is Universal Transverse Mercator.

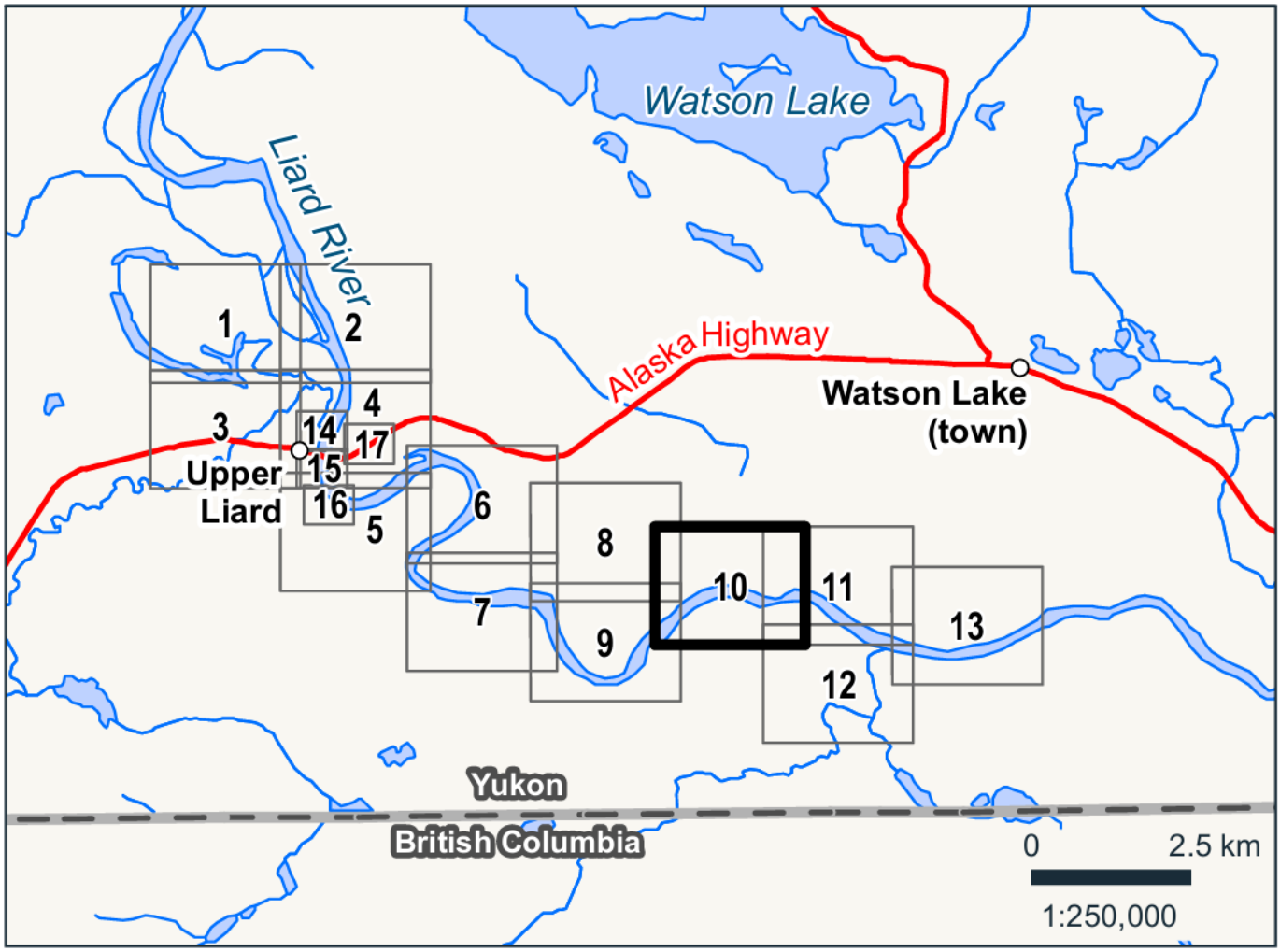

Figure 7-5 – Mapping Frame and Scales

7.4 Flood Mapping Community Engagement

A community engagement event was conducted to present the draft flood hazard mapping to local residents, communicate the project objectives and scope, and invite questions, feedback, comments, and suggestions from the community. Project team representatives included the Project Manager and a Hydrologist from the Government of Yukon along with technical staff from AtkinsRéalis, who were available throughout the session to explain methods, walk through the maps, and document questions and feedback for follow-up.

As part of the materials shared during the event, a poster map was prepared for each mapping scenario (Figure 7-3). The full set of draft maps was used to support discussion of local features, past flood observations, and the interpretation of draft inundation extents.

The engagement was designed to:

1. Share preliminary flood extents and associated hazard information in a clear, accessible format.
2. Provide an overview of the technical approach and key assumptions supporting the draft results.
3. Open a dialogue with the community regarding potential future planning and development considerations, recognizing that decisions on implementation, regulation, and enforcement rest with the responsible authorities.
4. Gather local knowledge and lived experience to help verify, contextualize, and, where appropriate, refine the mapping and explanatory materials.

This engagement strengthens transparency, builds shared understanding of flood risk, and supports informed discussion on future applications of the mapping (e.g., emergency preparedness, adaptation practices, and potential mitigation planning).

7.4.1 Event Format and Logistics

A preliminary project overview and orientation session was first delivered to Liard First Nation staff to introduce the study purpose, methods, and anticipated deliverables. This session provided context and ensured that key partners were briefed prior to the broader public engagement.

Subsequently, the formal community session was held as an open house with a presentation and facilitated Q&A at the Watson Lake Recreation Centre in Watson Lake, Yukon, on February 17, 2026. The format enabled drop-in review of materials, a structured presentation summarizing the study, and a question period to address comments and collect feedback.

Materials available at the event included:

- A slide presentation summarizing the project scope, methods, and draft results.
- Printed flood hazard map book showing inundation extents for selected AEP scenarios.
- A large-format poster with zoomed-in mapping for residential areas of interest.
- A plain-language handout summarizing the project and key terms (e.g., AEP).

Large-format residential-area maps supported detailed discussion of local features of interest. Staff recorded location-specific observations and questions for subsequent review as part of the draft-to-final refinement process. Approximately 15 residents attended to review the materials and provide comments.

7.4.2 Community Feedback

Community feedback gathered during the engagement session provided valuable local insights that helped refining the draft flood mapping and helped contextualizing the technical findings:

1. Several residents identified an unmarked logging road within the study area that does not currently appear on base mapping. This road was added to the final maps (see Appendix E.)

2. Participants with longstanding knowledge of local hydrology also highlighted groundwater outflows near the mouth of Albert Creek that may contribute to localized increases in water levels during high-flow periods. No modifications were made to the mapping based on this account. This localized inflow is expected to be very small in comparison to the total river discharge and should already be captured by the station used for the flood frequency analysis (Station 10AA001 - Liard River at Upper Crossing), located near the river crossing.

3. Residents also offered verification of the modelled flood extents based on personal experience. One attendee noted that during a specific historical high-water event, floodwaters reached a particular household. The extent depicted in the modelled inundation map aligned closely with this account, providing an informal but valuable cross-check of the mapping credibility and reinforcing confidence in the representation of observed conditions.

4. Several participants expressed interest in future planning discussions that may be informed by the flood mapping once finalized. These questions were addressed directly by the Government of Yukon representative, who provided general information on how such mapping may be considered by relevant authorities in future planning contexts, while emphasizing that any policy decisions fall outside the scope of this technical study.

5. Finally, attendees raised questions about the current year's snowpack conditions, noting that the heavy accumulation has heightened community awareness and concern regarding potential flooding. The interest and engagement on this topic suggest that the project is helping foster improved community dialogue around flood preparedness and risk awareness, demonstrating a positive outcome of the engagement process.

The community was also encouraged to provide feedback via the Government of Yukon Flood Hub. No online responses were received during the comment period, which closed on March 2, 2026.

References

AECOM (2021). Modeling Future Wildfire Risk in Yukon. Phase II – Modeling and Analysis. Technical Report

Bush, E. and Lemmen, D.S., editors (2019): Canada's Changing Climate Report; Government of Canada, Ottawa, ON. 444 p. https://changingclimate.ca/CCCR2019/chapter/8-0/

Brown, G., and Craig, J. R. (2020). Structural calibration of an semi-distributed hydrological model of the Liard River basin. *Canadian Water Resources Journal / Revue Canadienne Des Ressources Hydriques*, *45*(4), 287–303. https://doi.org/10.1080/07011784.2020.1803143

Canadian River Ice Database (CRID, 2025). Accessed on June 24, 2025. Link: https://data-donnees.az.ec.gc.ca/data/water/scientificknowledge/canadian-river-ice-database/

Chow, Ven Te (1959). Open-Channel Hydraulics. McGraw-Hill, New York, NY.

ClimateData (2025). About CanDCS-M6. Accessed on 05 September 2025. https://climatedata.ca/about-candcs-m6/

Craig, J.R., G. Brown, R. Chlumsky, W. Jenkinson, G. Jost, K. Lee, J. Mai, M. Serrer, M. Shafii, N. Sgro, A. Snowdon, and B.A. Tolson. (2020), Flexible watershed simulation with the Raven hydrological modelling framework, Environmental Modelling and Software, 129, 104728, doi:10.1016/j.envsoft.2020.104728

Curry, C.L., Ouali, D., Sobie, S.R., and Zwiers, F. W. (2023). Downscaled CMIP6 climate model subset selection. Pacific Climate Impacts Consortium. https://dspace.library.uvic.ca/server/api/core/bitstreams/1279e6d0-80ff-4b0c-b241-45de9562f18a/content

ECCC (2025). Environment and Climate Change Canada: Historical climate Data. Accessed on August 01, 2025. Link: https://climate.weather.gc.ca/index_e.htmls

Government of Newfoundland and Labrador (2025). Technical Guidelines for Flood Hazard Mapping Studies – Issued for 2025-26. https://www.gov.nl.ca/ecc/waterres/flooding/frm/

Government of Yukon (2022). Assessing Climate Change - Risk and Resilience in the Yukon, https://yukon.ca/sites/default/files/env/env-assessing-climate-change-risk-resilience-yukon-main-report.pdf

Government of Yukon (2025). Request for Proposals : Upper Liard Flood Mapping Study. Department of Environment – Water Resources Branch, Government of Yukon.

Hosking, J.R.M and Wallis, J.R. (1997). Regional Frequency Analysis: An Approach Based on L-moments. Cambridge University Press, UK. http://dx.doi.org/10.1017/cbo9780511529443

NRCan (2023). Federal hydrologic and hydraulic procedures for flood hazard delineation (2.0). Natural Resources Canada, General Information Product, 113e, 161. Natural Resources Canada. https://doi.org/10.4095/332156

Perrin, A. & Jolkowski, D. (2022). Yukon climate change indicators and key findings 2022. YukonU Research Centre, Yukon University, 126p.

Shrestha, R. R., Cannon, A., Schnorbus, M. A., Alford, H. (2019). Climatic Controls on Future Hydrologic Changes in a Subarctic River Basin in Canada. Journal of Hydrometeorology, vol 20, issue 9, page 1757-1778.s https://doi.org/10.1175/JHM-D-18-0262.1

USACE (2025). Hec-RAS User's Manual. Version 6.6. U.S. Army Corps of Engineers. Access on October 15, 2025. https://www.hec.usace.army.mil/confluence/rasdocs/rasum/6.6s

USGS (1989). United States Geological Survey: Guide for Selecting Manning's Roughness Coefficients for Natural Channels and Flood Plains. Accessed on March 16, 2026. Link: https://pubs.usgs.gov/wsp/2339/report.pdf

Water Survey of Canada (WSC, 2025). https://wateroffice.ec.gc.ca/index_e.html. Accessed on July 15, 2025. Link: https://wateroffice.ec.gc.ca/index_e.html

Walvoord, M.A., Barret (2016). Hydrologic Impacts of Thawing Permafrost—A Review. Vadose Zone Journal, Volume 15, Issue 6

Yukon Energy (2024). Climate Change Adaptation Plan – 2024 Summary Report. https://yukonenergy.ca/environment/climate-change/

APPENDICES

Appendix A. Historical Flow Records

A.1 Annual maximum discharge series

A.1.1 Station 10AA004 - Rancheria River near the Mouth

Table A-1 – Annual maximum daily and instantaneous peak discharge of Station 10AA004

No	Year	Q_{daily} (m^3/s)	Q_{inst} (m^3/s)	No	Year	Q_{daily} (m^3/s)	Q_{inst} (m^3/s)
1	1985	342	355	21	2005	317	351
2	1986	242	261	22	2006	400	469
3	1987	472	516	23	2007	479	522
4	1988	598	652	24	2008	381	412
5	1989	185	191	25	2009	363	392
6	1990	509	581	26	2010	162	165
7	1991	183	184	27	2011	202	215
8	1992	358	365	28	2012	901	985
9	1993	202	205	29	2013	353	388
10	1994	232	246	30	2014	249	267
11	1995	214	231	31	2015	221	224
12	1996	174	175	32	2016	167	178
13	1997			33	2017	173	188
14	1998	286	307	34	2018		
15	1999	364	372	35	2019	130	141
16	2000	217	222	36	2020	329	341
17	2001	288	300	37	2021	337	364
18	2002	238	246	38	2022	527	544
19	2003	141	143	39	2023	250	270
20	2004	257	264	40	2024	247	253

Note: red numbers are estimated values.

A.1.2 Station 10AA005 – Big Creek at Km 1084.8 Alaska Highway

Table A-2 – Annual maximum daily and instantaneous peak discharge of Station 10AA005

No	Year	Q_{daily} (m^3/s)	Q_{inst} (m^3/s)	No	Year	Q_{daily} (m^3/s)	Q_{inst} (m^3/s)
1	1989	27.1	28.5	19	2007	77.9	87.9
2	1990	50.0	54.0	20	2008	64.9	71.4
3	1991	17.8	18.0	21	2009	38.7	40.5
4	1992	51.2	53.1	22	2010	29.6	33.2
5	1993	25.1	25.5	23	2011	25.0	25.9
6	1994	35.3	35.9	24	2012	198.0	218.0
7	1995	22.8	23.5	25	2013	65.3	69.0
8	1996	31.4	33.9	26	2014	38.9	40.7
9	1997	93.6	105.0	27	2015	24.4	25.4
10	1998	49.3	51.8	28	2016	20.0	20.5
11	1999	50.6	52.0	29	2017	21.1	22.3
12	2000	21.7	22.3	30	2018	23.8	25.7
13	2001	65.8	73.9	31	2019	16.4	17.1
14	2002	32.2	34.6	32	2020	44.8	48.4
15	2003	19.0	19.7	33	2021	44.8	46.3
16	2004	34.8	36.6	34	2022	63.6	64.6
17	2005	63.3	66.6	35	2023	34.5	35.3

Note: red numbers are estimated values.

A.1.3 Station 10AA006 – Liard River below Scurvy Creek

Table A-3 – Annual maximum daily and instantaneous peak discharge of Station 10AA005

No	Year	Q_{daily} (m^3/s)	Q_{inst} (m^3/s)	No	Year	Q_{daily} (m^3/s)	Q_{inst} (m^3/s)
1	2017	228	263	5	2021	664	691
2	2018	324	333	6	2022	777	808
3	2019	250	256	7	2023	542	563
4	2020	490	505	8	2024	236	242

Note: red numbers are estimated values.

A.1.4 Station 10AB001 – Frances River near Watson Lake

Table A-4 – Annual maximum daily and instantaneous peak discharge of Station 10AB001

No	Year	Q_{daily} (m^3/s)	Q_{inst} (m^3/s)	No	Year	Q_{daily} (m^3/s)	Q_{inst} (m^3/s)
1	1963	852	861	32	1994	698	701
2	1964	1100	1110	33	1995	429	430
3	1965	481	484	34	1996	396	400
4	1966	654	660	35	1997	442	453
5	1967	818	830	36	1998	732	740
6	1968	595	603	37	1999	816	820
7	1969	530	532	38	2000	553	559
8	1970	538	541	39	2001	887	919
9	1971	858	861	40	2002	500	504
10	1972	1060	1080	41	2003	537	547
11	1973	782	782	42	2004	734	756
12	1974	671	691	43	2005	807	837
13	1975	776	779	44	2006	983	1020
14	1976	926	929	45	2007	965	992
15	1977	668	671	46	2008	833	850
16	1978	453	456	47	2009	917	932
17	1979	751	756	48	2010	437	442
18	1980	496	497	49	2011	738	755
19	1981	724	734	50	2012	1160	1190
20	1982	584	586	51	2013	1040	1050
21	1983	591	592	52	2014	578	581
22	1984	632	636	53	2015	718	725
23	1985	776	783	54	2016	611	629
24	1986	698	699	55	2017	555	562
25	1987	598	601	56	2018	401	406
26	1988	793	794	57	2019	479	484
27	1989	475	477	58	2020	806	817
28	1990	774	778	59	2021	857	871
29	1991	588	591	60	2022	1270	1290
30	1992	1190	1200	61	2023	710	722
31	1993	772	774	62	2024	401	404

Note: red numbers are estimated values.

A.2 Daily and instantaneous discharge relationship

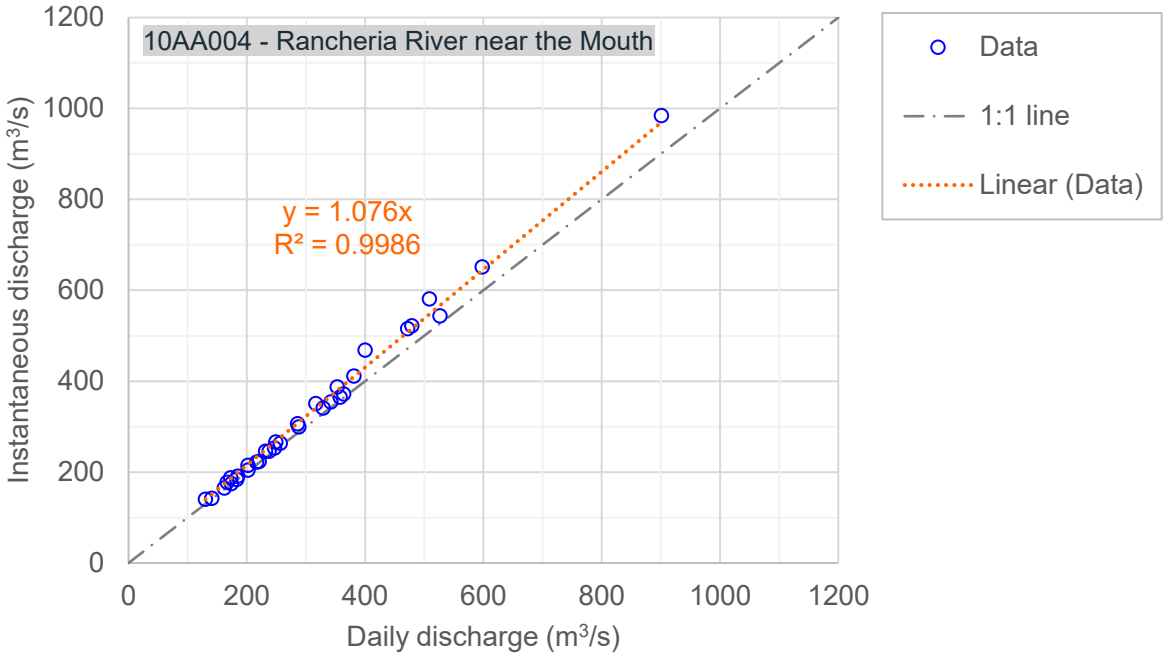

Figure A-1 – Relationship between maximum daily and instantaneous discharge of Station 10AA004

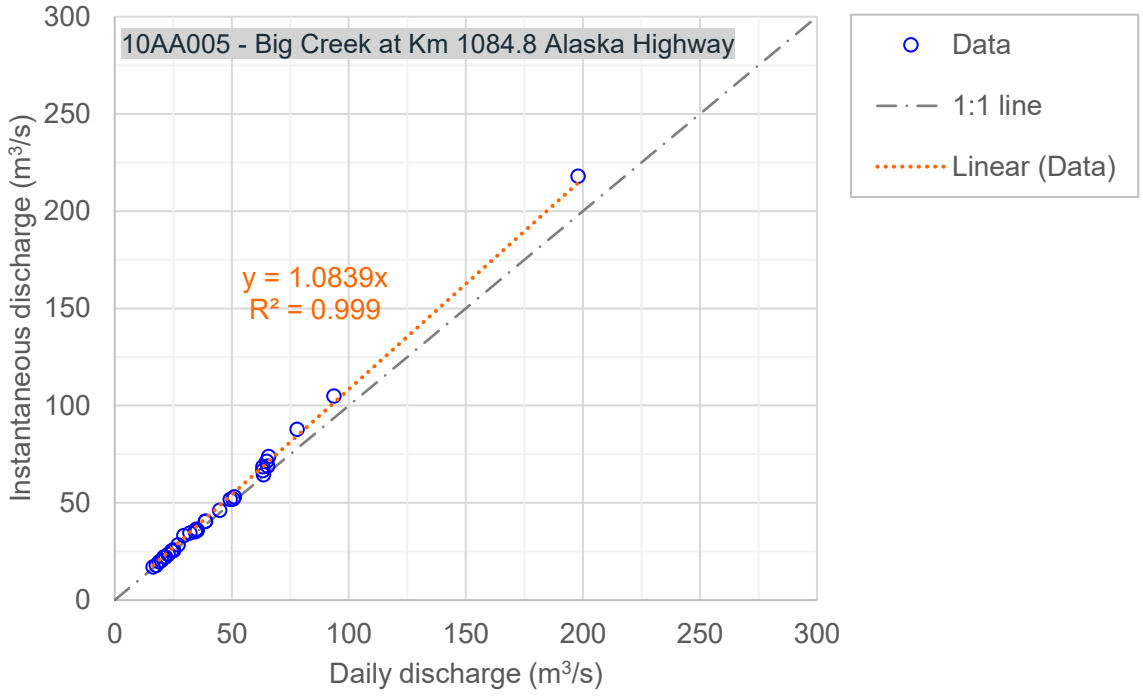

Figure A-2 – Relationship between maximum daily and instantaneous discharge of Station 10AA005

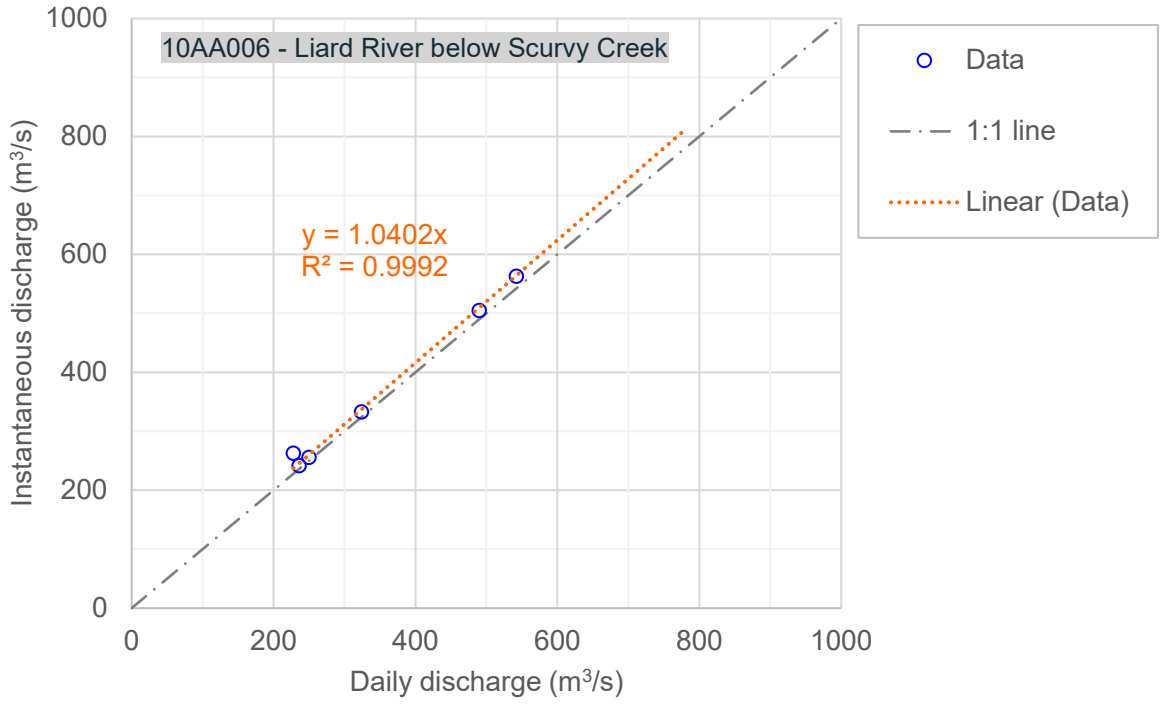

Figure A-3 – Relationship between maximum daily and instantaneous discharge of Station 10AA006

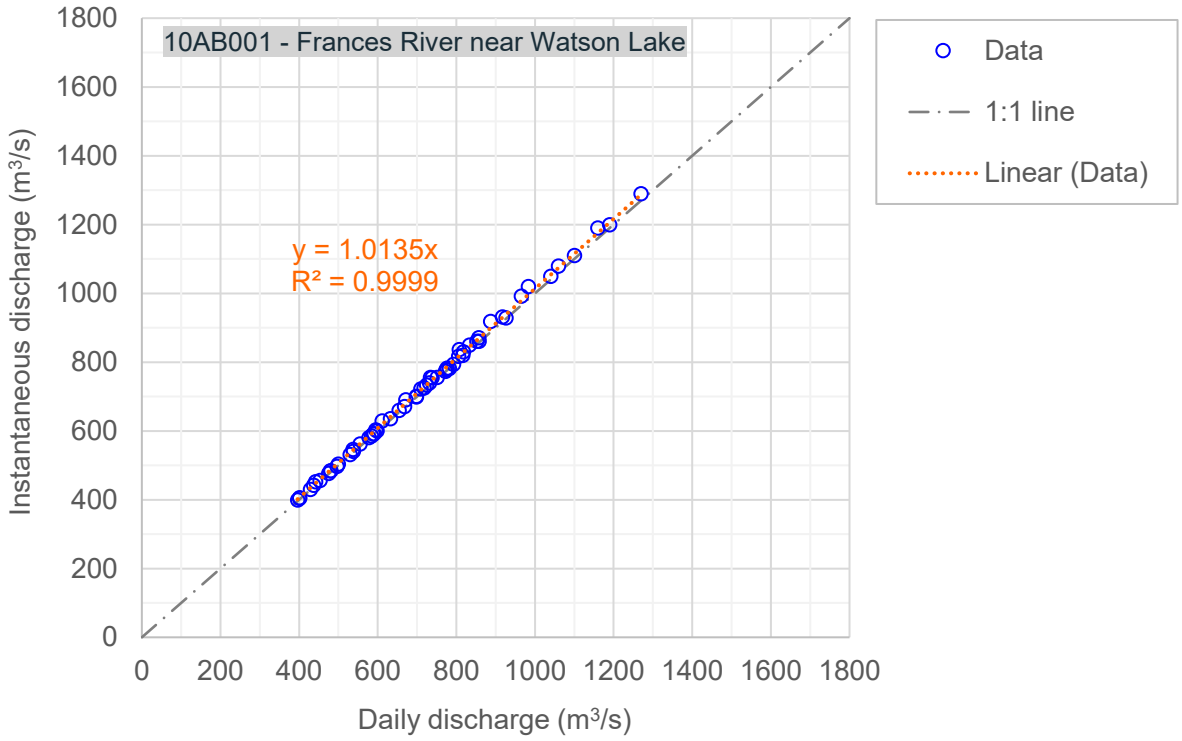

Figure A-4 – Relationship between maximum daily and instantaneous discharge of Station 10AB001

Appendix B. Hypothesis Testing

Table B-1 – Hypothesis Testing Results

Station	Hypothesis Testing		
	Test for Independence	Test for Stationarity	Test for Homogeneity
10AA004	We accept H_0 at a significance level of 5 %.	We accept H_0 at a significance level of 5 %.	We accept H_0 at a significance level of 5 %.
10AA005	We accept H_0 at a significance level of 5 %.	We accept H_0 at a significance level of 5 %.	We accept H_0 at a significance level of 5 %.
10AA006 *	n/a	n/a	n/a
10AB001	We accept H_0 at a significance level of 5 %.	We accept H_0 at a significance level of 5 %.	We accept H_0 at a significance level of 5 %.

* Test results are not available for Station 10AA006 as it contains less than 10 years of record.

Appendix C. River Ice Assessment

Appendix D. Fluvial Erosion Assessment

Appendix E. Flood Hazard Maps

AtkinsRéalis

Engineering Services Canada
AtkinsRéalis Canada Inc.
455 boul. René-Lévesque O
Montréal
QC
H2Z 1Z3

.